Politecnico di Milano

SCHOOL OF INDUSTRIAL AND INFORMATION ENGINEERING

Master of Science – Energy Engineering

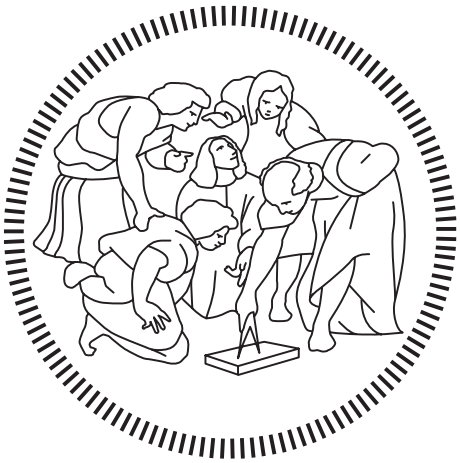

# Zn anode shape-change suppression in mildly acidic aqueous zinc-ion battery electrolytes containing quaternary ammonium salts

Supervisor

**Prof. Benedetto BOZZINI**

Co-Supervisor

**Dott. Francesca ROSSI**

Candidate

**Caielli TOMMASO– 928476**

**Academic Year 2020 – 2021**

# Ringraziamenti

Vorrei ringraziare la Dott.ssa Lucia Mancini di Elettra Sinctrotrone Trieste S.c.p.a. per le misure tomografiche, il Dott. Nicola Sodini di Elettra Sinctrotrone Trieste S.c.p.a. per la fabbricazione delle celle per tomografia, il Prof. Marco Boniardi e l'Ing. Andrea Casaroli del Dip. di Meccanica per il SEM e la stereomicroscopia e il mio amico Riccardo per avermi soccorso in extremis con l'impaginazione.

Un ringraziamento sincero soprattutto a Francesca Rossi e al prof. Benedetto Bozzini per avermi insegnato a fare ricerca, per avermi lasciato la libertà di sperimentare, e per avermi permesso di passare un anno bellissimo in un vero laboratorio scientifico. Lo desideravo da quando ero bambino.

# Sommario

La crescente domanda di batterie ricaricabili, unita alle le problematiche ambientali, di scarsità di risorse e di sicurezza associate alle batterie al litio, hanno spinto la ricerca a studiare tecnologie alternative per soddisfare tale domanda. Nell'ultimo decennio è infatti esploso l'interesse sulle batterie ricaricabili basate sullo zinco. Queste batterie adottano elettroliti acquosi, che sono intrinsecamente più sicuri, e anodi in zinco metallico, che permettono alte capacità specifiche. Inoltre, lo zinco è più abbondante e meglio geopoliticamente distribuito del litio. Sebbene le batterie con anodi in zinco siano una tecnologia ben nota fin dalla metà del diciannovesimo secolo e siano tuttora ampiamente prodotte e commercializzate, queste consistono esclusivamente in batterie non ricaricabili. La realizzazione di batterie ricaricabili con anodi di zinco in grado di competere con quelle al litio è teoricamente possibile ma deve affrontare importanti ostacoli tecnologici. Il principale è la sintesi di un catodo performante: l'interesse è attualmente principalmente focalizzato su catodi ad aria e su catodi ad intercalazione. Questa tesi si è pertanto concentrata però sulle problematiche relative all'anodo in Zn. Un anodo metallico si dissolve nell'elettrolita durante la scarica e si rideposita durante la carica. Questo processo non è purtroppo reversibile: l'alternarsi di fasi di carica e scarica comporta cambiamenti morfologici dell'anodo e l'evoluzione di strutture tridimensionali. Queste possono disconnettersi dall'elettrodo e causare una perdita di capacità, o nel caso peggiore, perforare l'elettrolita e dare luogo ad un cortocircuito interno alla batteria. Lo Zn è un metallo anfotero, la dissoluzione dello zinco metallico può infatti avvenire in elettroliti a pH sia acido che fortemente basico; a pH intermedi l'ossidazione dello zinco causa la formazione di ossidi insolubili e passivanti. Le batterie allo zinco possono quindi essere sviluppate in ambiente basico o debolmente acido. Le prime sono estensivamente prodotte come batterie primarie e sono state ampiamente, anche se non conclusivamente, studiate, le seconde hanno recentemente attirato l'attenzione per via della minore tendenza alla formazione di dendriti in questo tipo di elettrolita. Questa tesi si concentra sugli elettroliti debolmente acidi, la parte di revisione della letteratura sottolinea le differenze tra i due ambienti e studia l'applicabilità delle conoscenze dell'ambiente alcalino in elettroliti debolmente acidi. La principale differenza tra i due è che lo ione Zn in ambiente alcalino è complessato come zincato e porta una doppia carica negativa, mentre in ambiente debolmente acido questo porta una doppia carica positiva. In ambiente alcalino, inoltre, la reazione di dissoluzione porta ad una acidificazione locale della soluzione, che, in particolari condizioni, potrebbe favorire la passivazione dell'elettrodo. La reazione di dissoluzione in ambiente debolmente acido non comporta la modifica del pH, però la reazione secondaria di evoluzione d'idrogeno alcalinizza l'elettrolita e causa la formazione di ossidi sull'elettrodo. Le morfologie assunte dagli elettrodepositi di zinco a diverse densità di corrente sono analoghe nei due ambienti: al crescente della densità di corrente si ottengono depositi di tipo "mossy", compatto e dendritico. I depositi "mossy" sono porosi e fragili, il loro meccanismo di formazione è attualmente poco conosciuto. Depositi compatti, uniformi e regolari, sono invece la morfologia di elezione per il ciclaggio di un anodo in zinco. I dendriti sono strutture meccanicamente più resistenti che iniziano a formarsi quando la deposizione si sposta in uno

stato controllato dalla diffusione degli ioni di zinco. Le morfologie assunte da un anodo di zinco non si limitano a quelle descritte sopra, perché anche le fasi anodiche di dissoluzione influiscono fortemente sulla forma del deposito. La passivazione dell'anodo, per esempio, può causare irregolarità nella distribuzione di corrente che, a loro volta, danno luogo ad un deposito irregolare. Una ingegnerizzazione dell'anodo e dell'elettrolita è quindi necessaria per prevenire la passivazione, la corrosione e la formazione di strutture irregolari sull'anodo. Le soluzioni proposte sono: la strutturazione 3D dell'anodo, la formazione di interfacce che evitino il contatto del metallo con l'elettrolita, e l'aggiunta di specifici composti chimici (additivi) nell'elettrolita. Il lavoro sperimentale di questa tesi consiste nel testare l'efficacia di sei diversi sali quaternari d'ammonio (QAS): TBAB, CTAB, DMDTDAB, BDMPAC, BPPEI e PDADMAC, per contenere la variazione di forma dell'anodo. I QAS sono tensioattivi cationici comunemente usati come additivi per l'elettrodeposizione di rivestimenti protettivi in zinco. Sono state adoperate tecniche elettrochimiche (voltammetria ciclica, deposizione a corrente costante e ciclaggi galvanostatici) e di imaging (SEM, steromicroscopia, tomografia). Gli additivi sono stati utilizzati in una concentrazione pari a 0.1 g/l (ad eccezione del BPPEI, 0.01 g/l). Le voltammetrie hanno in generale evidenziato un effetto inibitorio degli additivi sulla reazione catodica, un effetto limitato sulla reazione anodica, e una più forte tendenza alla progressiva passivazione dell'elettrodo. Sebbene le voltammetrie abbiano permesso di evidenziare molti aspetti importanti del comportamento degli additivi, non possono fornire esplicitamente informazioni riguardo il loro effetto sulla morfologia del deposito. Questo è stato studiato tramite l'osservazione di depositi ottenuti con deposizioni galvanostatiche in un ampio range di correnti su un supporto di grafite. Tre additivi si sono rivelati particolarmente efficaci nella soppressione di strutture mossy (TBAB, PDADMAC, CTAB), garantendo un deposito compatto a basse densità di corrente (<20 $mA/cm^2$). Una volta accertato l'effetto benefico di questi additivi per deposizioni a bassa densità di corrente si è quindi testato il loro comportamento in ciclaggi sempre a basse densità di corrente (1 $mA/cm^2$), per verificane l'efficacia anche durante polarizzazioni anodiche. I test sono stati effettuati in celle simmetriche Zn-Zn a basse profondità di scarica (<1%). È stato osservato che il fallimento della cella senza additivo avviene per corto circuito poco dopo la passivazione della cella stessa, verosimilmente a causa di una disomogeneità della distribuzione di corrente causata da una imperfetta copertura dell'elettrodo con lo strato passivante. I test in presenza di additivo non hanno evidenziato differenze sostanziali nel comportamento del sistema, ad eccezione del PDADMAC, l'unico additivo che non ha portato al cortocircuito della cella. I campioni ciclati sono stati visualizzati al SEM. I depositi senza additivo hanno evidenziato nuclei sparsi ricoperti da ZnO formatosi per precipitazione. I depositi ottenuti in presenza di TBAB e PDADMAC sono risultati lisci, uniformi e con pochi ossidi precipitati. Gli altri additivi hanno presentato formazioni simili o più grandi del caso senza additivo. Per visualizzare nel dettaglio la progressiva trasformazione di forma dell'elettrodo, è stata progettata una cella simmetrica Zn-Zn per effettuarne una tomografia *in situ*. Questa era fabbricata in grafite, con geometria cilindrica, questa geometria comporta che sui due elettrodi vi siano due diverse densità di corrente con un rapporto proporzionale alle loro aree, pari a 2.5. Sono stati creati dei depositi di Zn sui due elettrodi in grafite e sono stati progettati dei trattamenti elettrochimici che permettessero una gestione ottimale del tempo-macchina: cicli galvanostatici a rispettivamente 12 e 30 $mA/cm^2$ con DOD inizialmente al 30% e in seguito al 60%. I test tomografici sono stati condotti sull'additivo risultato più promettente in base agli studi condotti in questa ricerca: TBAB, che ha presentato un eccellente effetto di limitazione della crescita instabile, peraltro comparabile a quello di PDADMAC, ma causando sovratensione catodiche notevolmente più basse. La

tomografia con TBAB è stata effettuata in modo comparativo rispetto al caso di controllo senza additivo. I risultati tomografici hanno confermato l'effetto benefico del TBAB sul lato a bassa densità di corrente, dove, al contrario del caso senza additivo, il deposito non ha presentato strutture mossy né ha subito un assottigliamento. Al contrario, sul lato a più alta densità di corrente l'effetto del TBAB è risultato dannoso; il deposito si è quasi totalmente distaccato dal substrato in grafite, causando il cortocircuito interno della cella. Gli effetti benefici di questo additivo a basse intensità di corrente sono stati provati, è stato però riscontrato anche un peggioramento delle prestazioni ad alte densità di corrente, associato al comportamento anodico dell'additivo. Questo potrebbe essere dovuto ad un adsorbimento non reversibile sulla superficie dello zinco, la cui passivazione è quindi favorita. L'ulteriore ricerca di additivi applicabili in un range di corrente più ampio deve quindi includere una analisi approfondita del loro comportamento sotto polarizzazione anodica.

Parole chiave: zinco, batterie, anodi, additivi, elettrochimica

.

# Abstract

The increasing demand of rechargeable batteries and the environmental and safety issues related to lithium batteries has driven research interest aimed at the developing of alternative technologies. Secondary batteries based on Zn could in principle solve the safety issues and offer an alternative to lithium. According to the properties of Zn, batteries with Zn metal anodes can be implemented with alkaline or mildly acidic electrolytes. The former is widely employed in primary batteries, the latter is receiving increasing attention for the development of secondary ones. Notwithstanding their appeal, major technological hurdles delay the development of secondary Zn batteries. The metallic Zn anode dissolves during discharge and is regenerated with the electrodeposition of Zn during discharge. The deposition of generally Zn does not produce regular and compact deposits: at low CDs, porous and mechanically weak deposits form, denominated "mossy". Shape changes and growth of irregular morphologies can lead to the loss of active material – with attending capacity loss - or, in the worst case, to the internal short circuit of the battery. Corrosion and passivation of the anode are other serious issues, which are expected to be strictly interconnected with the shape change, but the synergistic aspect of which received surprisingly little attention. The engineering of the anode and of the electrolyte are needed to obtain competitive performances. In this thesis six different quaternary ammonium salts (QAS) (TBAB, CTAB, DMDTDAB, BDMPAC, BPPEI, PDADMAC) have been investigated as electrolyte additives for the control of anode shape changes for 2M $ZnSO_4$ weakly-acidic electrolytes. Electrochemical (CV, galvanostatic deposition and cycling in coin-cell configuration) and imaging (SEM, stereomicroscopy, tomography) techniques were adopted for the purpose. Some aspects of the fundamental behavior of these additives were investigated through CV, which highlighted that these additives inhibit considerably the kinetics of the cathodic reaction and have limited instead effects on the anodic one, generally favouring passivation. Also, an increased tendency to passivation in presence of additives was observed, which was particularly strong for CTAB. The effect on the deposit morphology was investigated through the visualization of galvanostatic deposits obtained at different CDs on a graphite substrate. Three additives (TBAB, CTAB, PDADMAC) afforded the complete suppression of mossy structure formation. The evolution of the morphology after low CD (1 $mA/cm^2$) galvanostatic dissolution and deposition cycling was investigated in symmetrical Zn-Zn cells. The SEM inspection of the cycled samples evidenced that TBAB and PDADMAC yielded smooth and even morphologies. On the basis of the previous experiments, TBAB was selected as the single most promising additive, since it allowed the suppression of mossy Zn without an excessive inhibition of the deposition kinetics. The effect of this additive of the evolution of the anode morphology resulting from galvanostatic cycles, was studied more

in detail and dynamically by *in situ* tomography of a Zn-Zn symmetric cell at two representative CDs (12 and 30 mA/cm$^2$). TBAB showed beneficial capacity retention effects at low CD, but caused a serious degradation of the deposit at higher CD. This result was attributed to the anodic behavior of the additive, which brought about a more serious passivation of the deposit. The effectiveness in the shape control of the anode of TBAB at low CD was demonstrated and rationalized: of course, the further research for additives employable in a wider CD range is necessarily, specifically concentrating on the combined role of anodic and cathodic phase-formation processes.

Keywords: zinc; batteries; anodes; additives; electrochemistry

# Extended Abstract

The increasing demand of rechargeable batteries and the environmental and safety issues related to lithium batteries has driven research interest aimed at the developing of alternative technologies. Secondary batteries based on Zn could in principle solve the safety issues and offer an alternative to lithium, Zn is indeed more abundant and better geopolitically distributed than Li. Zn primary batteries have been a common technology since the second half of the 19th century and are still widely produced and commercialized. Some research in the development of a secondary battery with a metallic Zn anode has been done starting since the 60s, this subject however has gained interest only in the last 5 years. There are two main concepts of secondary batteries based on Zn: the rechargeable zinc air battery (ZAB), a battery which adopts atmospheric oxygen reduction as the cathode reaction and the zinc ion battery (ZIB) a battery which employs an intercalation cathode similar to that used in lithium batteries. ZIBs have potentially many advantages. With metallic Zn anodes it is possible to employ an aqueous electrolyte, which is cheaper and not flammable. The manufacturing of such batteries is also simpler and cheaper, since they can be assembled in air atmosphere. The commercialization of secondary Zn batteries must although face major technological challenges. The development of a performing intercalation anode is the main obstacle. This is due to the bivalent nature of the Zn ion, which intercalates less easily than monovalent lithium due to stronger electrostatic interactions. Most of the studies focus on MnO2 based cathodes, but a wide variety of different chemistries have been tested. This thesis focuses on the metallic Zn anode for secondary batteries, which also suffers major drawbacks which still need to be overcame. The typical problems of a primary Zn anode are corrosion, which causes a capacity loss, and passivation, which insulates the anode increasing battery internal resistance: these are traditionally solved by alloying Zn with other metals, but this is not a viable solution for secondary anodes. In a secondary metallic anode indeed, the metal dissolves in the electrolyte during discharge and deposits back onto the residual metallic portion during charge. This process however is not reversible, and the morphology evolves into tridimensional and dendritic structures, favouring the detachment of metallic Zn particles (loss of capacity), and, in the worst case, the perforation of the separator and internal short circuit of the battery.

The first part of this thesis is dedicated to the analysis of the literature on the electrochemistry of Zn with regard to the ZIB application. The state of the art of this technology will be also described with a particular focus on the engineering of the anode through the addition of additives. in the experimental part some QAS will be tested as electrolyte additive through

electrochemical (cyclic voltammetry, galvanostatic deposition and cycling) and imaging (SEM, stereomicroscopy, tomography) techniques.

Zn is an amphoteric metal: in aqueous solutions it dissolves into soluble species in both acidic/mildly acidic solutions and concentrated alkaline solutions, while its oxidation in intermediate pH windows yields insoluble oxidation products. There are indeed two main classes of batteries employing a Zn metal anode, with alkaline or mildly acidic electrolyte. Most of the literature available concerns the more traditional alkaline battery, recently however, mildly acidic electrolytes are gaining attention due to the lower tendency to develop dendritic structures. The chemistry of Zn in the two electrolytes is different, but it is possible to find some communalities. In alkaline environment the Zn ion is complexed with four hydroxyl groups and hosts a double negative charge, while in mildly acidic the Zn is solvated by water molecules and hosts a double positive charge. In alkaline environment the dissolution reaction causes a local acidification close to the anode that shifts the solution in a pH condition in which the formation of oxides is possible, this causes the passivation of the anode. In mildly acidic environments the dissolution reaction does not affect the pH. However, hydrogen evolution happening spontaneously on the anode, especially during cathodic polarization, causes a local alkalinization which also favours the formation of insoluble passivating oxides. The passivating layer on Zn seems to have a double nature in both the environments, a first porous layer is formed by the precipitation of oxides, driven by the aforementioned pH modifications. A second, thinner, and passivating ZnO layer is then formed through electrochemical oxidation of metallic Zn. The morphologies of electrodeposited Zn are also similar in both the environments: in alkaline ambient the conditions for the formation of such deposits are well documented, while there is a lack of specific literature on the characterization of the electrodeposit morphologies in mildly acidic solutions. In both environments, as CD increases the deposits appears subsequently mossy, compact, and dendritic. Mossy Zn is a porous structure, it is not mechanically resistant, and it easily detaches from the electrode, it generally starts forming below 15 mA/cm2, it grows under activation control and is hardly influenced by diffusion, Compact structures are the desired morphology for battery anodes, they are smooth and mechanically resistant. Dendrites start forming at higher current densities, the growth of dendrites is triggered by the switch to a diffusion-controlled deposition, their formation is indeed influenced by the concentration and stirring of the electrolyte. The evolution of the morphology after anodic and cathodic polarization cycling is however more complex than in pure electrodeposition experiments. Passivation and corrosion of Zn, as well as the deposition of tridimensional structures, are all interconnected and mutually enhancing processes. In fact, the corrosion in mildly acidic environment alkalinizes the solution, which favours passivation, an irregular passivation causes CD localization which, in turn, favours the growth of dendrites. Accurate engineering of the electrolyte and/or of the Zn anode is necessary to ensure an acceptable lifetime of the battery. Solutions include: 3D structured anodes supported by graphite or copper meshes, artificial interfaces which avoid the water-electrode contact, the

modification of the electrolyte composition with the addition of specific additive molecules. Additives are traditionally employed in the electrodeposition of Zn coatings to obtain a uniform, smooth deposit. The effect of these additives in different deposition conditions and the effect of different additives combined is poorly predictable. Their working mechanisms are manifold and hard to determine, in most of the cases these additives cause an inhibition of the deposition reaction. It is possible that the additive molecules are preferentially adsorbed on the tips of the deposits, inhibiting there the reaction through the occupation of favoured growth sites or through the electrostatic repulsion of incoming metal ions, the inhibition on the tip favours the deposition on the rest of the surface, creating an even deposit. Additives may also increase the nucleation rate, refining grain size, or impede the surface diffusion of the adatoms, hindering the formation of macrosteps and eventually projecting features. The action of the additive impact the metal ion chemistry, resulting in a variety of electrokinetic and mass-transport effects. In this thesis some additives have been tested with the aim to achieve a reversible dissolution and deposition of the Zn anode. Specifically, I concentrated on quaternary ammonium salts (QAS) a common class of cationic surfactants. The QA cation bears a positively charged nitrogen site, bonded to four organic groups, different organic functionalities give different properties to the QAS. Some QASs have also been tested as additives for the corrosion inhibition of steel and Zn, this is apparently a promising feature of this class of molecules, anyhow many times corrosion inhibitors act by favouring passivation or by suppressing the anodic reaction, which is not desirable in battery applications. Six QASs have been tested: TBAB, CTAB, DMDTDAB, which are QASs with aliphatic chains of different length, BDMPAC, a QAS with aromatic functionalities, BPPEI and PDADMAC, two polymeric QASs.

The experimental work of this thesis aimed to attain a better fundamental knowledge of Zn behaviour and morphology evolution in 2M $ZnSO_4$ electrolyte and to test the abovementioned QASs with regard to the reversible operation of secondary Zn anodes. The investigation was performed through different electrochemical and imaging techniques:

At first, CVs with three electrodes configuration were performed. Employing an Ag/AgCl reference electrode, two Pt CEs, and a glassy carbon WE. The electrolyte was 0.5M $NaSO_4$ + 0.01 M $ZnSO_4$, a low concentration of Zn ions in the electrolyte was adopted to appreciate mass transport limitation effects. CV electroanalytics can be effective only with concentrations of the electroactive species that are lower than those employed in batteries, and addition of conductivity salts is needed, nevertheless rich and relevant electrodic information can be obtained by this approach, that enables a rational screening of electrolyte chemistries. The solution was degassed with nitrogen to exclude the effect of dissolved oxygen. 0.1 g/l of QAS (0.01 g/l in the case of BPPEI) were added to the electrolyte. The CVs parameters were 10 cycles at 25 mV/s over a wide voltage range (from -1.6V v. ref CTV to -0.5 v. ref ATV), including both anodic and cathodic polarization. To study the effect

of HER on progressive cycling some similar CVs were performed with 500 cycles and -1.4V v. ref CTV.

The quality of the deposits could be appreciated through the imaging analysis of galvanostatic electrodeposits. These were performed with a current controlled power supply (2 electrodes configuration) in a small cylindrical cell, adopting a graphite rod as WE and Zn tube as CE, to keep the concentration of Zn constant during the deposition. The electrolyte was 2M ZnSO4 with the same amount of additive as in CV tests. Electrodepositions were performed at 10, 20, 50 and 200 mA/cm2, that encompass a range of mild to aggressive ZIB working conditions. The influence of Mn2+ on the electrodeposit morphology was also tested with this experiment. It is common practice to add 0.1M MnSO4 in the electrolyte to contain the dissolution of MnO2 based cathodes. Mn2+ ions could however affect the behaviour of the anode but no studies on these issues are available so far. The deposits without additive, with MnSO4, and TBAB were observed with a stereomicroscope at 5, 20, 40X magnifications.

The electrochemical behaviour of TBAB and PDADMAC was further investigated with the monitoring of the electrode voltage during galvanostatic deposition and dissolution. The experimental set-up consisted in a rectangular open cell with two vertical Zn plates, adopted as counter and WE, 2M ZnSO4 with the usual amounts of additives, was employed as electrolyte. the voltage was measured through an Ag/AgCl reference electrode, placed as close as possible to the Zn WE.

The study of the evolution of a ZIB anode morphology cannot be limited to the examination of the electrodeposits but must consider the effects of anodic polarization and cycling. Symmetrical Zn-Zn split cells were assembled for the purpose. The electrolyte, 2M ZnSO4 with and without the presence of additives in the usual amounts, was pipetted between the Zn plates. No separator was employed in order to allow the collection of samples for SEM inspection. The cells were cycled for half an hour at +/- 1mA/cm2 (<1% DOD), a low value of CD, which was chosen to investigate the effectiveness of the additives in the suppression of mossy structures.

To visualize the evolution of the deposit morphology with cycling, a cell suitable for an in situ tomography was designed. My work consisted in the testing and calibration of this cell with electrochemical techniques, in order to find its defects and suggest improvements. The testing also required to find an electrochemical cycling treatment which suited in the small times available for this measure and which had to be representative of a ZIB working condition. The cell was made of graphite; this material is an electrical conductor, is chemically inert and it is transparent to X-rays. It was designed with a cylindrical symmetry, which is optimal for this measurement. The first electrode, a graphite rod (diameter, 2mm, length 20 mm), was placed coaxially to the second electrode; a graphite tube (inner diameter

5mm, length 20 mm): these were supported by a Cu base, equipped with appropriate insulations and an insulating cap, that also acted as a spacer. The geometry of this cell is such that the CD on the inner rod is 2.5 times higher than that on the outer wall: this arrangement allowed to test simultaneously two different CD conditions in a single cycling experiment. 0.3 ml of electrolyte (2M ZnSO4 with and without additives) were inserted into the cavity between the rod and the graphite tube. The first task was to grow a uniform and appropriately thick Zn electrodeposit on both the inner rod and the outer wall. The formation of this layer on the inner rod was made extracting the rod from the cell, and depositing Zn at 100 mA/cm2 in a set-up similar to the second experiment (deposition on graphite) for 2400s. To obtain a compact deposit on the outer wall, ca. 40 mA/cm2 were required to simultaneously avoid anode passivation and cathode outgrowth. In fact, the ratio of the areas the current on the CE is around 2.5, in this high CD condition the CE passivates, and, after a prolonged deposition, it breaks. For optimal use of the beamtime to test systems without and with added TBAB, three slots of three hours were available for the electrochemical treatments of the cell for either case. The electrochemical conditions selected as most representative consisted in two series of two cycles of 2000s at +/- 60 mA (30 mA/cm2 in the inner rod and 12 mA/cm2 on the outer wall, 30% DOD), followed by a single cycle; 4000 s with the same CD (60% DOD).

The results collected with these experiments allowed to select and characterize the most performing additives among those tested, the evaluation considered the deposit levelling capacity, the grade of inhibition of cathodic reaction and the passivation tendency in presence of the additive.

CVs without additives showed that CTV increments brings about a progressive decrease of the cathodic currents, denoting that the tendency to passivation is favoured by parasitic hydrogen evolution at high cathodic polarization. The influence of the additives always brings about an inhibition of the cathodic currents and a stronger progressive reduction of CD as cycling proceeds. These effects were associated to a kinetic inhibition of the cathodic reaction and to a stronger and faster build-up of a passivating layer with cycling. CTAB was by far the most inhibiting additive. DMDTDAB, on the other hand, presented almost no deviation from the control case, this is unexpected because its chemical structure is similar to that of CTAB. This phenomenon was associated with the low solubility of DMDTDAB, which in solution is present mainly in the micellar form. PDADMAC presented a quite strong kinetic inhibition, BPPEI a strong progressive inhibition, probably due to the formation of a ionomeric film. TBAB and BDMPAC have a relatively lower influence on the cathodic currents.

The CVs provided information on electrokinetic aspects of the additive fundamental behaviour with only indirect insight into the deposit morphology. The galvanostatic

electrodeposition on graphite rods is an appropriate method to appreciate the deposit morphology at different CDs. In the case without additives, at 10 mA/cm2 the deposit was predominantly mossy, while at 1 mA/cm2 loose and incoherent mossy structures form. At 20 mA/cm2 mossy structures grew on a previously formed compact layer, these results are in accord with the literature on alkaline environments. Between 30 and 100 mA/cm2 deposits ate compact and even, some sparse dendrites appeared after 100 mA/cm2, above 150 mA/cm2 the surface was fully covered with dendrites. In alkaline electrolytes, dendrites grow starting from 30 mA/cm2, instead, in mildly acidic environment their growth starts at higher CD. At low CD MnSO4 resulted to have a minor influence on the deposit, however, it might increase the CD limit below which mossy Zn can form. It also manifested an effect on the shape of the high CD dendrites, this is due presumably due to the codeposition of Mn metal in these conditions. Depositions in the presence of additives showed that DMDTDAB has no influence on the deposit morphology, in keeping with CV results. BPPEI has a minor influence and cannot suppress mossy Zn formation, this is probably due to the lower concentration adopted for this additive. BDMPAC attained only a partial suppression of these structures. TBAB, CTAB and PDADMAC on the one had can totally suppress the formation of mossy Zn in the low-CD range, while, on the other hand, in the higher-CD range, these three additives give rise to morphologies that are more irregular than those obtained without additives. This phenomenon might be associated with mass-transport effects, in particular to convective flows developing in the free electrolyte. Since additives are present in a small concentration, mass transport could be important for their diffusion to the electrode, the reaction in zones with increased mass transport might result more inhibited by the additive than stagnant ones. This experiment and CV highlighted there is not a direct correlation between cathodic kinetics inhibition and effect on the deposit morphology. Complementary GS and CV experiments point out that a correlation between cathodic kinetics and deposit morphology cannot be straightforwardly established and more experimental information is required in order to appreciate their synergy.

Once evidenced the positive effect on the deposit of these additives at low CD, the evolution of Zn morphologies after low CD galvanostatic cycling were studied in a symmetrical Zn-Zn cell. In the absence of additives, the cell typically fails by short circuit, soon after a potential buildup associated with passivation: the slow alkalinization of the electrolyte due to parasitic cathodic HER presumably favours passivation. Passive layer failure associated with the rise of potential, gives rise to fluctuating voltage profiles and spikes. Defects of the passive layer led to high-CD spots that can trigger metal outgrowth, ultimately evolving into short circuits. All the other additives presented a similar failure mechanism, with the exception of PDADMAC which exhibited a different passivation behaviour, not associated with the formation of short circuits. Notwithstanding similarities in the electrochemical cell behaviour, the SEM micrography unveiled notable differences among the morphologies associated with the individual additives. The sample without additives showed large nuclei of freshly electrodeposited Zn above the corroded metal foil. These nuclei were covered with

precipitated ZnO crystals. BPPEI showed small differences from the case without additives. DMDTDAB, which exhibited almost no differences in electrochemical behaviour with respect to the case without additives, presented instead large tridimensional structures than were not found in the additive-free case. CTAB yielded large tridimensional crystallites. Use of BDMPAC, instead, was associated with a uniform oxide layer. TBAB and, in particular, PDADMAC yielded smooth and even morphologies, with small amounts of precipitated oxides, evidencing their beneficial effect at low CD cycling. On the basis of the previous experiments, TBAB was selected as the single most promising additive, since it allowed the suppression of mossy Zn without an excessive inhibition of the deposition kinetics.

A detailed visualization of the deposit shape evolution in the electroyte without additive and in the presence of TBAB was possible with *in situ* tomography at representative stages of cell cycling. The results showed that the morphology of the cell that was cycled without additives, was smooth and even on the inner rod, and less regular on the outer wall. The evolution of the inner deposit after the first two cycling periods highlighted a progressive coarsening of the deposit, with localized formation of a crust above the previously deposited layer, leaving a cavity between the material grown in the two subsequent steps. After the last cycle at higher DOD, the deposit was visibly thinner and the whole surface was covered in some tridimensional structures, attached to the cathode via a thin filament. The outer surface also went through stages of progressive thinning, and the evolution of mossy structures on the surface was clearly visible, as was expected at the prevailing CD. In the presence of the additive, after the first cycle the roughness and the porosity of the deposit increased. It was also possible to notice the formation of cavities, similarly to what happened after the second cycle in the deposit without additive. During the second cycle the inner rod showed passivation signs, after which the deposit appeared profoundly modified: some areas of the graphite substrate were exposed, and structures with a thin base were present. After the last, higher-DOD cycle, the deposit on the internal rod underwent major changes: a large portion of deposit on the inner rod detached from the electrode and the resulting Zn particles accumulated in the electrolyte causing a temporary short circuit. Differently from the inner rod, the pristine deposit in the outer wall of the TBAB cell was similar to that in the cell without additive. This allowed a much better comparison of the deposit evolution al low CD. After cycling no sign of mossy Zn formations was observable, the deposit presented a modified morphology, which appeared slightly less rough than the starting substrate, the thinning of the deposit was not clearly appreciable. This experiment gave a further confirmation on the beneficial effect of this additive on the deposit morphology evolution at low CD, at high CD however the effect is detrimental, this was associated to the anodic behaviour.

The effectiveness in the shape control of the anode of TBAB at low CD was demonstrated and rationalized: of course, further research for that can be effective in a wider CD range is

necessarily, specifically concentrating on the combined role of anodic and cathodic phase-formation processes.

# List of contents

# List of figures

# Chapter 1
# Introduction

The electrification of the mobility sector and the necessity to store electrical energy from renewable sources have increased the global demand for rechargeable batteries. However, there are many drawbacks of the technologies currently adopted for these scopes. Lithium ions batteries are now the standard technology in use on electric vehicles, due to their impressive performances in terms of low weight and high power density. The cost of Li-ion batteries is although high, due to the complex manufacturing process and the expensive materials. There are serious concerns about the long-term availability, the geo-political distribution, and the impact on the environment related to Lithium and Cobalt. Li-ion batteries also have major safety problems, due to the flammability of the organic electrolyte. The other main type of accumulators on the market is the lead-acid battery, a solid and simple technology, but suitable only for stationary applications due to the high weight, and with many concerns about the toxicity of lead. A secondary battery based on Zn would have many advantages and could solve the above-mentioned critical issues. Zn metal is slightly more abundant than lithium, but, most importantly, it is more evenly geo-politically distributed and has a broad range of low-cost widespread and consolidated applications. It is non-toxic, and it is possible to produce batteries with an aqueous electrolyte, which makes them intrinsically safer and environmentally friendly. Zn is a material adopted for battery anodes since the invention of the battery itself (section 1.3), anyway the development of a rechargeable device based on Zn must face many technological challenges, which have impeded the commercialization of Zn-based rechargeable batteries to this days. Today there are two main device concepts for the rechargeable Zn battery; the Zn-air secondary battery and the Zn-ion battery, the latter is going to be the subject of this thesis. The main obstacle to the production of Zn-ion batteries is the synthesis of a performing intercalation cathode, but the Zn metal anode[1] also presents many problematics which can led to a rapid performance drop or battery failure. In a metallic negative electrode, the metal dissolves during discharge and deposits during charge. this process however is far from reversible, the morphology of the metal changes, causing the detachment and loss of active material, or, in the worst case, the perforation of the separator and internal short-circuit of the battery.

[1] In the following thesis the author will refer to the negative electrode as “anode”, and to the positive electrode as “cathode”. this terminology might be questionable when referring to rechargeable batteries but it is commonplace in the specific literature.

Passivation and corrosion of the Zn anode are also serious problems. The literature relevant for this topic was examined in detail. Many studies on the fundamental behaviour of Zn during electrodeposition and corrosion were made in the second half of the 19th century, driven by the interest on Zn primary batteries, Zn electrowinning, Zn electro-deposited coatings, and Zn corrosion resistance. In recent times, many studies were made concerning secondary battery application, these generally focus on the engineering and performances of materials. No fundamental studies were found on the behaviour of Zn under the alternation of anodic and cathodic polarization conditions: it is extremely complicated to describe and model univocally this process due to the wide range of parameters involved. The work of the following thesis consisted in the observation of Zn morphology evolution with and without the presence of organic additives (quaternary ammonium salts), traditionally employed in the formation of electrodeposited coatings. This was done through electrochemical measurements and imaging techniques. The aim of the study is to investigate the fundamental electrochemical behaviour of Zn in near-neutral aqueous electrolytes, that the system of choice in ZIB research and are starting to be considered also for Zn-air battery technologies. I have deepened the working mechanism of the additives tested, providing factual information about the application of additives for the reversible operation of a Zn anode.

## 1.1 Zinc aqueous chemistry

### 1.1.1 Zinc element and basic zinc electrochemistry

Zinc is the 30th element in the periodic table and has a molecular weight of 65.39 g/mol, in its metallic form it has a hexagonal close packed (hcp) crystalline structure, some features of Zn crystalline lattice are shown in figure (1), along with the Miller indexes convention adopted later. A density of 7,14 g/cm$^3$ and a melting point of 419°C. In figure (2) is presented a zinc Pourbaix diagram: this diagram shows the thermodynamically stable species of Zn in aqueous solutions at different pH and potential conditions. It must be noted that this does not account for the participation of other species in solution different from Zn, water and their reaction products.

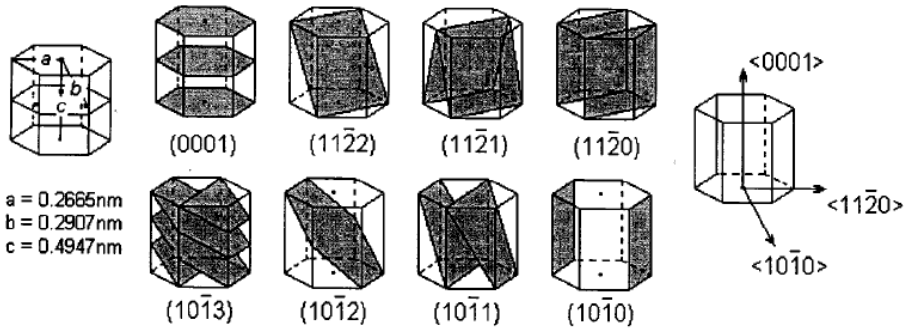


Figure 1 - Zn crystallyne structures and Miller indexes [3].

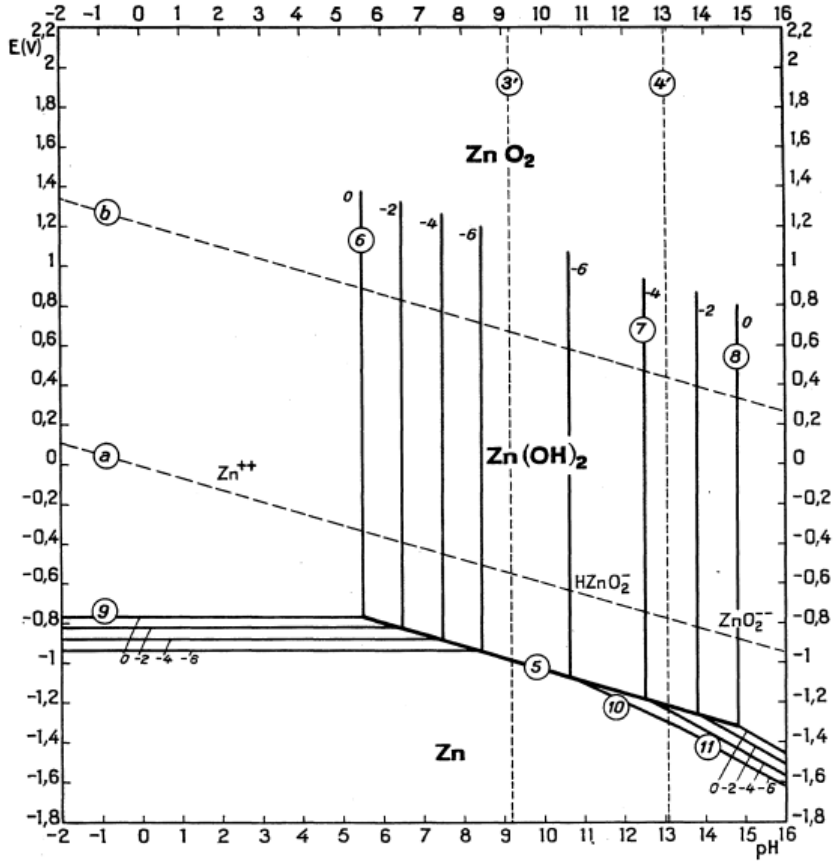


Figure 2 - Zn Pourbaix diagram [1].

(for example Zn salts anions such as $Cl^-$, $SO_4^{--}$, $CO_3^{--}$) which can form other compounds with Zn. Zn is an amphoteric metal, which means that there are soluble oxidation products in both mildly acidic[2] and strongly alkaline pH, indeed there is a pH window in which Zn metal oxidation reaction produces an insoluble oxide. The electrochemical dissolution and deposition of zinc are most conveniently carried out in these conditions. The electrochemical reactions of Zn are different under many aspects if they happen in alkaline or acidic environment. Beyond thermochemical computations, in practice, the chemistry of Zn is complex and unpredictable, the multitude of different crystalline faces all present on the surface, oxides layers of different nature which form as soon as the metal enters in contact with an aqueous solution, and the high sensitivity to impurities, are all parameters which make it hard to control and reproduce the experiments with this metal.

[2] The direct dissolution of Zn in $Zn^{++}$ (reaction (1)) is possible below a certain pH, batteries adopting $ZnSO_4$ electrolytes work at pH around 5, this condition are referred in literature as: mildly acidic, weakly acidic or almost neutral. In this thesis mildly acidic is going to be the adopted terminology.

### 1.1.2 Zinc dissolution and corrosion

The dissolution reaction of Zn happens differently in acidic and alkaline electrolytes.

In acidic solutions Zn dissolves according to the reaction:

$$Zn \rightarrow Zn^{2+} + 2e^- \qquad E° = -0.76\ V\ v\ SHE \tag{1}$$

The Zn++ cation in aqueous solution is solvated by six molecules of water to form a regular octahedral structure $[Zn(H_2O)_6]^{++}$.

In strongly alkaline solution the Zn ion carries a double negative charge and is called zincate ion $ZnO_2^{2-}$ which in aqueous solution is bonded to four hydroxyl groups to form a tetrahydroxozincate (or simply "zincate") ion $[Zn(OH)_4]^{--}$. The dissolution reaction in alkaline environment is the following:

$$Zn + 4OH^- \rightarrow (Zn(OH)_4)^{2-} + 2e^- \qquad E° = -1.2\ V\ vs\ SHE \tag{2}$$

The alkaline reaction has a lower standard redox potential than the slightly acidic one, (notice that the equilibrium potential in alkaline ambient, of course, is a function of pH). It is important to notice that the dissolution process in acidic environment has no effect on pH, while in alkaline environment it acidifies the solution because of the removal four OH- ions. The pH of the bulk electrolyte is not changed by this reaction, because at the cathode, considering 100% cathodic efficiency, the zincate anode is going to lose its hydroxyl groups, but the pH is going to be modified locally in the vicinity of the anode, later it will be shown that this has consequences of major importance.

The dissolution reaction mechanism and kinetics in mildly acidic Zn salt electrolytes is influenced by the concentration and nature of the anion. The reaction mechanism involves a two-step reaction which, like in the deposition reaction, involves a monovalent $Zn^+$ adsorbed species [14]:

$$Zn \rightarrow Zn^+ + e^- \tag{3}$$

$$Zn^+ \rightarrow Zn^{2+} + e^- \tag{4}$$

Even though the low nobility of Zn should in theory favour a fast corrosion, the low kinetics of HER on Zn and the formation of protective passive films often determines a slow corrosion rate.

HER exchange CD on Zn in aqueous solutions are between 10-9 and 10-8 mA/cm$^2$ [54] depending on the electrolyte and on the presence of impurities/alloying elements in the metallic Zn, the corrosion reaction is mainly under the cathodic reaction control.

Corrosion of Zn has been studied widely in aerated environments, mainly to evaluate the protection of Zn coatings. The corrosion conditions inside a battery are really different and corrosion information cannot be transferred straightforwardly to batteries; the battery electrolyte is not aerated and there is a high concentration of $Zn^{2+}$ ions. The corrosion rate of a metallic Zn anode depends on many different parameters and is hardly predictable, it is generally low because of the formation of passive films, although this is not desirable in batteries applications. Corrosion of Zn is often not uniform and under many conditions it forms pits [54].

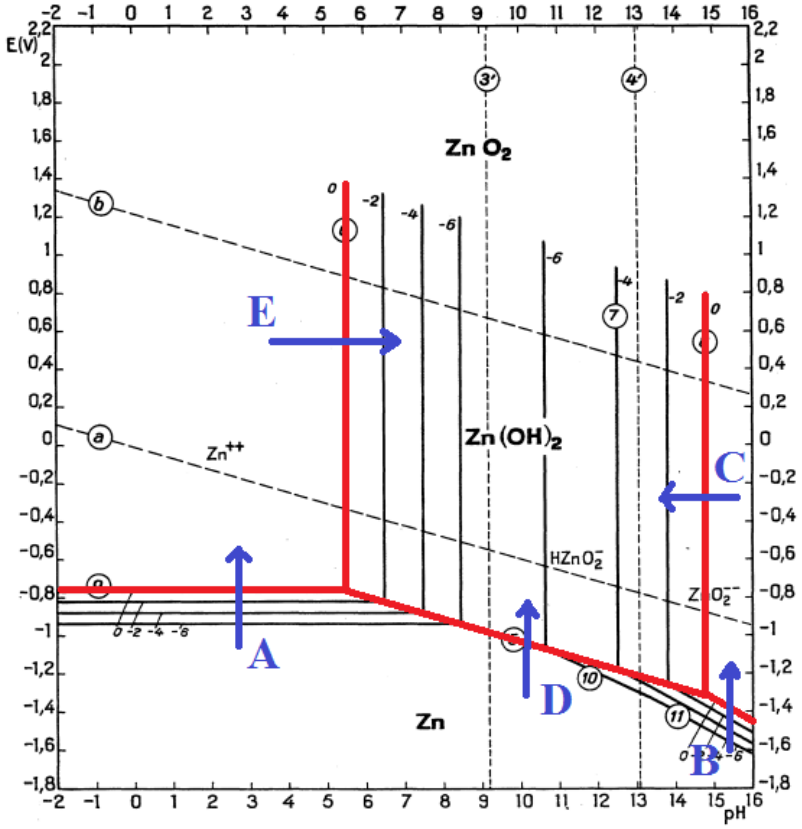


Figure 3 - Zn electrochemical reactions represented on the Pourbaix diagram. a) acidic dissolution, b) alkaline dissolution, c) alkaline oxide precipitation, d) electrochemical oxide formation e) acidic oxide precipitation.

### 1.1.3 Oxide formation and passivation of metallic zinc

The formation of insoluble products on zinc anodes is a key problem in the development of long-lifed anodes, they insulate the anode and limit ions transport. The characteristics of passivation layers on Zn are manifold in terms of composition and microstructure, depending on many factors such as polarization of the anode, pH, and electrolyte composition. The term "passive layer" is generally adopted for a non-porous layer that perfectly insulates the electrode and provides an almost perfect protection from corrosion. Zn typically in not prone to the formation of such protective layers, but even the formation of a partially insulating

layer is detrimental for batteries: it is common to refer to this layer as a "passivation layer" anyhow. The characteristics and the mechanism of formation of these passivation layers are different in acidic and alkaline environments.

Many studies [10, 11] were made on zinc passivation in alkaline battery electrolyte, the passive layer is composed of ZnO and γ-ZnOH or ε-ZnOH[3] (two different crystalline structures of ZnOH), zinc hydroxide however is present in minor amounts, and as the pH rises the composition becomes 100% zinc oxide. This oxide layer may have a duplex nature: it is composed by a first, thicker, porous layer (type I oxide) that hinders mass transport, but does not provide an effective insulation of the electrode, and a second thinner and denser film (type II oxide) more adherent to the surface, which is the actual the cause of passivation. The reaction mechanism is still not perfectly known, but, according to the "dissolution-precipitation" model, the first layer is believed to form when an excess of zincate ions, produced from the alkaline dissolution of zinc (2), locally decreases pH, increases Zn ion concentration in solution, and causes the precipitation of ZnO, according to the reaction:

$$Zn(OH)4^{2-} \rightarrow \ ZnO \ + \ 2OH^{-} \ + \ H_2O \qquad (5)$$

The first layer is indeed not present in convective environments. Notice that this is a chemical reaction, and does not involve electron exchange, so is not detectable by any electrical measurements.

Then, an oxidation of the metallic zinc take place at higher potential:

$$Zn \ + \ 2OH^{2-} \rightarrow \ ZnO \ + H_2O \ + \ 2e^{-} \qquad (6)$$

This is instead an electrochemical reaction and can be measured electrically. This oxidation reaction is favoured against alkaline dissolution by a local reduction of pH caused by the zincate formation (2) and enhanced by the fact that the oxide layer at the anode hinders the diffusion of OH- from the bulk electrolyte. It is worth noting that ZnO is a white solid and the inner layer appears black or gray, due to the presence of an excess of zinc in the oxide (non-stoichiometric type II ZnO).

Literature does not provide an exhaustive study of oxides formation mechanism in slightly acidic environments, studies were made only in aerated condition without Zn ions in solution, which is a condition radically different from that found in a ZIB [12,13].

[3] There is a dehydration equilibrium between the solid precipitates ZnO and $Zn(OH)_2$: in mildly acidic conditions the fraction of the latter was found to be higher than in alkaline, anyway the ZnO fraction is always preponderant [55], in this thesis ZnO will be assumed to be the only specie in the unsoluble precipitates

Passive layers in mildly acidic environments have a double nature like in alkaline environment [14] figure (4), there is an outer, thicker, porous layer formed by the reaction:

$$Zn^{2+} + 2H_2O \rightarrow ZnO + 2H^+ \quad (7)$$

that has the following equilibrium condition:

$$Log([Zn^{2+}]) = 10{,}96 - 2pH \quad (8)$$

From which we can calculate the pH of a $ZnSO_4$ solution (for 2M $ZnSO_4$ pH=5.3, also confirmed by [9]). An acidification of the solution will lead to the dissolution of ZnO, and any alkalinization will lead to ZnO precipitation. Indeed, at any $Zn^{++}$ concentration a local alkalinization brougth about by HER happening on the electrode during cathodic polarization, can cause the precipitation of oxides.

Eventually, depending on the anions present in solution, some insoluble complexes or compounds might also form with precipitation reactions, this is reported to happen in chlorides, carbonates and sulphates. In the sulphate case, the following reaction can happen:

$$4Zn^{++} + 6OH^- + SO_4^- + 5H_2O \rightarrow Zn_4(OH)_6(SO_4) * 5H_2O \quad (9)$$

Which is the formation reaction of Zinc hydroxide sulphate (ZHS), a compound detected by FTIR [16], XRD [25] and raman spettroscopy [14] on Zn electrodes in contact with sulphate-containing electrolytes.

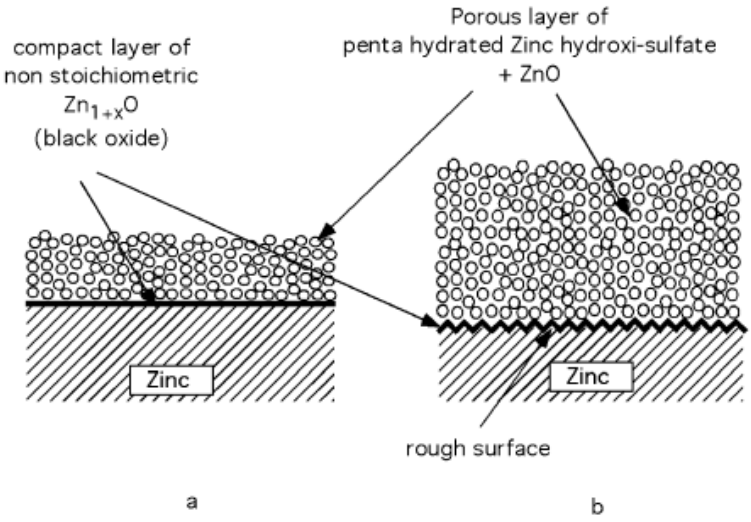


Figure 4 - Double nature of Zn passivation layer. during a) moderate corrsion b) strong corrosion conditions [14].

Notice that these are chemical precipitation reactions caused by the alkalinization and/or by the local oversaturation of Zn basic salts, hence not directly depending on electrode polarization. These reactions are favoured by a high $Zn^{++}$ concentration (such as is found

close to ZIB anode during discharge) and by a low pH (brought about by HER-induced alkalinization during charge). It is thus worth noting that, in principle, indeed, in a battery it is possible to expect the precipitation of such compounds not only during discharge but also during charge.

Electrochemical formation of ZnO in near-neutral ambient can indeed lead to some degree of passivation though the reaction:

$$Zn + 2H_2O \rightarrow (II)ZnO + 2H^+ + 2e^- \quad (10)$$

II-ZnO here, as in the alkaline case, is the non-stoichiometric "black" type II ZnO responsible for anode passivation. In mildly acidic environment it has a lower passivating effect and is generally not able to totally stop the dissolution of Zn.

It is worth noting that the origin of pH modification, which causes oxides formation, is different in alkaline and mildly acidic environments. In the former it is the normal anodic dissolution reaction, so acidification happens simultaneously to anodic polarization and is unavoidable, while in the latter it is HER, that happens under cathodic polarization and is proportional to the rate of a parasitic cathodic reaction, that can hardly be totally suppressed.

### 1.1.4 Zinc electrodeposition and electrodeposit morphologies

In order to create a metal deposit, the metal ion (which is normally hydrated or solvated) must move from the electrolyte to the electrode surface, driven by: electric field, concentration gradient, and/or convection. Once it reaches the electrode interface, the metal atom separates from its solvation shell or its hydroxyl complexing groups and it is adsorbed on the metal surface. The adsorbed atom (adatom) eventually diffuses on the metal surface and is incorporated in the metal crystalline lattice. The preferential sites in which adatoms are stably incorporated in the crystalline structure are the ones that minimize surface energy, where the atom is surrounded by the higher number of atoms of the crystalline structure such as kink or step positions figure (5). If after a mean residence time the adatom is not able to diffuse trough the surface to one of these sites, it desorbs from the electrode. The subsequent deposition of atoms at a kink position is referred to as 1D growth, and the deposition on step sites (that lead to a new kink position formation) as 2D growth, together 1D and 2D growths generate the "lateral" (or horizontal) growth of a new crystalline layer, while the deposition of atoms in a new layer is called 3D or vertical (normal) growth. Vertical growth is thermodynamically unfavourable with respect to lateral growth, since it requires higher energies and hence higher overpotentials.

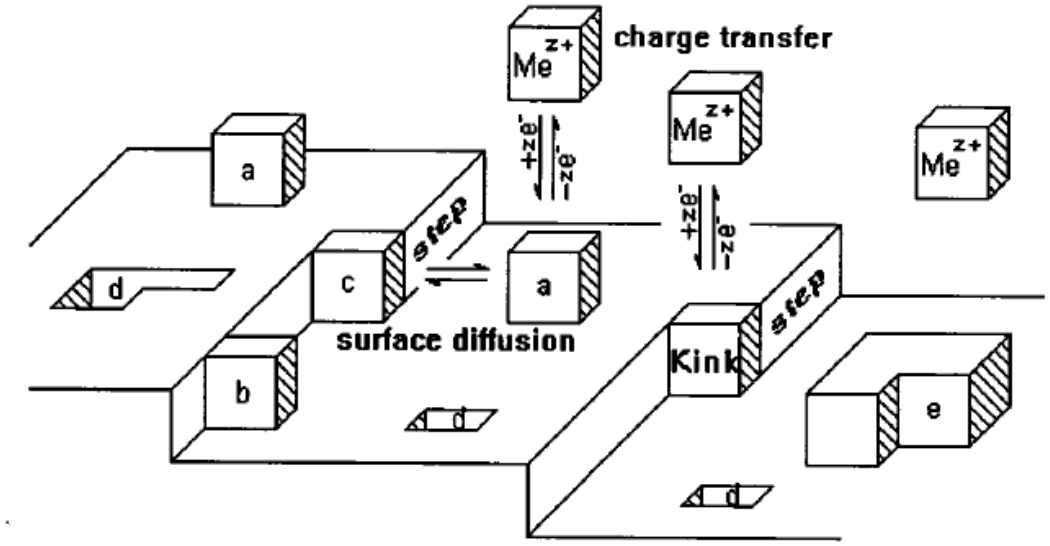


Figure 5 - Metal electrodeposition mechanism. a) adsorbed atom, b) atom in step position, c) atom in kink position [7].

In the case of zinc, according to the model in [2], developed mainly on the basis of EIS evidence, the adsorbed species able to diffuse through the surface is assumed to be a monovalent zinc cation ($Zn^{+}_{ad}$) which can be formed by the reductive adsorption of $Zn^{++}$ (11) or by the autocatalytic process (12).

$$Zn^{2+} + e^{-} \rightarrow Zn^{+}_{ads} \quad (11)$$

$$Zn^{2+} + Zn^{+}_{ads} + e^{-} \rightarrow 2\,Zn^{+}_{ads} \quad (12)$$

This latter reaction seems to be crucial for the overall reaction kinetics and for the final morphology of the Zn deposit. The 1D growth on kink sites (Zn*) proceeds by surface diffusion and incorporation of $Zn^{+}_{ad}$ (13) or by direct deposition of $Zn^{++}$ on kink sites (14).

$$Zn^{+}_{ads} + Zn^{*} + e^{-} \rightarrow Zn + Zn^{*} \quad (13)$$

$$Zn^{2+} + Zn^{*} + 2\,e^{-} \rightarrow Zn + Zn^{*} \quad (14)$$

The electrodeposition of Zinc always happens in the HER range, indeed the effect of $H_{ads}$ species is of fundamental importance for the deposition kinetics and for the final morphology of the deposit. Hydrogen adsorption on the metal surface is competitive with the adsorption of Zn, this determines an inhibition of Zn deposition at low pH values [42].

The formation of a new growth site Zn* (nucleation reaction) can happen through reactions (15) and (16), these reactions determine the number of growth sites and have an important influence on deposit morphology, (16) shows that nucleation can be favoured by hydrogen adsorption.

$$Zn^{+}{}_{ads} + \ e^{-} \rightarrow Zn^{*} \quad (15) \qquad (15)$$

$$H_{ads} + Zn^{+}{}_{ads} \rightarrow Zn^{*} + H^{+} \quad (16) \qquad (16)$$

The HCP structure of Zn has three main growth directions: the direction normal to the basal plane <0001> and the prismatic directions <1120> and <1010>. The previously described mechanism does not distinguish among different growth planes. The <0001> growth is considered to proceed through adsorption, diffusion and incorporation in kink sites (13), whereas on <1120> and <1010> planes the surface diffusivity is lower, and the deposition is supposed to happen preferentially through direct attachment of the incoming ion [3].

The applied overpotential is an important parameter which determines the final morphology of the deposit. The growth normal to the basal plane through adsorption, diffusion, and insertion into the crystal lattice on a kink position, requires the lowest energy, <0001> is indeed experimentally found to be the main growth direction at low overpotentials. On the other hand, the direct attachment on the surface requires less energy for prismatic planes, at higher overpotentials the growth on prismatic planes becomes indeed dominant. Beside overpotential, the other main factor which determines the structure of the deposit is the mass transport of metal ions to the cathode. If the morphology is determined by the charge-transfer overpotential, it is said to form under activation control, if instead it is determined by mass transport, it is called diffusion controlled, if both charge-transfer and mass-transport contribute appreciably to the final shape, the growth mode is defined to occur under mixed control.

The formation of an even, compact, and shiny electrodeposit is generally very hard to obtain: in fact, quite often the deposit presents tridimensional structures with many different shapes and properties. These structures can form and grow for a multitude of reasons, one of which is a direct consequence of the electric field laws: the electric field is increased near to a sharp edge. The increased electric field close to some already existing protrusions, causes a locally increase of current density: in this way the deposition rate increase on the tip, which grows faster than the rest of the electrode surface resulting in progressively increasing localization of the electric field. This phenomenon is called “tip effect”.

The morphologies taken up by electrodeposited zinc are manifold, depending on the deposition conditions, such as: overpotential, electrolyte composition, and electrolyte convection. So far, a model accounting for all these factor accurately and comprehensively, has not been devised.

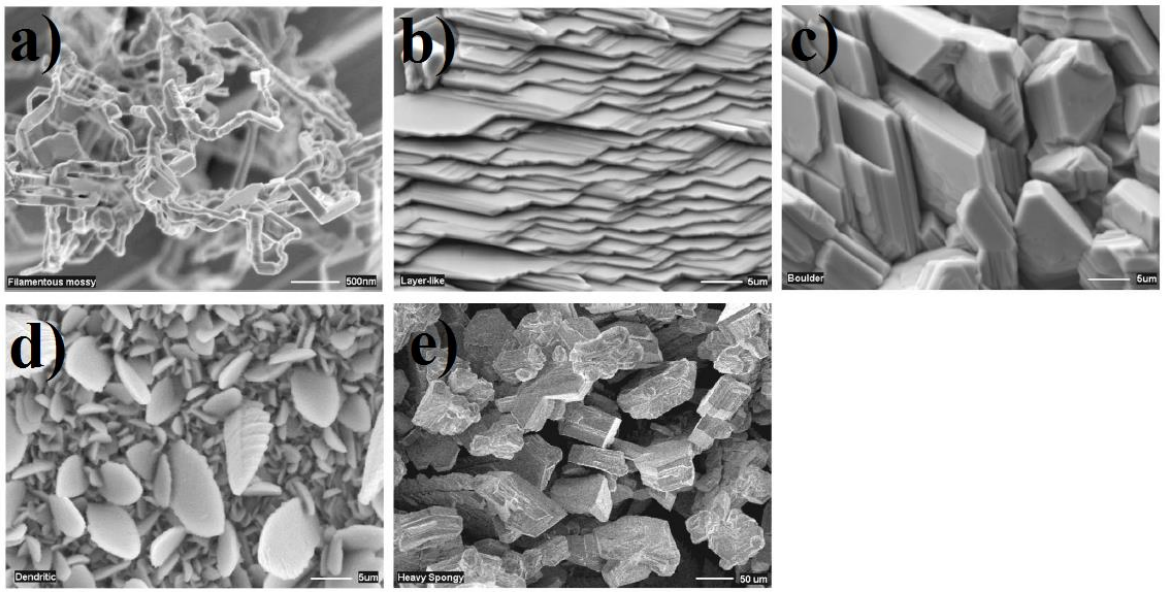


Figure 6 - SEM images Zn electrodeposits morphology in alkaline environment, a) mossy, b) layered, c) boulder, d) dendritic, e) heavy spongy [3].

Morphologies in alkaline solutions were characterized in detail by Wang [3], who identified five different classes of electrodeposits: mossy, layered, boulder, dendritic, and heavy sponge figure(6). This Author evaluated the effect of operating parameters such as: current density, concentration of zincate, temperature, stirring and substrate, on the formation of these deposits. Such an exhaustive study is still missing for mildly acidic electrolytes. Different pH values can have major effects on the deposit characteristics, even though, of course, the evolution of the deposits with current density and deposition conditions exhibits several commonalities with the better-known alkaline case. This is confirmed by [4] and by the experimental results of the present thesis work, that will be expounded below. It is always possible to distinguish three main classes of Zinc deposits: mossy, compact and dendritic. Each of these can be characterized by a set of characteristic properties, such as: appearance, microstructure, compactness, and adherence to the substrate, and by its formation and/or growth control mechanism: activation control, diffusion control or mixed control. It is commonplace to relate these different morphologies to different deposition CDs. Indeed, even if CD does not directly determine the deposits microstructure, both overpotential and ions transport limitations correlate positively with it, such that solid correlations can be established between morphology and applied CD. Broadly speaking, growing CDs correlated with Zn electrodeposit morphology in the following order: mossy<compact<dendritic.

Mossy (or spongy) zinc is a porous, non-adherent, non-compact, dark, and dull deposit that forms at overpotentials lower than a critical value (low current densities). This structure is characterized by macropores that can be easily observed at low magnifications under an optical microscope: higher magnifications achieved by SEM microscopy revealed a microscopic inner structure made of wiskers-like 50-100 nm thick figure (6a), this is the reason of the high specific volume of these deposits. Many studies were done to describe mossy Zn formation mechanism [2,3,8,32], but this is still not clear. The initiation of mossy structures seems to be triggered by some specific nucleation sites; sometimes indeed its growth can start directly on the substrate, more frequently though, it starts after the deposition of a previous compact zinc layer. The CD below which mossy structures forms is similar in alkaline and mildly acidic environments and is generally about 10 to 20 $mA/cm^2$. The effect on the threshold CD value of other plating parameters that influence the limiting current density (stirring and zinc ions concentration) seems to be minor, suggesting that mossy structures formation and growth is under activation control [3,7]. The tridimensional, macroscopic aggregates of these filamentary structures are sometimes also referred to as "dendrites", even though their microstructure and formation mechanism are quite different from those leading to the formation of dendrites that are characteristic of higher CDs.

Compact, non-porous electrodeposits (either of layered and boulder types) can appear like shiny metal or dull gray, depending on grain size. In particular, layered structures consist of layers of hexagonal platelets growing on <0001> direction, while at higher current densities the higher overpotential enables also the <1120> and <1010> growth directions. The simultaneous growth on basal and prismatic directions results in boulder-like deposits. There is no net border between layered and boulder structures, but, as the overpotential rises, the growth on prismatic directions becomes prevalent [50]. Perfect 3D epitaxial growth is hardly feasible, but this process was found to take place during the growth of the first deposited atomic layers. In most plating conditions after a critical thickness is attained, the morphology switches into boulder or mossy types, according to the applied CD.

At higher CDs, Zn dendrites start forming. These can grow in a multitude of different shapes and dimensions; the two most common ones are "hexagonal platelets" (single crystals hexagon) or "fractal/fern" (branched) like dendrites figure(6d-7). In alkaline environment, platelet-based structures may be regarded as an intermediate condition between boulder and "traditional" fractal/fern dendrites, while in mildly acidic electrolytes, dendrites are generally only of the platelet type, and fractal patterns are observed if the dimensions of the dendrites exceed one millimeter [6]. Zinc ion diffusion plays a major role in the formation and growth of dendrites: this is indeed influenced by Zinc ion concentration and electrolyte convection, of course, any condition that increases the limiting CD hinders dendrite formation. For this reason, the critical CD which triggers dendrite formation can vary over a wide range. Moreover, geometrical irregularities can determine local CD increase, which, in turn, can lead to the formation of dendrites at nominal CDs that are lower than expected. In alkaline environment dendrite formation happens at lower CDs than in mildly acidic electrolytes. It is reasonable to think that this happens because the mildly acidic electrolytes generally described in the literature have a Zn ion concentration that is ca. 20 times higher than that of alkaline ones. This difference in concentration might lead to confusion, with

respect to the role of the specific chemistry. No explicit information on these issues seems to be available in the literature, to date.

The mechanism of Zn dendrite formation and growth has been the subject of ongoing debate for a long time and it is a kind of standard in the metal electrochemistry literature. According to Diggle [5] its initial stages are controlled by diffusion, while growth control is taken up by activation. Later studies [7] claimed that also growth is under diffusion control. It is established, though, that the formation of dendrites happens in two stages: a first one in which a tip is formed in the diffusion layer and grows faster than the recesses, owing to an increasing concentration gradient developing through the diffusive layer.

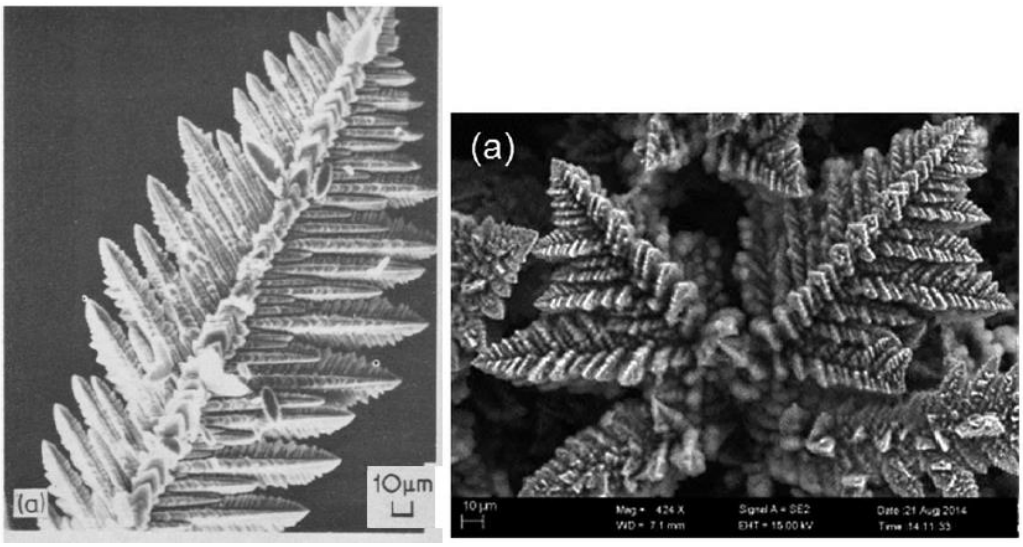


Figure 7 - SEM images of fractal/fern like dendrites [52,53].

When the tip has grown higher than the diffusion layer thickness, the diffusion of metal ions to the tips changes from planar to hemispherical, further stabilizing faster growth of the tip. Dendrites indeed are empirically found to develop after a given initiation time, after which it is possible to clearly observe the typical effects, such as current increase in potentiostatic measurements or crystallite formation by microscopy/tomography. Such initiation time is associated to the time necessary for the initial tip to grow outside the diffusion layer. Rich experimental evidence shows that the formation of zinc dendrites is influenced by mass transport: dendrite formation is hindered if the solution is stirred (i.e., it does not occur under otherwise identical conditions, or, instead takes place at higher CDs), if the temperature is increased (diffusivity of ions increases), if the current is pulsed (allowing the ion concentration in the catholyte to relax to the bulk value) and if the concentration of zincate ions is increased [7].

Heavy sponge-type deposits are black, porous and sponge-like. Their formation has been correlated with the convective flow induced by the concurrent hydrogen bubble formation. It is worth noting that these high-CD plating conditions in fact exceed the range currently considered relevant to batteries applications.

There are many other parameters influencing the morphology of a Zn deposit, such as the nature of the substrate, the presence of a separator or of a gelled electrolyte and the presence of impurities/additives. The knowledge of the morphologies in the battery field is indeed mainly empirical and generalizing is complex.

When Zn is deposited on a Zn substrate, the condition of the latter is important for the determination of the final morphology. This is one reason of the poor reproducibility and predictability of Zn electrodeposition behaviour on Zn metal: different grain sizes, exposed crystalline faces, surface finishing and oxides layers, all may have an influence on the final shape of the deposit. Irregularities already present on the surface favour non-compact structure formation, generally through tip effect. The deposition on a substrate (such as copper or graphene) has the tendency to proceed at first epitaxially, continuing the structure of the support, with the formation of a compact deposit. After a layer of Zn is formed, the influence of the substrate is lower, and the deposits evolves as a function of electrolyte and plating conditions.

Gelled electrolytes and separators may have strong effects on the nature of the deposits. Both reduce the diffusivity of ions, probably enhancing the formation of dendrites. Dendrites growing through the separator were studied with tomography [51], which demonstrated that the growth of dendrites is favoured by the separator. The geometry of the dendritic structures observed was totally different from that in the free electrolyte, since dendrites grew through separator's micropores. The formation of non compact structures (mossy structures like), typical of low CDs, inside separators has not been the subject of publications, so far.

## 1.2 Electrolyte additives

It is common practice to include in the electrolytes small amounts of specific substances to modify or control different parameters of the electrochemical reaction happening in the bath, these substances are referred to as additives.

### 1.2.1 Additives to improve deposit quality

The improvement of many aspects of the deposit quality, such as roughness, compactness, and brightness, is often achieved including additives in the electrolyte. The most widespread application of these is in the formation of metallic coatings, many studies were made though for the application in secondary batteries with metallic anodes.

Many organic and inorganic chemicals are employed for this scope, a classification attempt was made in [29]. Additives can be cationic, anionic, or non-ionic (these generally have functionalities with marked polarity). Charge and charge distribution of the additive molecule is of fundamental importance for the interaction with the electrode surface, and with the depositing metal ion.

The effects on the deposition of a given additive in different plating baths are hard to predict, the correlations between an additive and the effects on the deposits are based mainly on empirical observations. The classes of additives more extensively studied for electrodeposition are generally identified by their effect on the deposit such as levellers or brighteners. Levellers are additives which can suppress the irregular growth of three-dimensional structures and expand the current density range in which compact deposits are formed. Levellers normally cause a reduction of the grain size and an increased polarization of the cathode (two phenomena that are strictly interconnected). In a few cases, such additives can reduce the cathodic polarization, e.g. by resonant tunneling [73]

The mechanisms through which additives allow to obtain a compact and uniform electrodeposit are manifold, plus generally complex and hard to determine. Often an additive can act through more than one mechanism and have different effects at different plating conditions. Moreover, the synergic effect of two or more additives or of an additive in different electrolytes is often unpredictable. Old – but extremely well documented and organized - reviews of the possible working mechanisms, with a focus in electroplating are given in [29,30], more modern studies were made also for ZIBs [32,35,56]. The additives studied in this thesis are cationic surfactants, the possible mechanisms associated to these additives are the following:

(i) most of the additives work with a surprisingly low concentration (less than 1 mM): this suggests that their inhibiting effect, is focused on specific areas, like the tips of the deposit. The increased electric field on the tip restricts the migration and adsorption of the additive molecules to these projecting features, locally inhibiting further deposition. The metal will consequently deposit preferentially on the flat surface of the electrode. It has been proved [56] that an excess of additive is detrimental, because if the concentration is too high the effect is not going to be focused on the tips, but on the whole surface.

The inhibition mechanisms of the additives are different and complex. The additive might react on the surface; some metallic ions co-deposit on the surface, some organic compounds are reduced and their reaction products locally coat the surface, creating are either adsorbed or form a film. Many additives are reversibly adsorbed on the electrode surface, the inhibition might be a consequence of the covering of active area by additives molecules or, if the adsorption happens preferentially on specific growth sites or crystalline faces, an effect on the reaction kinetics. Another possibility is that the steric hindrance of large, adsorbed molecules repels incoming ions, or that the presence of positively charged species on the tip shields the negative charge of the electrode, this last mechanism is called “electrostatic shield effect” [56] (figure 8) additives that are not adsorbed on the surface might also act through this last mechanism [57].

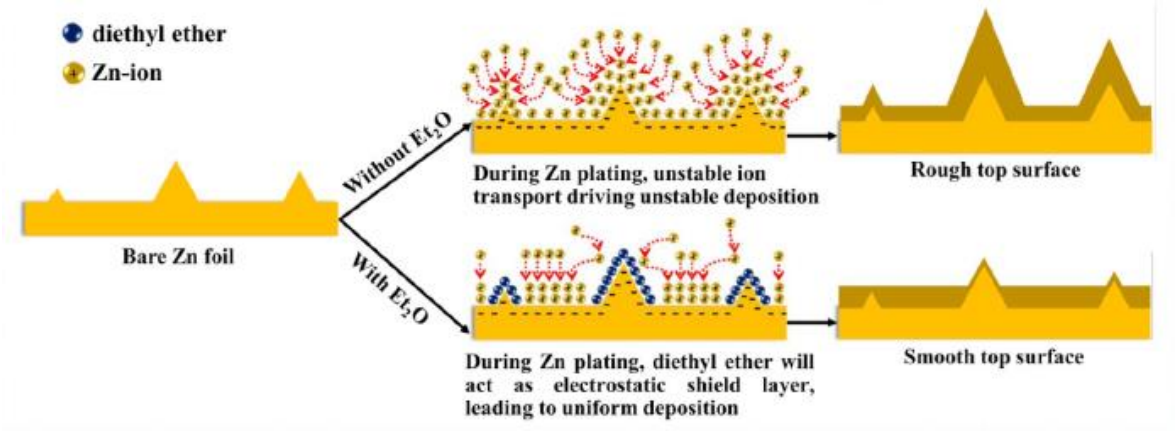


Figure 8 - Representation of the electrostatic shield effect mechanism [56].

Some additives can limit the adatom surface diffusivity [35]: in this way the migration to a single large tip would be impeded, leading, as noted before, to a high surface density of nucleation sites, resulting in the formation of many smaller tips (figure 9).

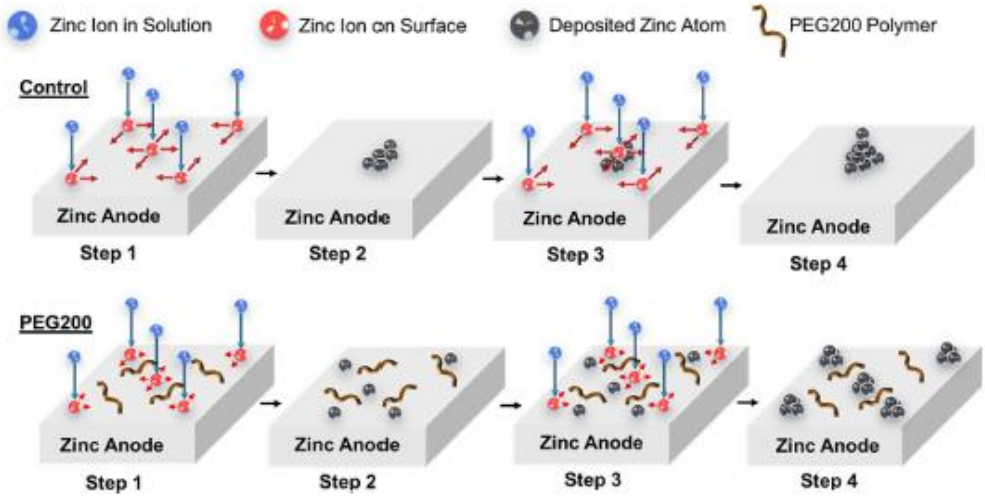


Figure 9 - Zn adatom diffusivity limitation mechanism [35].

Many additives increase the nucleation overpotential of Zn deposition: this increases the nucleation rate, leading to a homogeneous electric field and finer grain size. The increased nucleation potential/nucleation rate and the inhibition of growth sites are two strictly interconnected phenomena. Some EIS studies [58] in both alkaline and mildly acidic environment, reported an increase of cathodic polarization effects with addition of $TBA^{+}$ and $Pb^{++}$ ions (two well established additives for Zn electrodeposition), owing to a decrease of active surface fraction and surface density of growth sites, resulting from additive adsorption on the electrode and/or suppression of the autocatalytic reaction (11). Instead, the formation of new growth sites, which is observed as an inductive loop in the low frequency part of the EIS spectrum (around 0.01 Hz), is improved by additives. This is consistent with

an increased nucleation rate: the increment of growth sites is related to the formation of a bigger number of finer grains and to the consequent modification of the deposit microstructure.

It is important to underline that, if a compound increases the cathodic polarization, it does not necessarily have a positive effect on the deposit morphology, and that the increased overpotential is an energetically negative consequence of the additive action on the deposition, since increased polarization decreases voltage efficiency. Of course, an additive which can ensure a compact deposit without increasing excessively polarization is preferable.

Some additives act on the depositing metal ions: this is the case of complexing and ion pairing mechanisms [30]. In the first case the adsorbed additive may complexes metal ions, facilitating the adsorption on the electrode and increasing the rate of reduction (induced adsorption) or favouring the flow of electrons from the electrode to the metal ion (ion bridging). It is also possible that the depositing ion is paired with an additive molecule with opposite charge, when the depositing ion has a negative charge (this is the case of amphoteric metals like zincate ions in alkaline environment) these are repelled by the negatively charged cathode, the previous pairing with a cationic additive might facilitate the adsorption of the metal atom. It is worth noticing that, even if the nominal concentration of the additive it is low, migration of cationic species cathode might lead to locally increased additive concentrations in the catholyte, enabling ion-pairing favoured adsorption for all the approaching zincate ions.

### 1.2.2 Additives for corrosion inhibition

Additives are used also to prevent corrosion: these are commonly called corrosion inhibitors. Their application is well established in numerous sectors, such as, quite extensively in corrosion prevention of steel in the Oil&Gas industry. Many studies were made also regarding their application to zinc batteries, but their application is limited because other corrosion inhibition methods are preferred (section 1.3.2). Corrosion inhibitors are also manifold and different in terms of chemical nature and working mechanism. They can be organic or inorganic, neutral, anionic, or cationic. Regarding the working mechanism, these additives can favour the passivation of the metal or, similarly to many levellers, adsorb on the surface creating a protective film or modify the reaction kinetics. Specifically, anodic, cathodic or both electrokinetics can be inhibited by additives. The efficiency of these additives in corrosion reduction is generally proportional to their amount, which is generally below 0.01% w/w. [71]. In order to reduce the corrosion of metallic anodes in secondary batteries, a corrosion inhibitor acting on the cathodic reaction (HER) is preferred, the inhibition of the anodic reaction would interfere with the normal discharge reaction, and an additive which induces passivation would insulate the anode increasing the battery impedance.

### 1.2.3 Quaternary ammonium salts (QAS) as additives

Quaternary ammonium salts (QAS) are cationic surfactants, widely employed as electrolyte additives. QASs have a quaternary ammonium cation, which is a nitrogen atom, bonded to four alkyl groups and hence hosts a single positive charge. QAS are stable toward most of bases and acids and highly soluble in water. Under cathodic polarization they can degrade through an irreversible reduction reaction, producing an amine and a hydrocarbon [59], the reaction conditions in the reference were of really high cathodic polarization but it cannot be excluded that some reactivity may occur also under milder conditions. No information can be found in the literature about the oxidation of such compounds. QASs are generally biodegradable and, even if they are generally toxic for aquatic organisms [60], they typically do not represent an environmental issue in the really small amounts required for battery applications.

The use of QASs to improve electrodeposits quality is already well established, but their working mechanisms are poorly understood. QAS adsorption on the Zn cathode is generally taken for granted: blockage of favourable deposition sites, tip growth inhibition [38] and increased nucleation rate [58] are their commonly reported mechanism. QASs are also a class of additives strictly associated to the ion-paring mechanism [30], since this mechanism is effective only for negatively charge depositing ions (zincate ions in alkaline environment): one can thus suppose that some differences in the behaviour of these additives found in alkaline and mildly acidic electrolytes, might be associated with the fact that the ion pairing mechanism is not active in mildly acidic aqueous ambient. A strong positive effect on the deposit quality is clearly observable also in mildly acidic solutions: this suggest that the adsorption on the cathode is the most important mechanism through which these additives work in both environments. The effect of QASs on the electrodeposit morphology depends also strongly on the nature of the alkyl groups; for aliphatic QASs the cathodic inhibition and the ability to suppress dendrites seems to increase along with the chain length [45,67]. Bigger alkyl groups delocalize the positive charge of the nitrogen on the whole molecule, decreasing the cation polarity as well as, presumably, the strength of its adsorption on the cathode. Long aliphatic chains, of course, also decrease the QAS solubility.

QASs are also studied as corrosion inhibitors for both steel [61] and primary Zn batteries [62,63]: the possible double effect as levellers and corrosion inhibitors makes them particularly attractive for the application on rechargeable ZIBs.

## 1.3 Zinc ion batteries (ZIBs)

### 1.3.1 Zinc based batteries

Zinc has been a material exploited as a battery primary electrode since the beginning of this technology; the very first battery built by Volta (figure 10a) at the end of 18$^{th}$ century, adopted metallic Zn anodes. The Daniel cell (1836) (figure 10b), the Grove cell (1838) and the Leclanché cell (1866) were the three main batteries used in the 19$^{th}$ century, all employed Zn metal anodes in acidic or mildly acidic electrolytes, and adopted different cathode

chemistries. During the 50s of the 20th century the "alkaline" battery (figure 10c) was invented, employing a KOH electrolyte, a Zn powder that oxidized to $ZnO_2$ as the anode and the reduction of manganese(IV) oxide to manganese(II) hydroxide as the cathode reaction. Nowadays this is still the most common primary battery employed in portable electronics. During the 20th century, the Zn-air battery was invented: this is a technology based on a metallic Zn anode in an alkaline electrolyte, coupled with the cathodic reaction of catalysed atmospheric oxygen reduction. Use of a metallic anode and the absence of cathodic reactants stored inside the device, allow to reach high energy densities: primary ZABs are commercial devices for both low- and high-power applications. None of the previously described batteries is rechargeable. Studies on secondary batteries with Zn anodes were done starting from the seventies, but with the breakthrough of Li-ions batteries the research interest on this technology faded until the last decade, when the subject exploded, driven of the need to find substitutes for Li-ion batteries, mainly for transportation applications.


Figure 10 – Different primary batteries. a) Volta pile b) Daniel cell c) alkaline batteries.

The secondary Zn batteries research focuses mainly on rechargeable Zn-air batteries and secondary Zn ion batteries (ZIB) a technology which employs an intercalation cathode which hosts $Zn^{++}$ ions similarly to Lithium batteries. Before this, very few studies were done to investigate a way to obtain a reversible deposition of Zn in electrolytes different from those developed and optimized for metal plating. Literature for Zn electrodeposition was driven by Zn electrowinning and electrochemical Zn plating. Zn electrowinning is a process to extract metallic Zn from mining ores, which are generally an impure, acidic, sulphate solution. Zn plating is done to create a corrosion protection layer, mainly on steel. This process is capable of yielding smooth, resistant, and uniform deposits, generally from concentrated $ZnSO_4$ acidic electrolytes or cyanide-based alkaline ones. These electrolytes

are deeply different from those considered for secondary batteries anodes with mildly acidic electrolytes. The literature on Zn anodes before the last decade focuses mainly on primary batteries, hence on the prevention of corrosion and passivation during open circuit and discharge. This is useful, but not immediately appliable to secondary mildly acidic ZIBs, because the electrolytes used were most often those employed in the Leclanché or the alkaline cells.

### 1.3.2 ZIB anodes

Zinc metal has a high mass specific capacity (820 mA h/g) and a very high volumetric capacity (5855 mA h/cm^3), the redox standard potential is low (-0,76 V v SHE), compared to those of alkali metals. Moreover, gravimetric power densities achievable with alkali metals are indeed higher than those of zinc. Nevertheless, Zn is still an attractive anodic metal for many technological and economic reasons. First of all, Zn can be used in aqueous electrolytes directly in its metallic form. Instead, alkali metals exhibit standard reduction potentials that are low with respect to HER and direct contact between them and water would result in highly exothermic oxidation. Still, use of Zn metal as an efficient and long-lived anode is not trivial; proper engineering of Zn anode and electrolyte has not been achieved so far.

The development of secondary Zn anodes must face three main problems: corrosion, passivation and non-compact deposits formation.

Free corrosion of Zn anodes happens mainly during long shut down periods. It yields major drawbacks in the battery performances and durability, such as self-discharge, loss of active material, and formation of hydrogen gas inside the battery. Moreover, it rises the pH of the electrolyte, which in mildly acidic electrolytes causes the precipitation of insoluble ZnO (section 1.1.3), which can insulate the anode. Since in battery applications it is not possible to reduce the corrosion rate by inducing the formation of a passive layer, the approach traditionally adopted in primary batteries consisted in alloying the metallic Zn with some elements which inhibits HER. Hg amalgams (up to 10% of Hg in weight) were used for the scope, which was later substituted by a wide variety of different alloying elements such as Bi, Sb, In. This solution, though, is not appliable to secondary batteries; the reversible co-deposition of the alloying elements along with Zn is hardly achievable.

HER does not only happen during shut down after free corrosion, but also, at increased rate, during charge (cathodic polarization): this limits the charge rate to a level which prevents the formation of too much hydrogen.

Passivation of Zn anodes has the direct consequence of increasing the impedance of the electrode, causing an efficiency loss and a performance drop. Moreover, an uneven passivation which insulates only some portions of the electrode surface causes a non-homogeneous CD distribution, which leads to the formation of pits during discharge and favours the formation of non-compact structures during charge, (section 1.1.3).

Non-compact deposit structures are a major issue for the cyclability of ZIB batteries, indeed dendrites and mossy aggregates can grow through the electrolyte separator and reach the

cathode, short-circuiting the battery and causing an immediate failure, moreover non-compact Zn structures are brittle, they tend to break, disconnect electrically from the anode, and be oxidized under free corrosion in the electrolyte, which is detrimental because it favours the accumulation of oxides close to the anode and mainly because it causes a loss of anode material. This decreases the battery capacity and mandates to oversize the mass of Zn in the anode, to compensate these losses. Problems related to deposits morphologies are more pronounced in alkaline environment, where non-compact structures have a higher tendency to grow. This is one main reason for the increasing interest in mildly acidic electrolytes. It is worth noticing that the formation of mossy zinc happens at lower CD than compact deposits, so the CD working range during charge which allows to have a high cyclability, has not only an upper limit due to dendritic growth but also a lower one, since ZIBs anodes might have problems also working at low CDs.

All these unwanted processes, that take place at the anode, are interconnected and synergistic: the inhibition of one of those will likely have inhibiting effects also on the others.

### 1.3.3 Anode engineering

Techniques to improve Zn anode life include 3D micro-structured supports, coatings, and electrolyte additives, this last one is the main subject of this thesis and will be analyzed in detail in section 1.3.7. It is noteworthy that often, even though some engineered anodes exhibit good performances, their composition or synthesis process is in contrast with some of the ZIBs' original development purposes, such as environmental friendliness and manufacturing simplicity.

The synthesis of anodes by the deposition of Zn on a 3D structured support, brings the advantage of an active area increment, that decreases locally the CD, and hence the electrode polarization, increasing voltage efficiency and power density. The reduction of current density decreases the dendrite formation risk. In principle though, this should favour the formation of mossy structures: it is worth stressing that, to the best of the author's knowledge, the literature did not address this issue, to date. 3D anodes can be adopted effectively, in synergy with electrolytes additives. Beside allowing a stable and compact Zn deposit, the support needs to be electrically conductive and mechanically resistant: copper foams [17][18] and carbon clothes [19] have been tested. Deposition on carbon cloth supported carbon nanotubes [20] favours a homogeneous electric field distribution during deposition, leading to compact deposits. Even though these techniques seem to provide good performances, one main drawback is that volumetric and mass capacity are reduced with respect to a monolith zinc anode, not only for the presence of the inactive material of the support, but also owing to the porosity of the material.

The formation of coatings on zinc to form an artificial anode-electrolyte interface has a double advantage: it allows a homogeneous distribution of depositing Zn ions through coating nanochannels, that reduces tip effects and guarantees compact deposits, and creates a buffer between metallic Zn and the water solvent of the electrolyte, suppressing water-involving side reactions (corrosion, passivation). The coating needs to be an electrical insulator and an ionic conductor, otherwise, obviously, Zn would deposit on it instead of

going through and deposit on the bulk Zn; moreover, it must be hydrophilic to ensure a good wettability, but at the meantime insoluble, otherwise it would dissolve in the electrolyte. Finally, it must also be mechanically resistant and flexible, to follow anode thickness changes during charge/discharge cycles. A wide range of different materials was tested for this purpose, some promising attempts include coatings based on: $CaCO_3$ [21], poli-amide [22], and ZnO [23], $TiO_2$ [24], In [25].

### 1.3.4 ZIB cathodes

Notable and steadily increasing research efforts are being made to find a competitive, long-life, cathode for rechargeable ZIBs; the cathode is probably the single most critical component to develop, and the main factor delaying ZIB industrialization.

Intercalation cathodes developed for Li-ion batteries are not suitable for $Zn^{++}$ ions, since the bivalent nature of $Zn^{++}$ causes a stronger electrostatic interaction that hinders solid state diffusion of this species inside the cathode material. Moreover, at the cathode/electrolyte interface, the strong solvation shell of Zn ion penalizes the desolvation of the ion which is preliminary to its intercalation. [42]

The two more promising cathode materials are reported to be $MnO_2$ and V-based materials, but also cobalt, Prussian blue analogues, layered sulphides, and organic materials have been tested so far.

$MnO_2$-based materials exist in many different polymorphs, corresponding to different geometries of the intercalation sites: tunnel (alfa, beta, gamma), layered (delta), or spinel (lambda), each of these structures is composed by $MnO_6$ octahedral units. Mn-based materials are relatively simple to synthetize and cheap, have an average working voltage of (1,4 V vs $Zn/Zn^{++}$) and high capacity (200 to 300 mAh/g), but suffer of poor electrical conductivity. It is still unclear whether the working principle of $MnO_2$ cathodes is chemical conversion or ion intercalation, it is possible that the actual storage process involves both mechanisms. Mn dissolution, crystalline structure modification, passivating layer formation and $H^+$ intercalation are the main unwanted processes, responsible for the low cyclability and fast capacity fading reported in the literature. [42]

Vanadium-based cathodes are generally vanadium oxides $V_2O_5$, $V_6O_{13}$ or vanadium oxides salts (vanadates); they are more expensive than $MnO_2$, have a lower output voltage (0,7 V vs $Zn/Zn^{++}$) but higher capacity (300 to 400 mAh/g). [42]

### 1.3.5 ZIB electrolytes

Liquid water, water in salt, ionic liquid, organic liquid, gel and quasi solid electrolytes have been studied for ZIB applications, in this thesis only aqueous electrolytes will be analysed. As already mentioned, the electrolytes for ZIBs can be of alkaline, or mildly acidic pH. The traditional alkaline electrolyte is a 5 to 7M KOH + 0.1 to 0.6 M ZnO solution. In mildly acidic ambient, the search for the best electrolyte is still subject of research: a wide range of Zn salts has been tested and good results are obtained with $ZnSO_4$, $Zn(CF_3SO_3)_2$ and

$Zn(TFSI)_2$. $ZnSO_4$ is the most common Zn salt while and $CF_3SO_3$-based salts are complex and expensive, even though they exhibited better performances in terms of dendrite suppression [26,27].

Aqueous electrolytes have the advantage of being generally highly conductive. When the concentration of salt is not too high, the ionic conductivity $I_c$ [S/m] is, with a reasonable approximation, directly proportional to the concentration of ions in the electrolyte, the specific value, of course, depending on the ion nature. When the concentration of salts is high, the viscosity of the electrolyte increases, lowering $I_c$, so there is generally an optimum salt concentration that maximizes conductivity. 2M $ZnSO_4$ solution has an ionic conductivity of 1.3 S/m while it is 3.6 S/m 3M $Zn(CF_3SO_3)_2$ [31]. Is possible to obtain an extremely high concentration of salt (up to 20M for TFSI [26]) to the point that the mixture is not liquid anymore and is referred as "water in salt" electrolyte: the advantages of such a mixture are described later but, since its viscosity is really high, these have a decreased $I_c$. The ionic conductivity of water-based electrolytes is anyhow always high if compared to organic or solid electrolytes: the improvement of ionic conductivity is thus not a fundamental aspect for ZIBs development.

Another important characteristic on a battery electrolyte is the transport number, defined as the ratio of the sum on the product of anions and cations diffusivities:

$$\mathrm{T} = \frac{D_+ + D_-}{D_+ D_-} \tag{17}$$

This is an index of the concentration polarization losses, the lower the transport number, the higher the concentration polarization losses. In the best case, T is equal to one if the negative charges are fixed, if the diffusivity of anionic and cationic species is the same, T=0.5. However, $Zn^{++}$ cations in aqueous solutions are surrounded by a large solvation shell, that limits their diffusivity, so their transfer coefficient is usually lower than 0.5. In [22] the transport number of 2M $ZnSO_4$ was estimated without separator and in the presence of different separators: it was always found to be around 0.38. A liquid water-based electrolyte has indeed bad transport characteristics, to improve the ion transference number it is possible to increase the salt concentration, to employ big anionic species with lower diffusivity or polymeric coatings with fixed anionic charges.

The electrolyte electrochemical stability window (ESW) is the maximum cell voltage compatible with the electrochemical stability of the electrolyte, this is one of the main obstacles to the achievement of high energy densities in aqueous batteries, because it limits the maximum cell output voltage. Organic or polymeric electrolytes that are normally adopted in Li-ion batteries normally have ESW above 4V, but the theoretical ESW of aqueous electrolytes is 1,23 V, which is the potential difference between HER and OER equilibrium potentials. Electrolyte stability is particularly critical during charge, especially at high SOC and high C-rates since charging currents must be limited to avoid electrolyte deterioration. Thus, a wide ESW is important, not only to achieve a high energy density, but also to allow low charging times. If the cell voltage is higher than the ESW, there are the thermodynamic conditions for the reaction of the electrolyte, but this may happen even at

lower voltages, if just one semi-reaction of water splitting takes place. Limiting the cell's voltage below 1,23 V is typically not enough to ensure electrolyte stability; the potential difference related to one of the two electrodes can be high enough to let one semi-reaction happen. As already described, in aqueous electrolytes stability issues are generally related to HER, even if also OER can be an issue. OER normally requires high overpotentials but can be problematic if high voltage and oxygen-activating cathodes are employed, this aspect limits the cathode choice to low-voltage ones. High concentration and water-in-salt electrolytes have a decreased water activity because water molecules are bonded in the solvation of ions, this allows to expand the ESW to around 1.5V, matching the OCV of a Zn-$MnO_2$ cell.

### 1.3.6 Separator

In a battery with a liquid electrolyte, it is not possible to keep the anode and the cathode close but separated just with a liquid phase in-between. The electrolyte is hosted inside an inert microporous support called separator. Even if the separator does not react chemically, it has a significant effect on the anodic reaction. Mass transport in the vicinity of the electrodes is drastically reduced if compared to a free-flowing electrolyte: it is thus fundamental to take this in consideration if a material or an electrolyte is tested with an excess of electrolyte solution.

### 1.3.7 ZIB additives

To suppress the unwanted processes on the anode side of a ZIB, a wide range of different additives has been tested. The ideal additive must prevent the formation of non-compact structures, suppress corrosion, and avoid passivation, without reducing excessively the reaction kinetics. Differently from the additives previously tested for deposit levelling and corrosion inhibition, battery additives must work during both anodic and cathodic polarization cycles. The additive effects in a condition different from the nominally sought after one (cathodic polarization for levellers and anodic polarization for corrosion inhibitors) are not investigated in the existing literature. The application on ZIB anodes requires to study the additive behaviour on both polarization conditions and the effect of the cycling between the two at various current densities.

Levellers are traditionally studied for processes such as coatings formation, which are commonly done at a single, optimum, value of current density, generally in the tens of $mA/cm^2$ range. The electrodeposition of Zn on a ZIB anode during charge must ideally ensure the growth of a compact and uniform deposit in a CD range that is as wide as possible. As described before in section 1.1.4, the CD range of compact deposits for Zn has an upper and a lower limit imposed by the formation respectively of mossy structures and dendrites. Anyway, literature available often does not distinguish between these unstable growth regimes, or it focuses exclusively on dendrite suppression and, less commonly, mossy structures. In this thesis work, I have shown that mossy Zn formation is probably the single most critical unstable growth mode during recharge of Zn anodes in the CD range of practical interest for ZIBs. If an additive guarantees an effective suppression of high-CD dendrites, it

does not necessarily suppress also mossy structures formation and vice versa (this will also be demonstrated in this thesis), although many additives demonstrated to be effective in both the scopes.

A wide number of additives aimed at ensuring a uniform and compact Zn deposit have been tested. Anyway, most of the studies were made in alkaline environment, only recently attention has been paid to mildly acidic environments. Additives tested so far include both metallic ions and organic additives. Pb [32,40,41] and Sn [32] demonstrated to suppress mossy structure formation in alkaline environment, Pb and Ni [33] suppressed low-CD structures in a mildly acidic electrolyte. Organic additives tested for this purpose are several and of varied chemical nature. The most promising in mildly acidic environment are polymeric additives and surfactants. Polymeric additives include polyethylene glycol (PEG), which suppressed dendrites growth in a 0.1M ZnCl electrolyte [34] and sulphate electrolyte [35]. Branched polyethyleneimine (BPEI) was found to be effective in dendrite suppression in 2M $ZnSO_4$ electrolyte [36]. Cationic surfactants like QAS are known to be good levellers for Zn electrodeposits [42,43] and have been tested widely for secondary batteries in alkaline environment [37,39,40], but there are only a few examples of application in mildly acidic electrolytes [38, 44], also anionic surfactants like SDS seem to have an influence on the quality of the Zn electrodeposit in mildly acidic environment [44].

Additives for Zn anode corrosion suppression in batteries cannot rely either on the passivation of the anode, or on the suppression of anodic reaction (dissolution of zinc), otherwise the performances of the battery would be impaired. The ideal additive inhibits only the cathodic reaction (HER). In this way, both corrosion and passivation of the anode (potentially favoured by alkalinization due to HER) are hindered. It is difficult, though, to measure the effect of the additive on HER and corrosion: moreover, even slight changes of environment and/or working conditions can change drastically their behaviour. Most of the studies evaluating corrosion inhibition of ZIB additives are based only on potentiodynamic measurements and sometimes provide controversial information about their ability to suppress corrosion. None of the reported additives – apart from the traditional alloying used in primary Zn anodes, or the application of coatings that are incompatible with recharge - seems to have outstanding performance in terms of HER suppression [44].

Some additives adopted for the suppression of non-compact structures might also be able to reduce corrosion rate and/or passivation of the anodes. Anionic surfactants like SDS seems to extend the ESW of ZIBs, reducing both HER at Zn during standby and discharge and OER during recharge of the Zn anode, in both acidic [64] and alkaline [65] environments. Cationic surfactants like CTAB in alkaline ambient seem to increase HER overpotential in [63] but to increase corrosion rate [44,65]. TBAB, according to [66] (tests were made in on a zinc-bismuth alloy), can decrease HER to a certain extent. PEG [34] was also proved to decrease HER. The suppression of HER might be explained with the formation of films of adsorbed molecules, which reduce the water-electrode contact, or with the kinetic inhibition of specific reaction sites. A difference between anionic and cationic surfactants is that their charge is presumably influencing their adsorption behaviour: cationic surfactants are expected to be strongly adsorbed on the surface during cathodic polarization, whereas anionic surfactants during anodic operation. In [46] some aromatic QAS have been

investigated as corrosion inhibitors in primary alkaline batteries: the author suggests that they might be adsorbed on the surface during open circuit, thus inhibiting corrosion, and desorb from the surface during discharge (anodic polarization), avoiding inhibition of the discharge process. This might explain why the influence of QAS on the polarization is stronger during cathodic processes.

Dissolution suppression of MnO2-based ZIB cathodes is often achieved through insertion of $Mn^{++}$ ions: in this way, the activity of the metal anion in solution is increased and further dissolution of cathode material is less favoured. To this scope, when $MnO_2$-based cathodes are employed in mildly acidic $ZnSO_4$ electrolytes, a significant quantity of $MnSO_4$ (generally 0.1 M) is added. It should be taken into account, though, that $Mn^{++}$ might have a non-negligible effect on reactions such as Zn deposition and HER, and, under strongly cathodic polarization, can event codeposit along with Zn. Some studies indeed showed that HER on zinc is increased both with $Mn^{++}$ in solution [48] and Mn alloyed with Zn [49]. [48] highlighted also a change in crystallographic orientations of the deposit. Anyway, an exhaustive study on the influence of $Mn^{++}$ ion on Zn electrodeposition and corrosion in ZIBs, or about its synergy with any other additive was not found in the literature.

In the experimental section below, seven different QAS will be tested as additives for Zn electrodeposition figure (11). These additives were already tested in alkaline environment by our group [39]. Tetra-butyl ammonium bromide (TBAB) is a QAS with four identical four carbon aliphatic chains. The efficacy of similar QASs but with two, three, and five carbon atoms chains has been tested in chlorides electrolyte [45] and TBAB is resulted to be the best dendrites suppressor. Hexadecyl tri-methyl ammonium bromide (CTAB) differs from TBAB mainly for its long 12 carbon atoms aliphatic chain, TBAB and CTAB are two of the most common QAS employed in electrochemical processes and have already been tested for ZIB applications. Di-methyl di-tetradecyl ammonium bromide (DMDTDAB) has 2 long aliphatic chains which makes it more insoluble than CTAB, so that, at the concentrations commonly adopted for the other additives, it is present mainly as a micelle rather than as a free molecule [68]. No documents were found in the literature in which DMDTDAB was adopted as an electrodeposition additive. Benzyl dimethyl phenyl ammonium chloride (BDMPAC) is an additive employed in gold deposition, with two aromatic functionalities. Benzyl-phenyl modified polyethyleneimine (BPPEI) is a polymeric QAS with the same functionalities of BDMPAC, this compound is interesting because it is a QAS but has the structure of PEI, which is also an additive studied for ZIB anodes. Poly di-allyl di-methyl ammonium chloride (PDADMAC) is a polymer in which the tetravalent nitrogen is included in a five-atoms ring, was adopted as component for an artificial SEI in metallic lithium batteries, but, to the best of my knowledge, never in Zn involved experiments, beside the previously cited work [39].

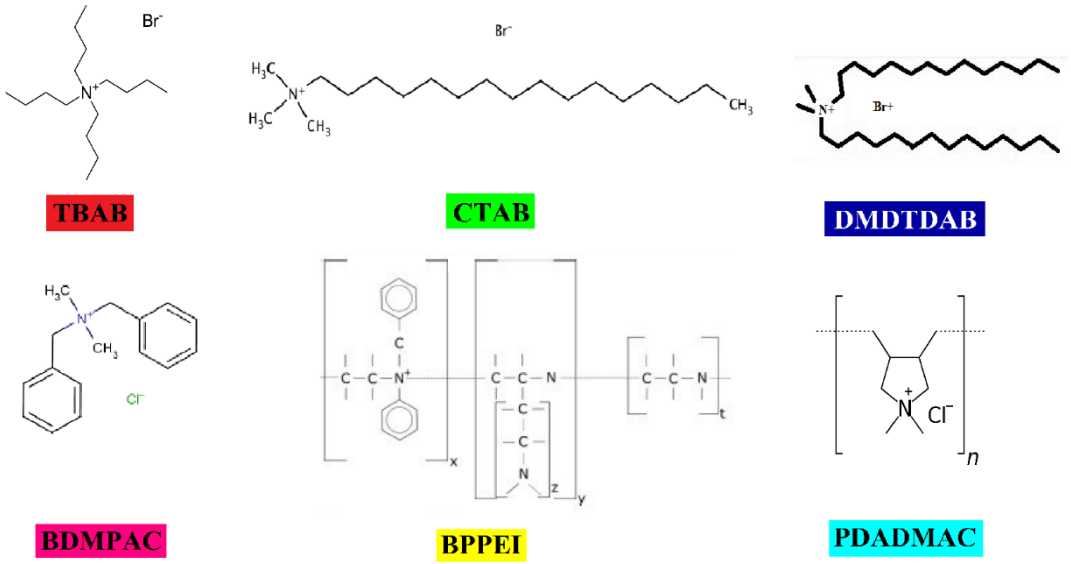


Figure 11 – Molecular structure of the QAS tested in this thesis.

# Chapter 2
# Experimental section

The experimental work of this thesis consists mainly in the testing of the six QAS listed in section 1.3.7 (figure 11) as additives for a reversible Zn stripping and deposition. Some considerations are also going to be made about the behaviour of Zn in 2M $ZnSO_4$ solutions ad on the influence of $Mn^{++}$ ions on the Zn electrode, topics on which there is lacking information in literature. The testing of the six QAS is going has been performed through three experiments: CV in a low $Zn^{++}$ concentration electrolyte, galvanostatic deposition on a graphite support at different CD, and symmetric cell cycling at low CD with SEM inspection of the samples. The cathodic and anodic behaviours are both explicitly taken into account. On the basis of these experiments, the most promising additives (TBAB and PDADMAC) have been selected for further investigations with galvanostatic deposition and stripping tests on a Zn substrate. Deposits made in the presence of TBAB and $Mn^{++}$ ions have been visualized with stereomicroscopy. The influence of TBAB on Zn morphology after galvanostatic cycling has been visualized through *in operando* tomography in an originally developed cell.


Figure 12 - The six QAS chemicals tested in this thesis.

## 2.1 Cyclic Voltammetry

The task of this experiment is to obtain fundamental knowledge of how QA additives influence the deposition and corrosion of zinc. For electroanalytical reasons, as explained below, the operating conditions are not identical to those prevailing in a typical Zn-based battery but allow to highlight better the physico-chemical role of the organics on electrocrystallization. Achieving a good reproducibility with this experiment is a not a straightforward task and often literature reports solely rely on single measurements, without indication of confidence bands.

### 2.1.1 Instrumentation and reagents

The CVs were performed with a classical three electrodes configuration (figure 13). in a cylindric closed cell with an Ag/AgCl 3.5 M KCl reference electrode, all the voltages in the following sections are going to be expressed vs. Ag/AgCl. Two identical platinum CEs were employed (small Pt rods; 1mm diameter, 5 mm long), placed symmetrically with respect to the WE and RE, to improve the uniformity of the current distribution and reduce ohmic contribution. For most electrochemical measurements, a glassy carbon WE with a surface of 0.07 $cm^2$ was employed A plastic tube (2mm diameter) was placed in the cell to degas the solution, the gas mass flow was controlled with a MaterialsMates GF-MF flow controller. The cell was placed under a magnetic stirrer and a magnetic anchor was placed inside the cell to enhance mass-transport. CVs were performed with a VersaSTAT 3F potentiostat.

The electrolyte consisted in an aqueous solution, containing 0.5 M $NaSO_4$ supporting electrolyte, to which 10 mM $ZnSO_4$ and 0,1 g/l (except 0,01 g/l for BPPEI) of organic additive were added according to the experimental requirements detailed below. The zinc ion concentration was way lower than the concentration in a battery electrolyte, with a higher concentration the currents would have been too high and the ohmic drops would hide some behaviours of the system, moreover in this condition a limiting current is reached soon, giving detailed information on mass transport effects and the deposition of a limited amount of metal that in principle allows complete voltammetric stripping. For this experiment we neglected the role of $Na^+$ ions on deposition and corrosion of zinc, on the basis of its thermodynamic stability in the potential window we are working in. It is nevertheless worth noting that [69] highlighted an impact of $Na^+$ on dendrite suppression, through the so-called electrostatic shield mechanism.

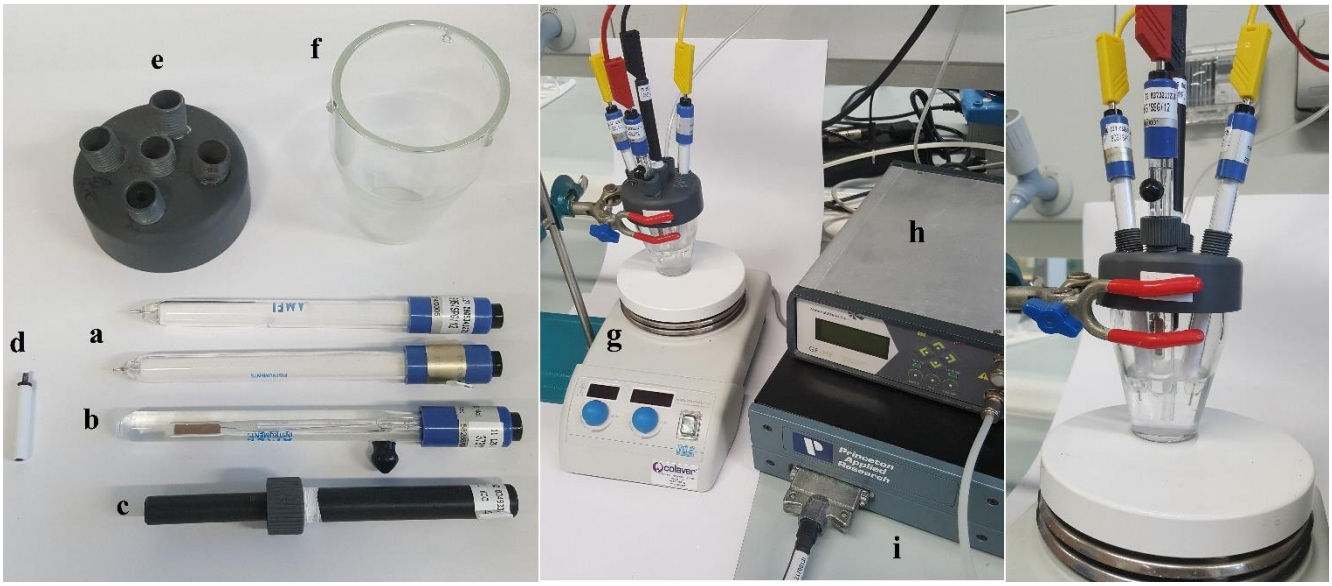


Figure 13 - Instrumentation and set up for the CV. a) Pt CE, b) Ag/AgCl REF, c) WE support, d) Glassy carbon WE, e) cell cap, f) cell, g) magnetic stirrer, h) gas flow meter, i) potentiostat.

### 2.1.2 Measurement protocol

In order to reliably assess the impact of the different organics on the voltammetric behaviour of Zn, we devised the following protocol, that was repeated three times in correspondence of each organic investigated. All the CV were made at 25 mV/s, unless otherwise specified. (i) The cleaned GC electrode was subjected to CV cycles in the pure supporting electrolyte, (5 cycles in range 0.5÷-1.8V, starting from OCV), to verify the WE condition and to ensure additional anodic cleaning. (ii) $ZnSO_4$ was added to the electrolyte. The electrolyte was stirred and deaerated with N2 to eliminate the dissolved oxygen. On the basis of voltammetric data, the ideal deaeration conditions were found to be 0.5 nl/min of $N_2$ bubbling for 10 min before the electrochemical measurements, after which bubbling was stopped and the electrolyte was kept under a blanket of flowing $N_2$. Then, a second CV was performed, 10 cycles from -0,5 to -1,6V starting from anodic terminal voltage (ATV). The aim of this measurement was, again, to verify the regularity of the behaviour before proceeding with the measurement in the presence of a given additive. (iii) One ml of concentrated additive solution was introduced into the cell. For the less soluble additives, DMDTDAB and CTAB the solution was totally replaced with a previously prepared one. The solution was degassed again as before, and a third CV was performed, with the same parameters of the second one.

Notwithstanding the high chemical stability of GC, accurate chemical cleaning and mechanical polishing of the WE are required after each measurement, to achieve a high reproducibility. Specifically, chemical cleaning is aimed at removing residual Zn, Zn basic salts, and traces of organics. On the basis of voltammetric evidence, the optimal pre-treatment condition for GC was found to be: electrode immersion in 70% nitric acid for a

few seconds, thorough rinsing with DI water, gentle polishing with 2500 grinding paper, and finally sonicated for 5 min in DI water. To ensure complete removal of zinc compounds and organics from the analysis system, the Pt CEs were washed with 10% nitric acid and accurately rinsed with DI water and the RE and all the cell components were thoroughly washed with DI water.

## 2.2 Galvanostatic depositions on graphite

This experiment aims to visualize the different morphologies of galvanostatically electrodeposited Zn at different current densities.

Galvanostatic depositions (figure 14) were performed with a QL355TP power supply, in 5 ml cylindrical vials, using a zinc tube obtained by shaping a zinc sheet (5mm diameter, 250 um thickness) as anode, and a graphite cylindric rod (2 mm diameter) as the cathode. The basic electrolyte was 2M $ZnSO_4$, into which the additives were introduced in the same concentrations used for CV measurements. To investigate the effect of $Mn^{++}$ ions, also a 2M $ZnSO_4$ + 0.1M $MnSO_4$ was tested. 3 ml of fresh electrolyte were inserted in the vial prior to each deposition experiment.

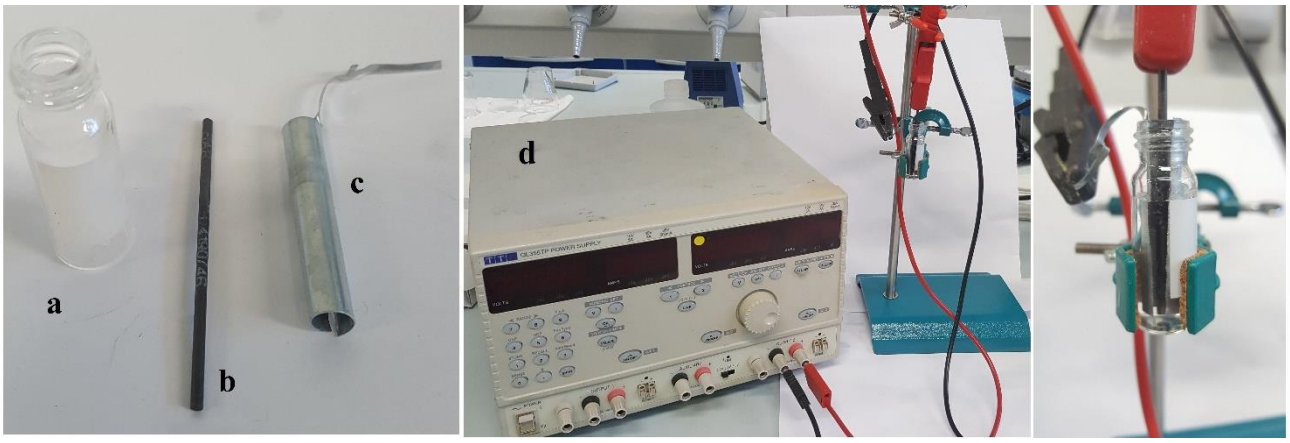


Figure 14 - Experimental set-up of the galvanostatic deposition on graphite, a) cell, b) graphite rod, c) Zn CE, d) power supply.

The graphite rods were immersed in 70% nitric acid to clean any residual zinc, then rinsed with DI water. The Zn anodes were degreased with acetone and rinsed with DI water.

Galvanostatic depositions were performed at 10, 20, 50 and 200 mA/ $cm^2$. The depositions at 10 and 20 mA/cm2 lasted respectively 4 and 2 hours, depositing always, nominally, 40 mAh/ $cm^2$. While those at 50 and 200 mA/cm2 were carried respectively for 4 and 1 hour (nominally 200 mAh/ $cm^2$). Some depositions were performed also at 1 mA/$cm^2$, these were kept running for around 14 hours, in many cases the cells short circuited before the end of the planned deposition interval, moreover the deposits often exhibited poor adherence and it was not possible to collect them for an inspection, for this reason the deposition at such a low CD were not carried on systematically. These growth experiments were performed out

in a two-electrode configuration, monitoring the cell voltage on the display of the power supply but without the possibility to collect voltage measurements.

After the deposition, the samples were washed gently with DI water and dried with nitrogen.

## 2.3 Symmetrical cell galvanostatic cycling

In this experiment two symmetrical zinc electrodes undergo many low current galvanostatic cycles, alternating positive and negative currents. The aim of this measurement is to understand the behaviour of zinc anodes under low-current cycling: the experimental conditions are similar to those of a realistically working ZIB, in terms of electrolyte composition and geometry of the cell. The long times required for this experiment have not allowed systematic replicates of the measurements. In any case, selected measurements were replicated, in order to gain some quantitative insight into the failure times of the cells.

Cycling experiments were performed with a versaSTAT 3F (by Princeton Applied Research) potentiostat, in the electrochemical test cell ECC-air (by EL-CELL) (figure 15), using two stainless steel as outer current collectors and two Zn sheets of 18mm diameter and 250 µm thickness as electrodes. Experiments with free electrolyte employed, as spacer, an O-ring of 3 mm diameter cross section. The basic electrolyte was 2M $ZnSO_4$, to which additives were introduced, in concentrations equal to the ones used for the CV experiments.

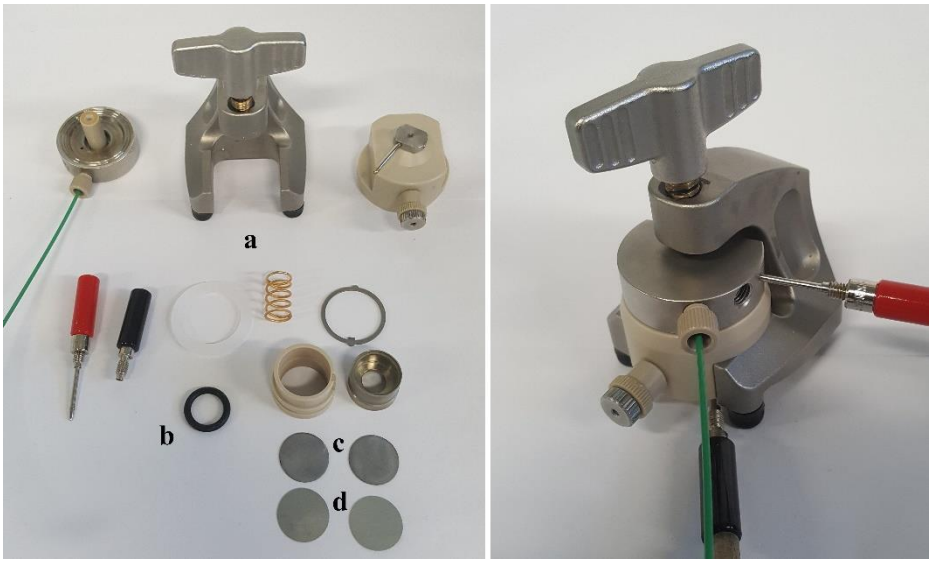


Figure 15 - Experimental setup of the symmetric cell cycling. a) carious cell components, b) O-ring, c) stainless steel current collectors, d) Zn electrodes.

The two Zinc discs were degreased with acetone and rinsed DI water, the cell was assembled and 300 µl of electrolyte solution were added. Electrochemical measurements were carried out in the two-electrode configuration. The galvanostatic pulses were set at +/- 2,54 mA (1 $mA/cm^2$) for 30 min each, starting with deposition on the lower electrode. The charge transferred in each cycle is 0.5 $mAh/cm^2$. It must be noted that this amount of charge

transferred for each cycle, though a classical literature benchmark for ZIB studies, is notably lower than that of practical battery operation [70].

The measurements were considered failed after a threshold voltage of +/- 1V was reached, indicative of electrode passivation, or if the voltage dropped to low values, constant during each galvanostatic half-cycle, indicating short circuiting.

After the completion of the measurement, the cells were disassembled and the two Zn discs were washed gently with DI water, dried with $N_2$, and collected to be analysed with SEM microscopy.

## 2.4 Galvanostatic deposition and stripping tests on Zn

The additives which mostly exhibited a tendency to suppress the formation of mossy structures during galvanic electrodeposition on graphite and that showed a uniform surface at SEM after cycling were TBAB and PDADMAC. These were further analyzed through a three electrodes cell during both anodic and cathodic polarization.

The experiment was made with a three electrodes configuration in a rectangular cell made of polypropylene 5x1.5 cm in section, 3 cm height. Two identical Zn sheets (5x3 cm) were adopted as working and counter electrode, placed vertically on the two large faces of the cell. This configuration allowed an even current distribution and low border effects. The reference electrode (3.5 M KCl Ag/AgCl) was placed horizontally at ca. 2 mm from the center of the working electrode Zn foil: this configuration allows minimal ohmic drop and negligible distortion of the current lines. The cell was filled with 2M $ZnSO_4$ without or with 0.1 g/l of additives in the measurements with TBAB and PDADMAC. To further control the effect of ohmic drop prior to each experiment, this quantity was directly measured with an on/off technique and the position of the reference electrode was adjusted to get the same ohmic drop before each measurement. Galvanostatic measurements were carried out at 10 $mA/cm^2$ for four hours at anodic and cathodic polarizations.

## 2.5 Zn symmetric cell tomography

### 2.5.1 Calibration of the tomography cell

The aim is to test an electrochemical cell designed to be suitable for in situ tomography of Zn electrodeposits evolution. This cell necessarily needs to be made in a material which is both transparent to X-rays and conductive, moreover it must be chemically inert in the testing conditions. Graphite is a cheap and resistant material suitable for this application. The cell must be of small dimensions to fit the sample holder of the tomograph, and preferably of cylindrical symmetry to allow an easier reconstruction of the 3D model. The first design attempt of such a cell consisted of a 20 mm high graphite cylinder composed by an inner 2mm diameter graphite rod and an outer graphite tube (5mm inner diameter, 1 mm thick), supported by a threaded base, in order to be fixed to the tomograph support, and closed by a cap, both made of PVC.

The first step to make the cell operative is to create a Zn layer on the surfaces of the electrodes; this was done initially by rolling a Zn strip on the inner rod, filling the cell with a 2M $ZnSO_4$ solution and using it as an anode to galvanostatically deposit the first layer on the outer surface. Then the Zn strip was removed, the cell was closed, and the polarity was switched to deposit on the inner rod. In this way deposits were created at a current density on both sides of 10 mA/cm$^2$ for 4h. In this way, we obtained on both electrodes fully developed mossy deposit, appropriate for calibration of the tomography acquisition conditions.

After the first attempt some small improvements were made in the design of the cell: the holes in the top and in the bottom were eliminated, since they caused spills and evaporation of the electrolyte. The support at the bottom part was replaced with a copper cylinder for a better electrical contact with the external graphite cylinder (figure 16). It is important to note that the geometry of this cell necessarily works with different current densities on the rod and on the external cylinder, because of the different area, the ratio of these currents is 5/2=2.5. we took advantage of this characteristic of the cell, which allowed to follow the behaviour of the Zn electrodes simultaneously at two different current density levels.

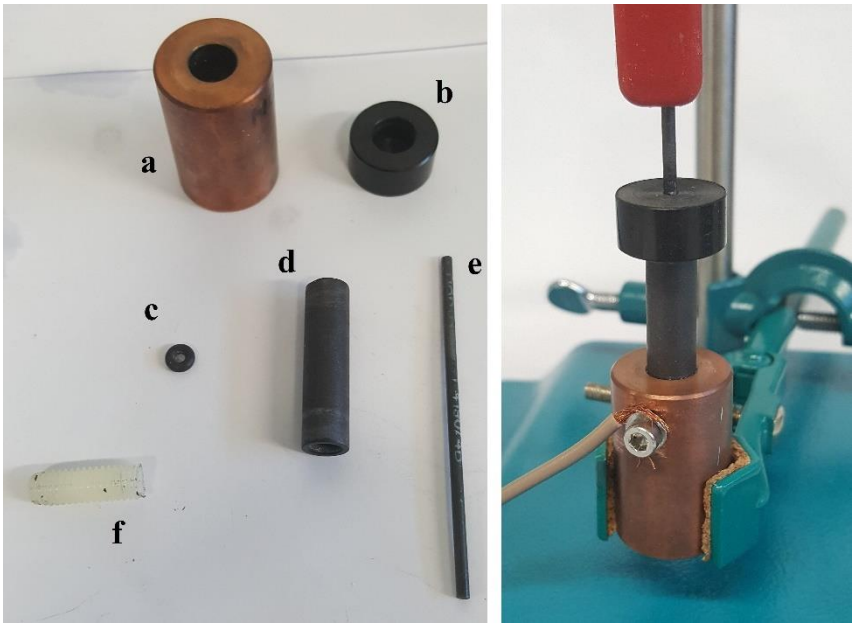


Figure 16 - Tomography cell. a) copper support, b) PVC cap, c) O-ring, d) graphite tube, the external electrode, e) graphite rod, the internal electrode, f) screwed plastic cylinder for the setting on the tomograph.

The first sample analysed with the tomograph needed to be representative of an evolved morphology to calibrate the tomography measurement. Instead, the ideal starting condition for subsequent cycling, is a couple of compact Zn layers, representative of a pristine anode.

The procedure for the formation of the initial Zn layers was also improved to obtain compact layers as starting condition. The deposit on the external cylinder was grown with 2400s of deposition at 200 mA (100 mA/cm$^2$), outside the cell, in a setup identical to that of the galvanostatic deposition in section 2.2. The formation of the initial Zn substrate on the

internal cylinder required currents above 30 mA/cm$^2$ to obtain a compact deposit. However, if the internal rod is adopted as CE, its CD is almost three times higher (>75 mA/cm$^2$) and this causes anodic passivation, and results in the formation of fragments of dead Zn that impair the electrolyte performance. Moreover, concentrations gradients rapidly built up in the cell at such high currents and favour the passivation on the bottom where the concentration of $Zn^{++}$ species is higher. The final protocol for the formation of this Zn layer was thus to assemble the cell with an inner rod similar to that described above, but deposited for 3600s, and to use this as the CE to charge the cylinder surface. The deposition was carried out at 200 mA (40 mA/cm$^2$ on the cylinder and 100 mA/cm$^2$ on the inner rod) for 2400 s, in order to deposit a charge equal to that of the previously made pristine inner rod, which was substituted to the consumed one, adopted for this deposition. The deposit on the outer cylinder was thinner on the bottom and with some small irregularities on the top but was considered adoptable for the purpose.

The selection and preparation of the samples to examine was constrained by the strict times available at the tomograph. We choose to analyse the deposition without additives and in the presence of TBAB, these were made separately on two identical cells, which were alternatively examined at the tomograph and subjected to galvanostatic cycling. Since the typical measuring time was of three hours, the cyclings were designed so that they could be completed in this time, to fully exploit the beamtime and start a measurement as soon as the previous one was over. The first measurements were done on two pristine cells, then both cells (with and without additive) were cycled two times at 60 mA (10 mA/cm$^2$ outer cylinder and 25 mA/cm$^2$ outer rod) for 2400s (DOD 30%), starting with the inner rod under anodic polarization. After this electrochemical treatment, a tomographic scan was collected. This protocol was repeated three times. The last cycle was made always with the same currents but held for 4800 s (DOD 60%)

The choice of the cycle current was driven by many factors. The low times available for the cycling, which imposed to do an aggressive cycling transferring high charges in small times, mandated the adoption of high current densities. The application in the battery field though, makes of low practical interest to study currents above 50 mA/cm$^2$. The selected current density configuration thus, on the one hand, is of full practical interest and, on the other hand, allowed to follow simultaneously the evolution of morphologies in conditions that typically lead to the formation of both compact and mossy Zn.

### 2.5.2 Data analysis for tomography

The raw data collected after the measurement session at the tomograph were 1200 frontal radiographs of the cell (frontal plane, including the rotation axis) taken at different angles. Reconstruction generated 1270 transverse slices, that were assembled into 3D renderings with the Fiji software. A first file was made to join all the 1270 images of the different sections into a 3D matrix, 8-bit black and white colour resolution. Brightness and the contrast of the image were adjusted to highlight the interesting features of the deposit. The reconstructed slices were cropped to isolate the deposits on the external surface of the inner rod electrode and of the internal surface of the external hollow-cylinder electrode.

The key advantage of *in situ* imaging is that the evolution of the deposit in the very same region could be observed, after appropriate registration. Adventitious highly-absorbing inclusions in the bulk of the graphite and surface scratches provided useful reference points. Larger electrodeposit features could be easy spotted and tracked at different cycling stages. Appropriate sections and renderings were selected in order to pinpoint the key morphological features of the cycled material.

# Chapter 3
# Results and discussion

## 3.1 Cyclic voltammetries

### 3.1.1 Electrolyte without additives

In Figure 17 we report one typical instance of the 18 replicated CVs (10 cycles) measured in the additive-free electrolyte in order to achieve a thorough grasp on instrumental and reproducibility issues. The results from these measurements are in excellent quantitative matching, with a well defined and controlled deviation of the current values, which was always below 15%. The cathodic deposition of Zn (Figure 18) starts at ca. -1.15 V in the first cycle, in which Zn nucleation occurs at the bare glassy-carbon surface, and at ca. -1.10 V in the following ones, in which Zn nucleates in the presence of a film or residual corrosion products. After an initial current-density growth that follows Butler-Volmer kinetics, a mass-transport controlled peak forms, with a maximum at ca. -1.17 V. The limiting current density under stagnant conditions is attained during the anodic-going scan, as one can appreciate from the plateau extending in the range ca. -1.5÷-1.3 V. At high cathodic potentials, close to -1.5 V, an additional peak can be observed, that can be explained with the reduction of zinc oxides/hydroxides, forming in the catholyte owing to local alkalinization brought about by

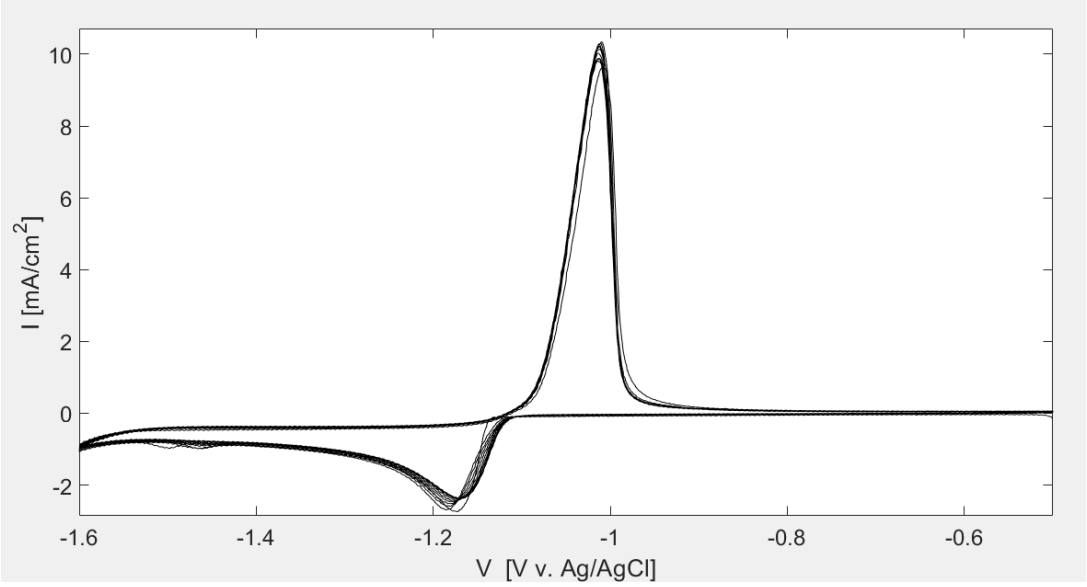


Figure 17 - Cyclic voltammograms recorded with a glassy carbon electrode in contact with a 0.5M NaSO4 + 10mM $ZnSO_4$ aqueous solution. Number of cycles 10. Scan rate 25mV/s.

HER concomitant with Zn electrodeposition. It can be noticed that the current densities in the whole cathodic loop tend to decrease with the number of CV cycles, owing to the accumulation of oxidation products that can neither be fully solubilized in the anodic interval, nor completely reduced in the cathodic period.

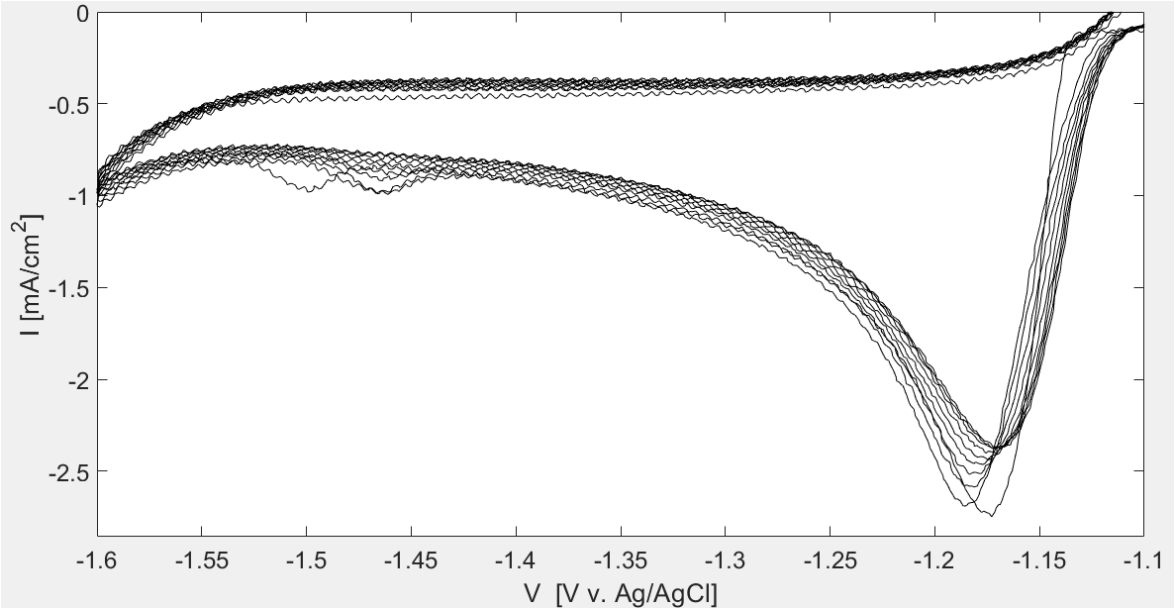


Figure 18 - Expanded cathodic range of Figure 17.

The anodic range of the CVs (Figure 19) is dominated by the stripping of Zn deposited in the cathodic range and exhibits a prominent peak, followed by a sharp decrease and terminating with a low CD tail extending for some tens of mV. Since in mildly acidic electrolytes the tendency to passivation is weak, the negative-resistance range of the peak is dominated by Zn consumption rather than by oxide formation, as in alkaline solution. Evaluation of the anodic-cathodic charge ratios (figure 27e) over all cycles of all replicated runs confirms this view.

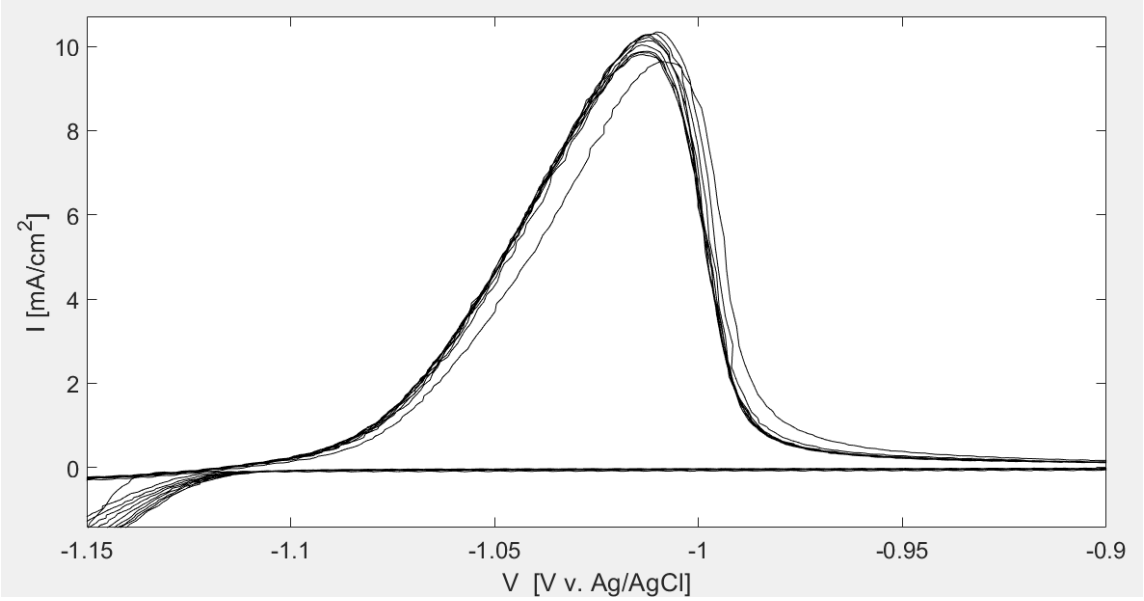


Figure 19 - Expanded anodic range of Figure 17.

Notwithstanding dominating active corrosion, the residualCD. tail observed in the CVs measured with a glassy-carbon electrode, can be justified with the formation of Zn(II)-containing species, imparting some degree of pseudopassivation, impeding the completion of Zn stripping, and forming a compact and hard-to solubilize layer of corrosion products, favoured by the presence of an inert electrode material. The progressive decrease of the CD values, already noted in the cathodic loop and confirmed in the anodic one, is fully compatible with the buildup of an anodic film over cycling.

To further investigate cathodic alkalinization and anodic pseudopassivation processes occurring during the operation of Zn anodes in a near-neutral aqueous electrolyte, we carried out prolonged voltammetric cycling (500 scans) and assessed the effect of lowering the cathodic terminal voltage (CTV) from -1.6 to -1.4 V (Figure 20). It is worth nothing that after 500 cycles with both CTVs, the WE was covered with an evident white layer – that we did not investigate further –, that was clearly thicker after the experiment with CTV of -1.6 V.

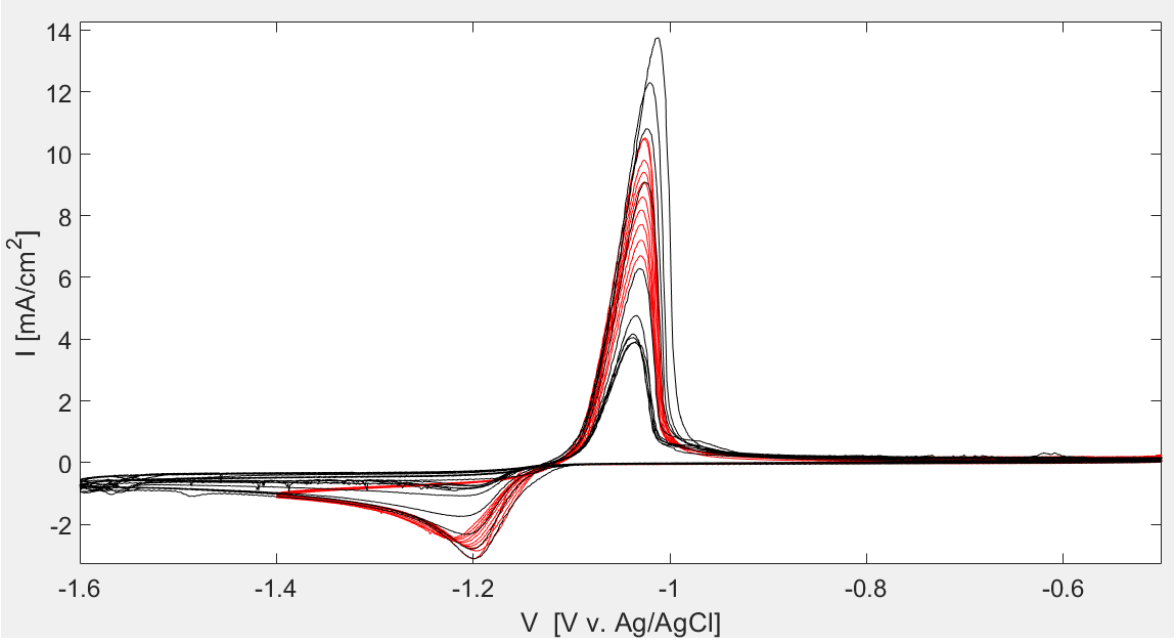


Figure 20 - Cyclic voltammograms recorded with a glassy carbon electrode in contact with a 0.5M $NaSO_4$ + 10mM $ZnSO_4$ aqueous solution. Number of cycles: 500. Scan rate 25mV/s.

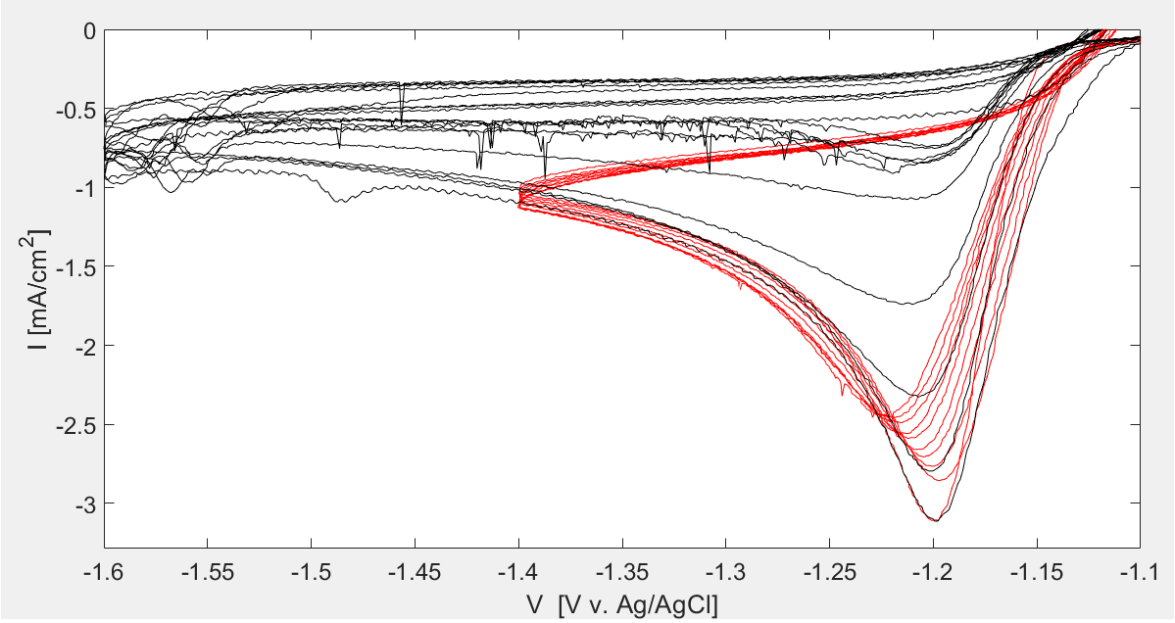


Figure 21 - Expanded cathodic range of Figure 20.

From the results of Figure 20 it can be noticed that, coherently with the CVs of Figure 17 and irrespective of the CTV, there is a progressive decrease of current density in both the cathodic and anodic ranges. A closer look at the CVs in the cathodic range (Figure 21) reveals that while with a CTV of -1.4 V the limiting current density is not affected by cycling, the rising portion of the cathodic CD before the mass-transport control peak is systematically lowered, though not as much as with the CTV set at -1.6 V. The cathodic and anodic consumed charges as a function of the cycle number in the CVs with the two CTVs are represented in Figure 22.

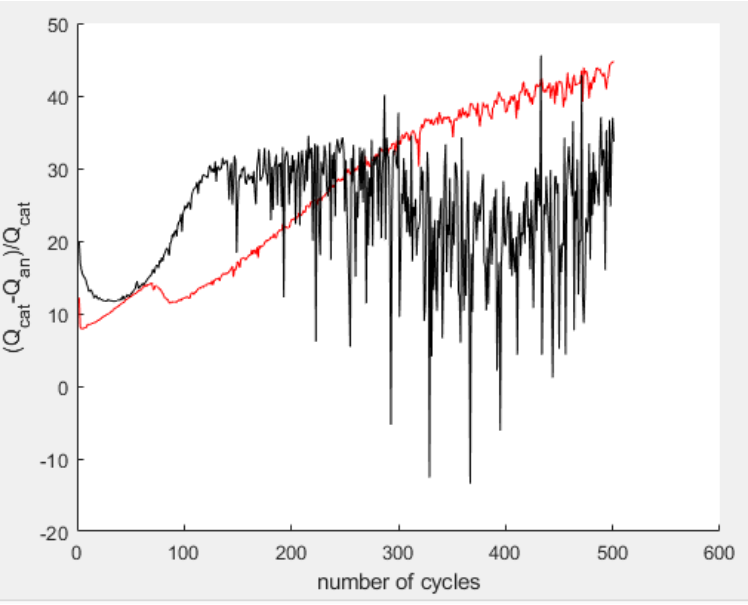


Figure 22 - Relative variation of consumed charge as a function of cycle number from the CVs of Figure 5.

The relative variations of consumed charge reveal that the cathodic charge is systematically higher (in the range ca. 10÷40 %) than the anodic one: in principle a difference between the anodic and cathodic consumed charges can be due to HER and to the formation of Zn-containing species, that cannot be solubilized anodically and impede the complete stripping of the deposited zinc. HER thus leads to the fact that the trend of Figure 21 is dominated by the build-up of an insoluble film, which impedes the completion of Zn dissolution. This tendency is quantified by the $Q_{an}/Q_{cat}$ parameter (figure 22, 27e), which is also going to be adopted in the interpretation of the CVs in presence of additives.

Mechanistically, this scenario is compatible with the anodic formation of type II oxides, as well as with the cathodic precipitation of zinc basic salts, resulting from the alkalinization of the catholyte and favoured by a CTV of -1.6 V: the presence of both species has been demonstrated in neutral environment by quasi-in situ XAFS, recently performed in our group and in a 1M $ZnSO_4$ electrolyte by Cachet [14].

Of course, both processes tend to reduce the active area of the electrode and, in addition, can also give rise to a porous layer of type-I oxide [72] that also hinders mass transfer. A further piece of evidence hinting at the occurrence of the cathodic precipitation process is that, with the CTV set at -1.6 V, after ca. 100 cycles, random c.d. spikes can be observed both in the cathodic and anodic ranges, that are characteristic of pseudopassivation conditions.

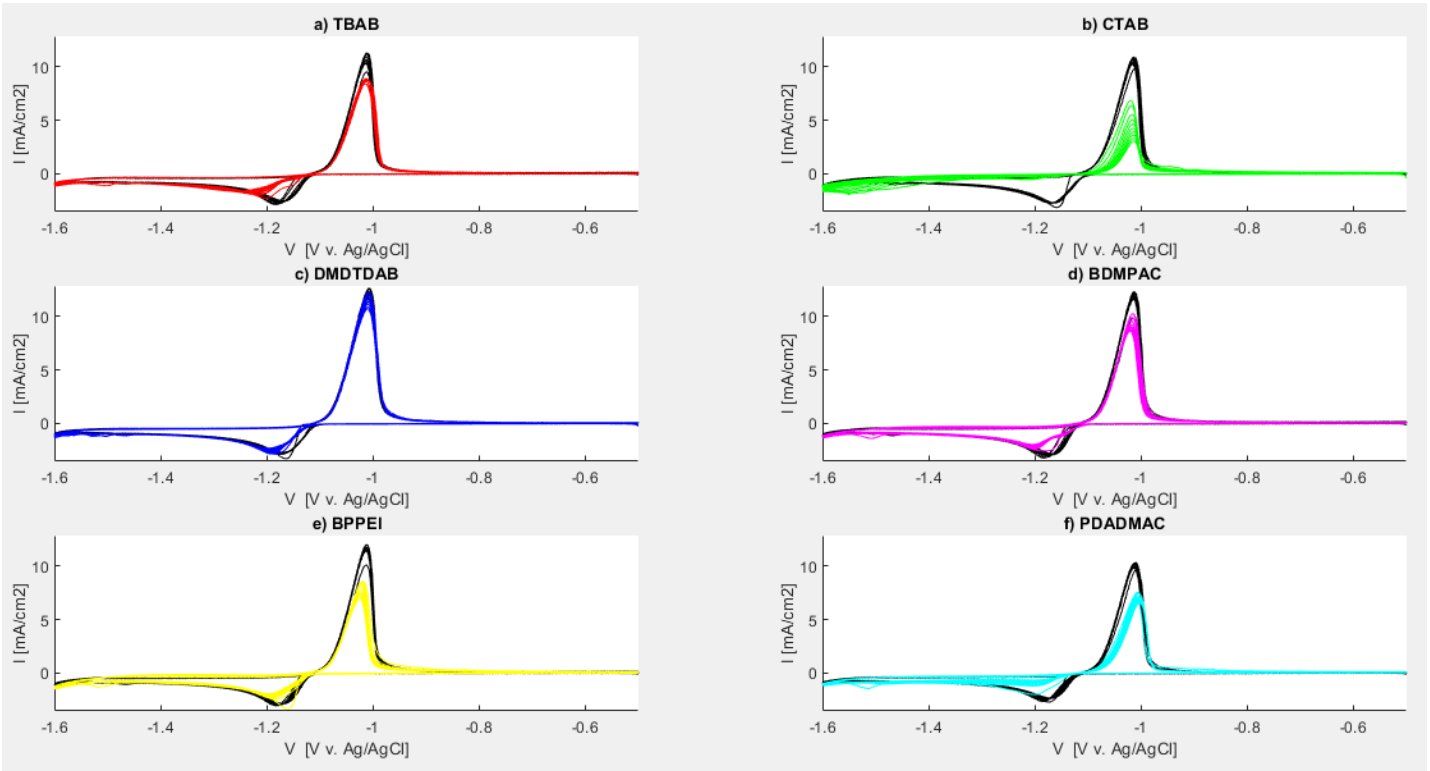


Figure 23 - CV with the additives compared with the correspondent CV without additive. CTV=-1.6V, ATV=-0.5V, scan rate 25mV/s, 10 cycles.

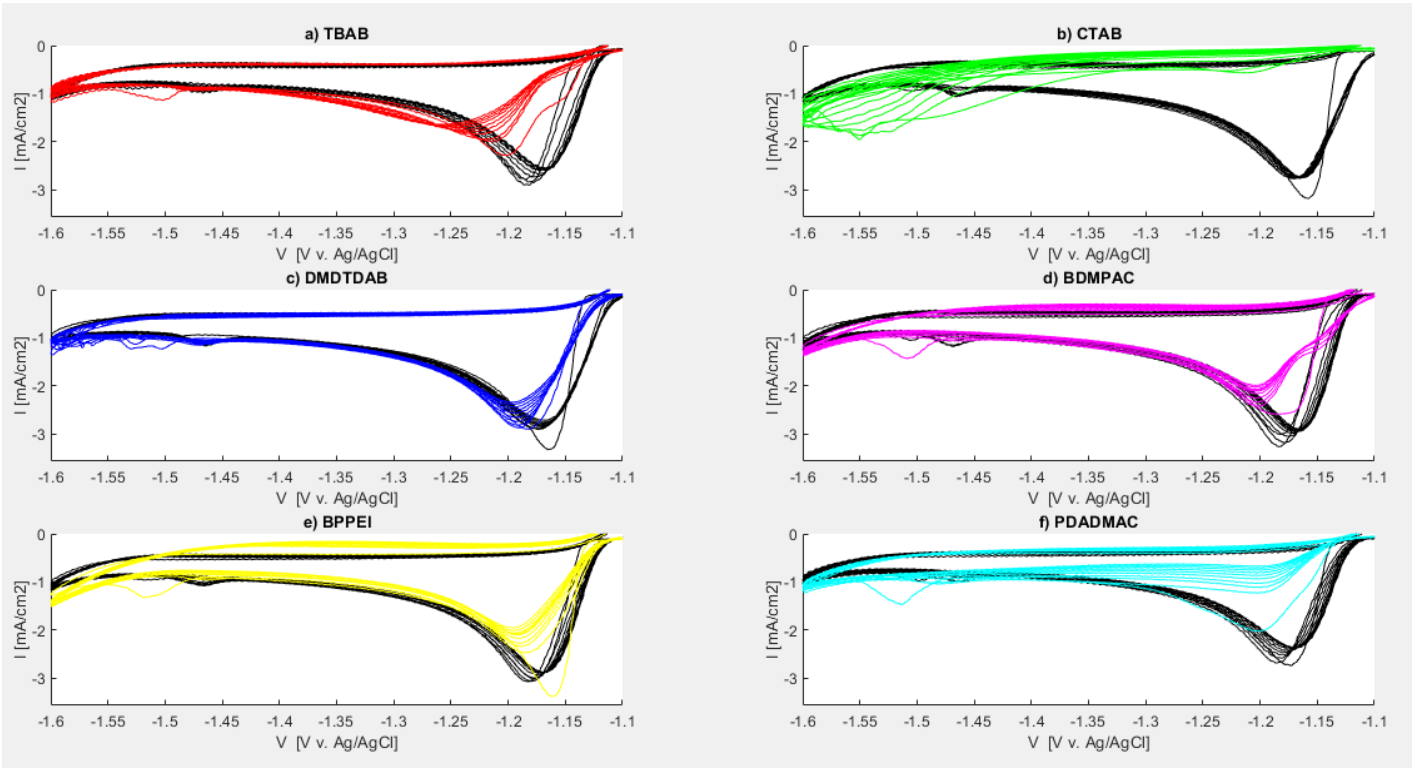


Figure 24 - Expanded cathodic range of figure 23.

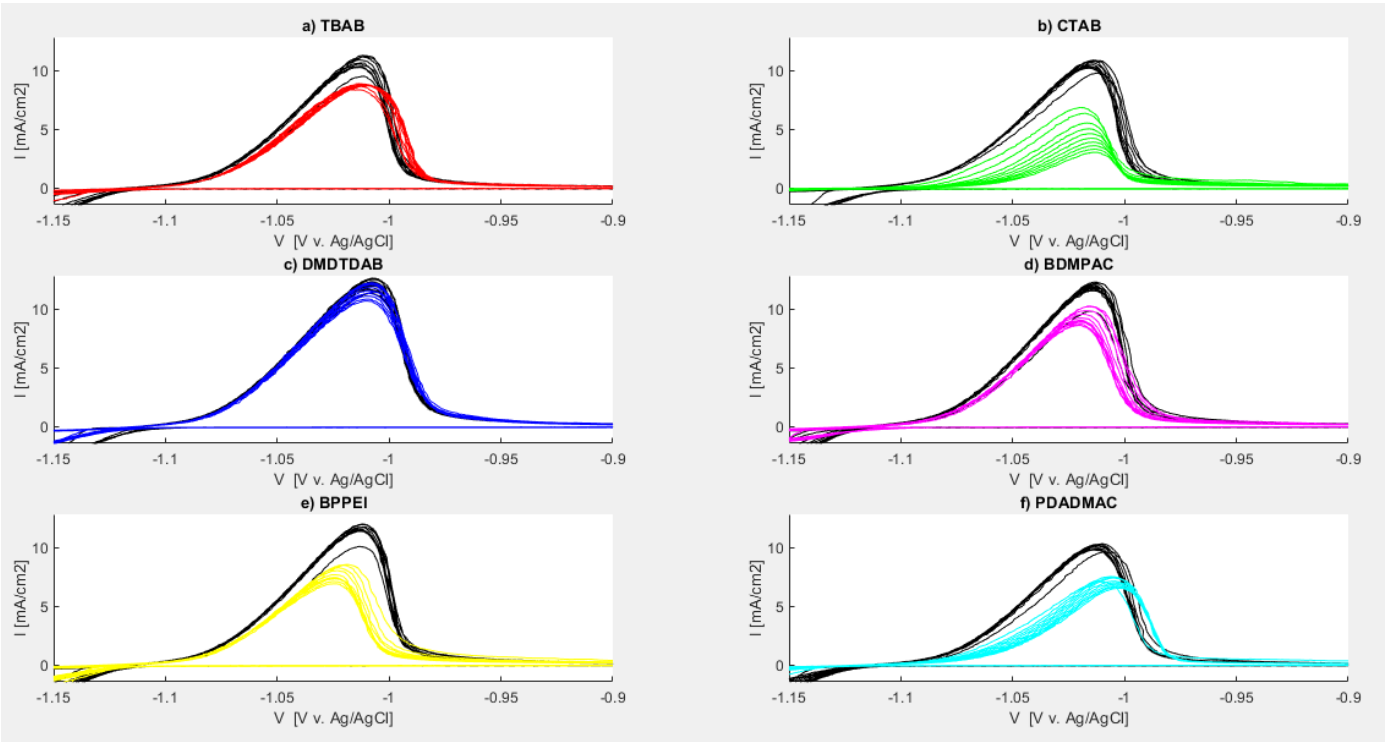


Figure 25 - Expanded anodic range of figure 23.

### 3.1.2 Influence of the additives

**TBAB**
After the introduction of 0.1 g/L of TBAB the cathodic Tafel-type slope is notably reduced, as well as the mass-transport controlled cathodic peak (Figure 23a, 26a). The cathodic limiting CD and the anodic Tafel-type are only slightly affected by the presence of the additive: this possibly shows that the effect of the additive is mainly on the cathodic reaction kinetics. The most characteristic CV feature related to the addition of TBAB is that two cathodic Tafel-type slopes appear, possibly denoting the presence of two electroactive species.

**CTAB**
CTAB exhibits a notable cathodic inhibition, such that an appreciable CD can be measured only for potentials lower that ca. -1.4 V (Figure 23b 27h). The slightly fluctuating behaviour of the CD at high cathodic potentials might be due to a strong HER contribution or to the reduction of zincates formed by alkalinization of the catholyte, as commented in section 3.1.1. Moreover, there is a strong progressive increment of this inhibition because the CD, both in the cathodic and anodic ranges, decreases systematically with the number of cycles. The anodic kinetics are also progressively reduced, even though not as much as the cathodic one.

**DMDTDAB**
DMDTDAB brings about very slight modifications of the CV behaviour of the additive-free system (Figures 23,24,25c), essentially resulting in (i) a limited degree of cathodic inhibition; (ii) the progressive decrease of the anodic CD with cycling is slightly more marked. It is worth noting that, owing to the very low solubility of this salt in aqueous solution, the effective concentration of the QA cation, that is the key species interacting with the cathodic surface, might be very low.

**BDMPAC**
Apart from minor quantitative details, BDMPAC behaves in essentially the same way as TBAB, and the same comments apply (Figure 23, 24, 25 d).

**BPPEI**
BPPEI shows the lowest degree of cathodic inhibition in the Tafel-type region, among the investigates additives, accompanied by a sizable progressive decrease of the CD upon cycling (Figures 23, 24, 25 e). The formation of a ionomeric film at the cathode surface, highlighted in aqueous alkaline solutions [39] could explain the strong reduction of the limiting CD. The anodic branch is quite similar to that of BDMPAC, that contains the same moieties, though in a polymeric network, with a slightly higher inhibiting action.

**PDADMAC**

Similarly to CTAB, but with differences in quantitative details, PDADMAC brings about a notable cathodic inhibiting effect, but, at variance with CTAB, the progressive nature of the inhibition is far less marked and most of the inhibiting effect seems to develop after the first cycle (Figures 23, 24, 25 f). In the anodic range, stable and relatively strong inhibition.

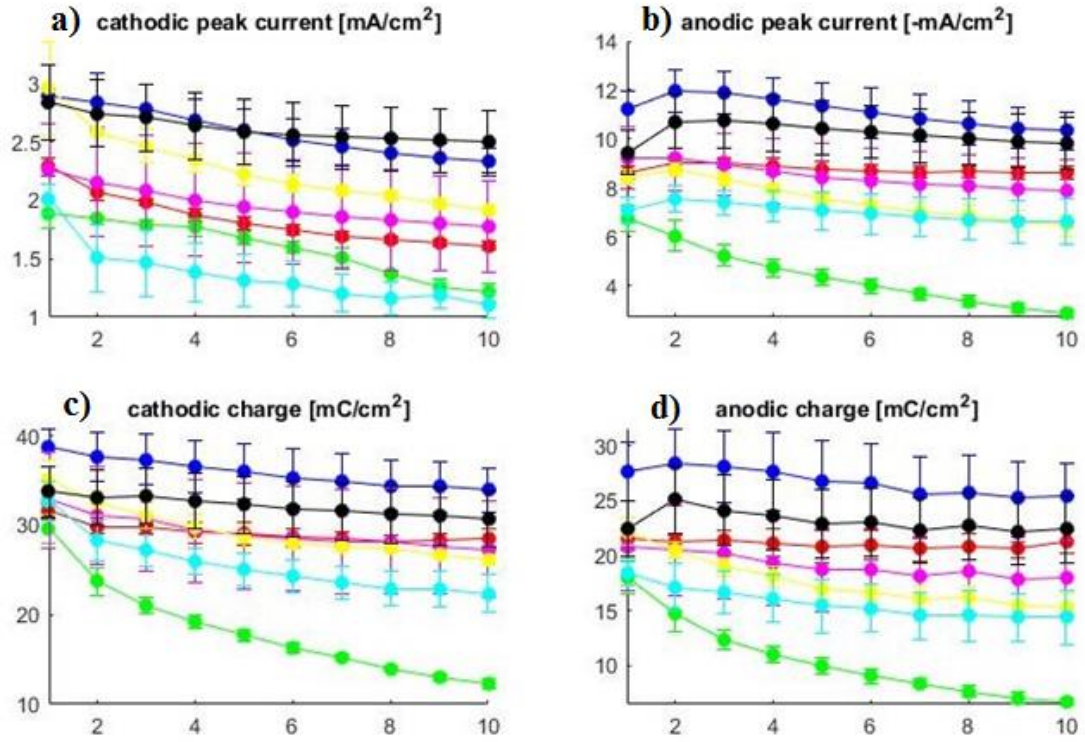


Figure 26 – Electrochemical parameters computed from the CVs of Figure 23, as a function of the cycle number.

### 3.1.3 General considerations about the effect of the additives

The inhibition of the deposition reaction brought by the investigated additives, can be associated to two effects: (i) the kinetic inhibition of the deposition reaction, a purely cathodic effect, and (ii) the formation of a layer of oxides and/or reacted additives which reduce the active area, a process which is influenced both by cathodic (alkalinization by HER or reduction reactions/irreversible adsorption of additives) and anodic behaviour (oxides formation). The following criteria are adopted to establish a ranking of the additives.

(i) reduction of the cathodic Tafel slope in the first cycle → kinetic inhibition of deposition reaction

CTAB < PDADMAC < TBAB<BDMPAC < BPPEI < DMDTDAB=NOADD

(ii)Progressive reduction of cathodic currents with cycling + low $Q_{an}/Q_{cat}$ ratio → increased passivation or inhibiting layer formation.

progressive reduction of cathodic currents:

CTAB < PDADMAC < BPPEI < TBAB = BDMPAC < DMDTDAB < NOADD

Low $Q_{an}/Q_{cat}$ ratio:

CTAB < PDADMAC < BPPEI < TBAB = BDMPAC < DMDTDAB < NOADD

It seems that there is a correspondence between the three effects. hypothesis to explain this behaviour is that both, cathodic inhibition and increased passive layer formation are correlated with the surface coverage and adsorption/desorption rates of the additive molecule on the Zn electrode. Strong adsorption / slow desorption of the additive might impact the passivation of the anode. Of course, thus conjecture will require explicit testing e.g. by spectroelectrochemial methods. The only exception is BPPEI, which brings small inhibition in the first cycles but has a high progressive effect and a low $Q_{an}/Q_{cat}$ ratio, this would confirm its tendency to create a ionomeric film.

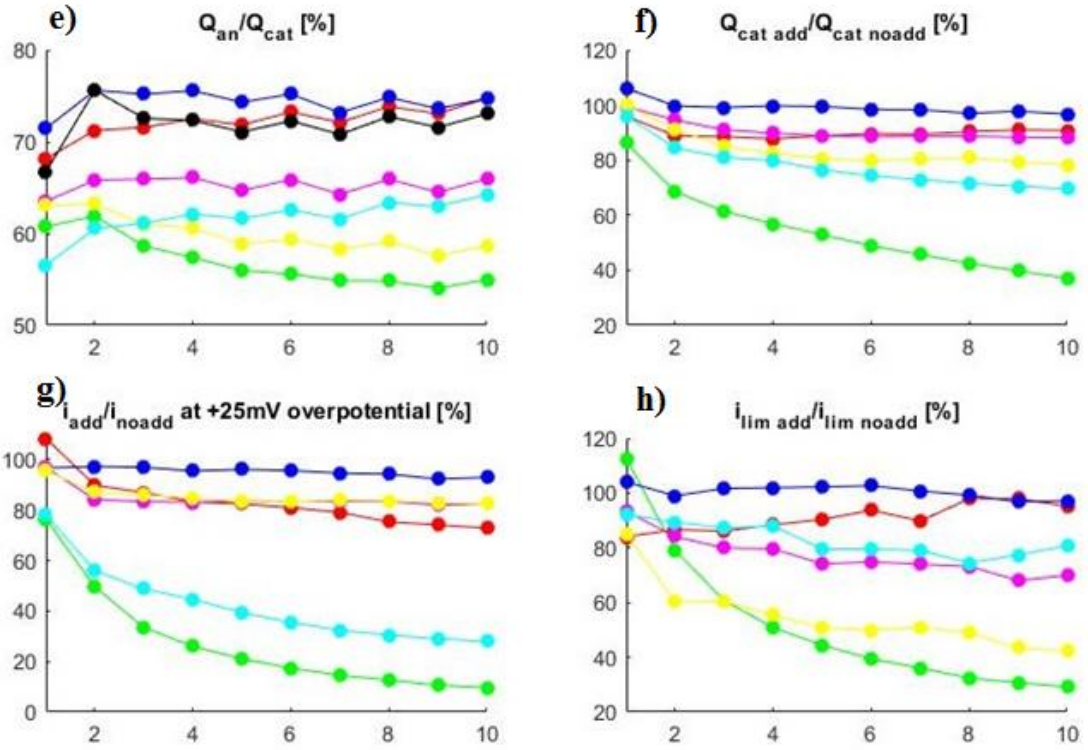


Figure 27 - Electrochemical parameters computed from the CVs of Figure 23, as a function of the cycle number.

## 3.2 Galvanostatic electrodeposition on a graphite support

This experiment aims to study the impact of additives in a range of practically relevant Zn electrodeposition conditions. In fact, the most common case of battery control is of the galvanostatic type. Moreover, galvanostatic growth experiments allow to work with the $Zn^{2+}$ concentrations that are employed in real batteries. The data from the CVs indeed provided useful information of the fundamental behaviour of additives in the electrodeposition and corrosion processes but cannot yield information about the quality and morphology of the

deposits. Prolonged growth experiments (> 10 mAh) were carried for the electrolyte without additives and for the most promising additive: TBAB. Moreover, we also considered the effect of adding 0.1 M $MnSO_4$, that is typically present in ZIB electrolytes. The thick Zn films grown galvanostatically without additive, with $MnSO_4$ and with TBAB were imaged by stereomicroscopy. As already stated in section 2.2 it was not possible to collect the voltage data of this measurement, moreover, the two electrode configuration along with the different conditions of the CE made not significative the voltage value read on the display of the power supply, that was however generally higher in the presence of additives.

### 3.2.1 Galvanostatic electrodeposition from additive-free electrolyte

Even though no positive experimental information of this type has been published so far for Zn electrodeposition from neutral sulphate solutions, deposition on graphite support section (2.2) in absence of additives confirmed the commonly accepted literature vision of metal

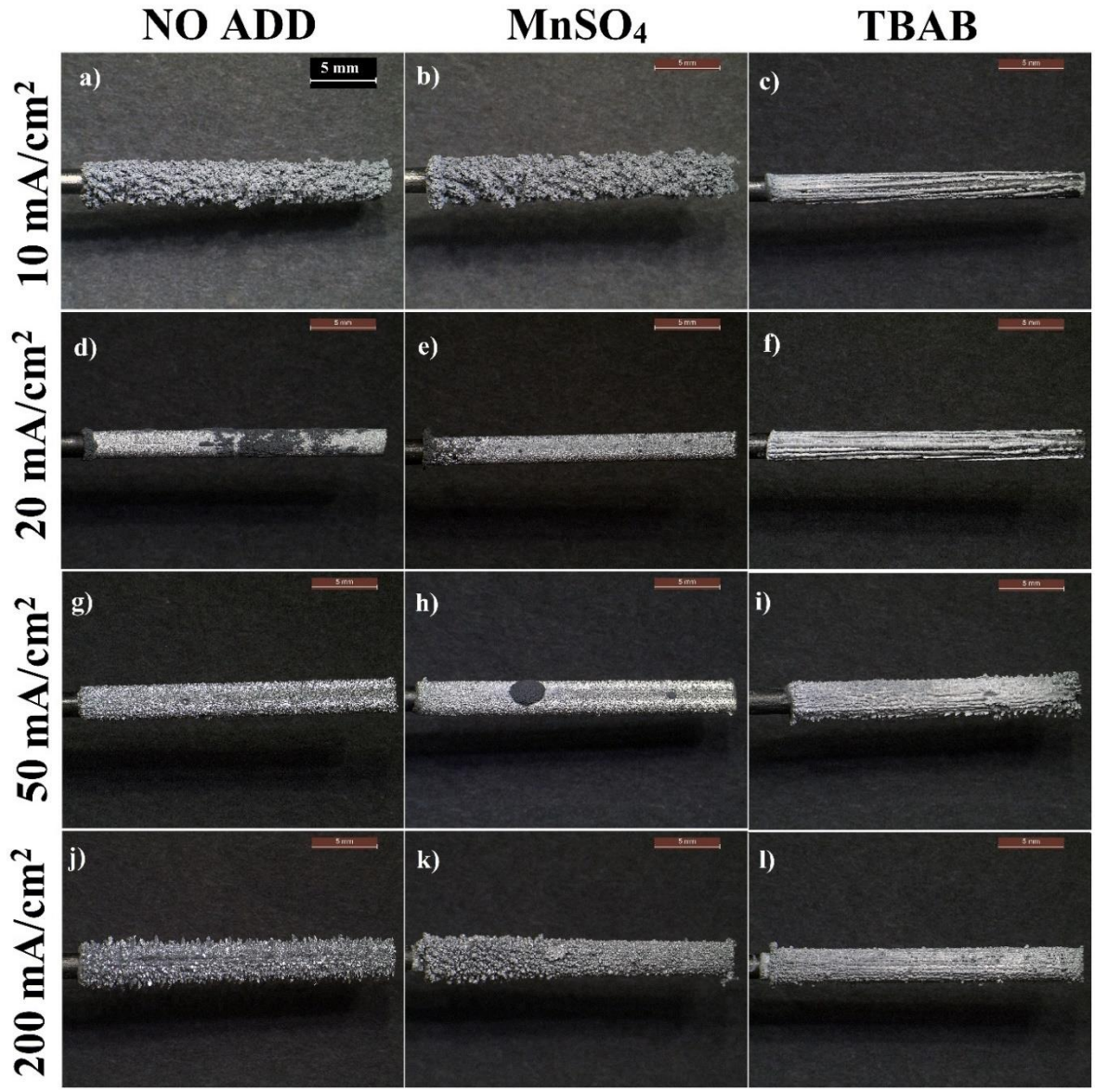


Figure 28 - Stereomicrographs of the Zn deposits on graphite in 2M $ZnSO_4$ electrolyte, from left to right: without additive, with 0.1 M Mn++, with 0.1 g/l TBAB. From up to down: 10 mA/cm$^2$, 20 mA/cm$^2$, 50 mA/cm$^2$, 200 mA/cm$^2$

plating: as CD grows the metal morphology changes progressively from mossy to compact and finally to dendritic. Below 10 mA/cm$^2$ the deposits are fully mossy (figures 28,29,30 a). Imposing 1 mA/cm$^2$ dark and dull grey muddy and non-adherent deposits form unevenly on the graphite support. Instead, at 10 mA/cm$^2$ initially a uniform layer forms, then 3D structures start growing perpendicularly to the electrodes, which are well-adhered to the substrate, but mechanically weaker than the compact structures formed at higher CD. At 20 mA/cm$^2$ a first compact layer forms (figure 28,29,30 d), above which mossy structures start growing after a given deposition time. The same behaviour can be observed in a range of current densities between ca. 15 and 30 mA/cm$^2$. Compact boulder structures, without any sign of dendritic formations grow between 50 and 100 mA/cm$^2$ (figure 28,29,30 g). These deposits are metallic, shiny, uniform, compact and adherent and exhibited an increasing grain size with increasing CD. Above 100 mA/cm$^2$, well defined dendrites start to grow and their density increases with CD. At 200 mA/cm$^2$ the sample was totally covered with dendrites (figure 28,29,30j). These current density values are characteristic of electrodeposition with a free electrolyte, the presence of a separator might modify the

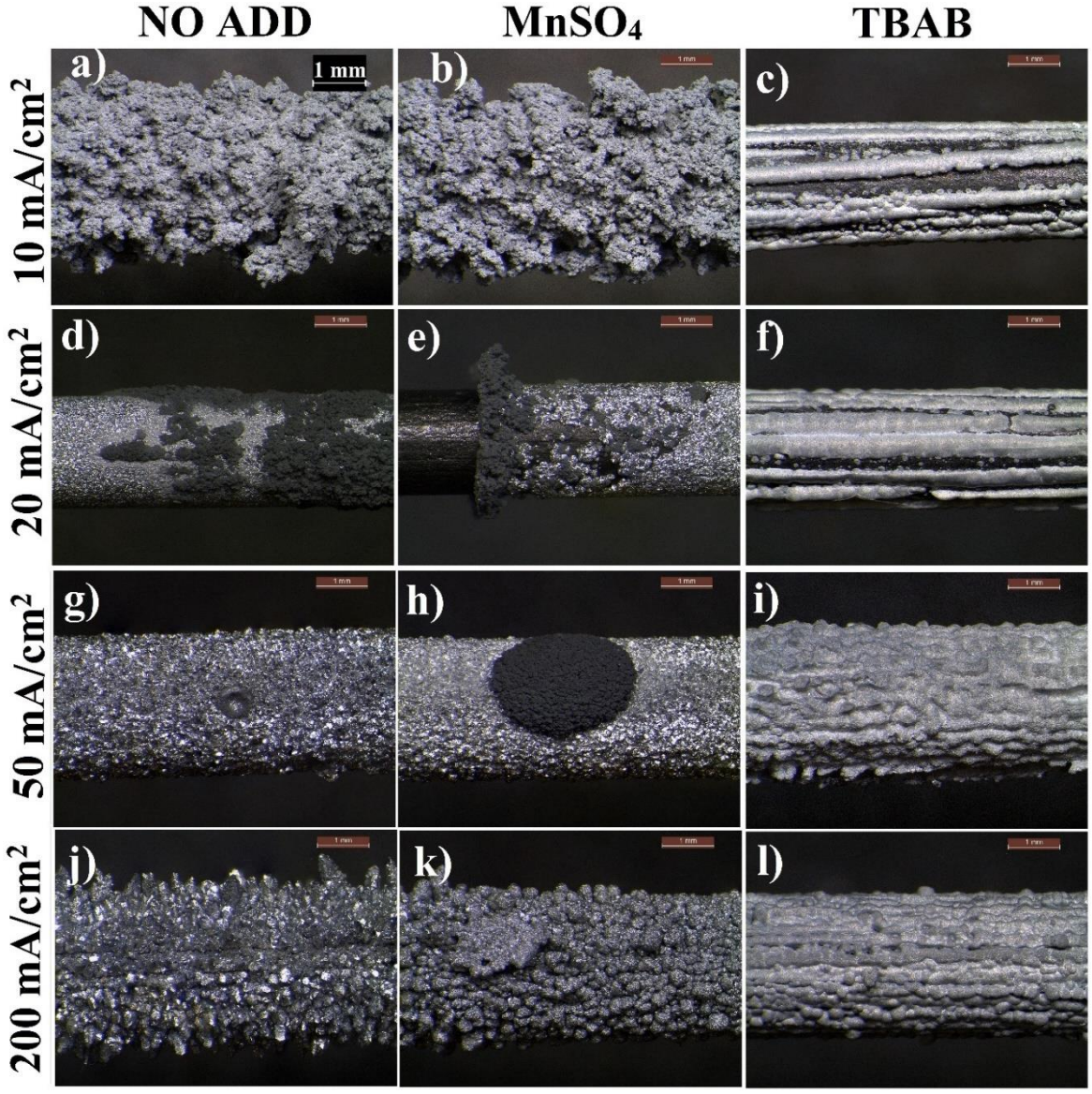


Figure 29 - Magnifications of the stereomicrographs of figure 28.

window in which non-compact structures are obtained. Yet, is worth to underline that, if we consider 50 mA/cm$^2$ as a reasonable upper bound for battery operation, the high current density dendrites do not represent a threat, while the formation of mossy structures is possible basically in all the relevant current conditions. If compared to the results given in [7], there is a marked difference from the alkaline environment, in which dendrites are observed at current sometimes already above 10 mA/cm$^2$, mossy structures on the other hand do not seem to be appreciably affected by the pH of the electrolyte. The theory which states that these dendrites are formed under diffusion control [5], the parameters of the deposits in alkaline environment at different zincate concentrations in [7] and these observations of this work, jointly suggest that the lower tendency to form high current density dendrites in acid environment is mainly due to the higher concentration of Zn ions (generally 20 times higher section(1.3.4)) that can be more readily achieved in non-alkaline conditions. [78]

Changes in the refractive index of the electrolyte developing during electrodeposition, both in the presence and in the absence of TBAB, witness that concentration gradients develop in

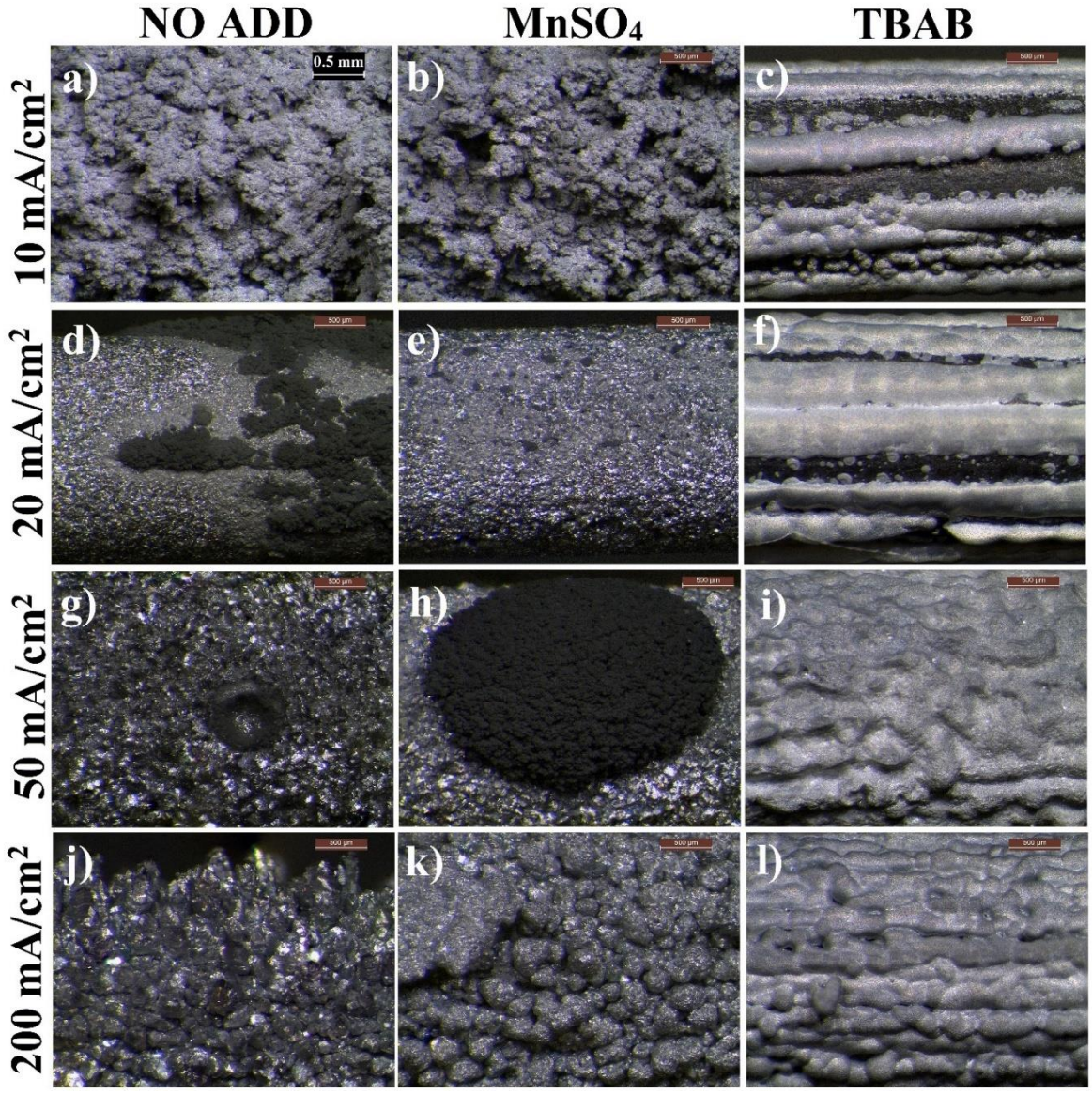


Figure 30 - Magnifications of the stereomicrographs of figure 28.

the cell. In fact, increased $Zn^{2+}$ concentration close to the anode gives rise to electrolyte stratification and convective flows, as a function of the collocation of the electrodes. In the cell geometry adopted in this work, electrolyte stratification prevails, with higher $Zn^{2+}$ concentrations towards the bottom of the cell. It can be noticed that the dendrites, forming at high current densities, are more developed at the top of the electrode fig (28j), where the diffusion control sets in at lower CD levels.

### 3.2.2 Galvanostatic electrodeposition from $MnSO_4$-containing electrolyte

The addition of 0.1 M $MnSO_4$ brings about some slight, but well defined, morphology changes. Mossy structures at low CD are similar to those found without $Mn^{2+}$ (figure 28,29,30 b), the CD required to obtain compact deposits is the same, although large aggregates of mossy structures can be observed up to 50 $mA/cm^2$ (figure 28,29,30 h). The dendrites forming at 200 $mA/cm^2$ were of different shape, smaller and with a less sharp tip. At such high CDs co-deposition on Mn metal happens along with Zn, is expected, influencing the morphology of the deposit [74-77]. The effect of a significant amount of this ion is not as strong as the effect of small amounts of QAS additives (see next), still is not negligible, in particular it could be detrimental for the formation of mossy structures. Further studies evaluating the combined effect of $Mn^{++}$ and QAS might have to be taken into consideration.

### 3.2.3 Galvanostatic electrodeposition from additive-containing electrolytes

A scheme of the morphologies obtained as a function of the c.d. in the presence of additives is provided in figure 31. A complete suppression of mossy structures at low CD is achieved by TBAB, PDADMAC and CTAB. These additives were tested also at 1 mA/cm$^2$ and were found to enable the growth of compact deposits also in this critical condition. Some degree

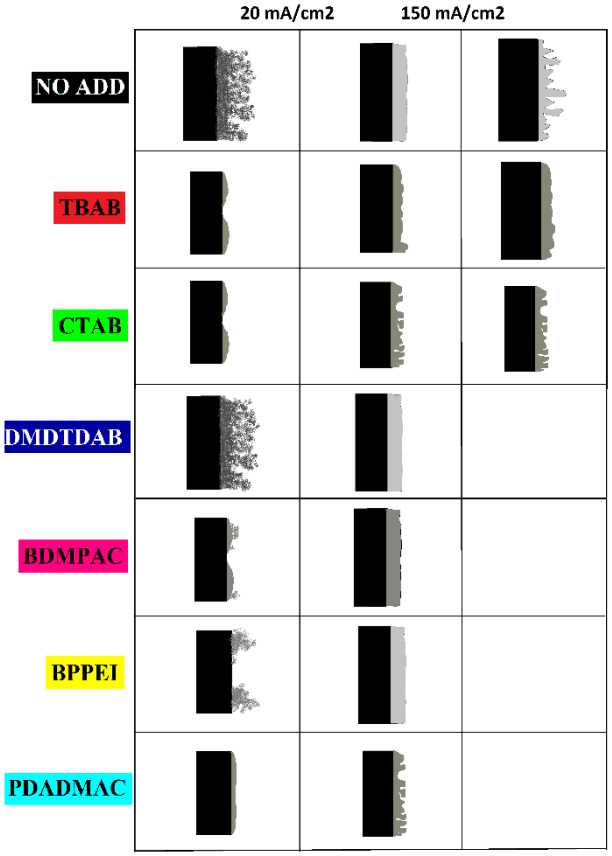


Figure 31 - Qualitative representation of the Zn deposits on graphite with all the additives.

of mossy structures prevention is show also by BDMPAC, while BPPEI and DMDTDAB deposits showed no appreciable improvement with respect to the additive-free electrolyte: this behaviour is consistent with the lower concentration of the former and the low CMC of the latter.

All the stereomicrographs of deposits from TBAB-containing solutions showed vertical patterns in the whole CD range, that were not found in the absence of the additive. These patterns might correlate with electrolyte flow by convection under the $Zn^{2+}$ concentration gradient, developing with vertical electrodes. The fact that an additive effect is triggered by electrolyte flow points towards the partial cathodic current mechanism of smoothing by additives.

While without additive the deposit was uniform, the morphologies obtained at 50 mA/cm$^2$ in the presence of additives often present irregularities and tridimensional structures. This is the case of TBAB (figure 28 i) and of PDADMAC and CTAB, the additives with the best performances in terms of mossy structures suppression. It is worth noticing that the deposit

in the presence of PDADMAC at 10 mA/cm$^2$ was more uniform than that from TBAB in figures (28,29,30 c), the graphite was not exposed, and vertical patterns were barely observable, anyway the deposit observable at 50 mA/cm$^2$ was more irregular than that from TBAB-containing solutions.

The deposit obtained with TBAB at 200 mA/cm$^2$ (figures 28,29,30 l) is far less dendritic than that obtained at the same CD without additive. Interestingly is more regular also than the one obtained with TBAB at 50 mA/cm$^2$, presumably, owing to higher nucleation rate.

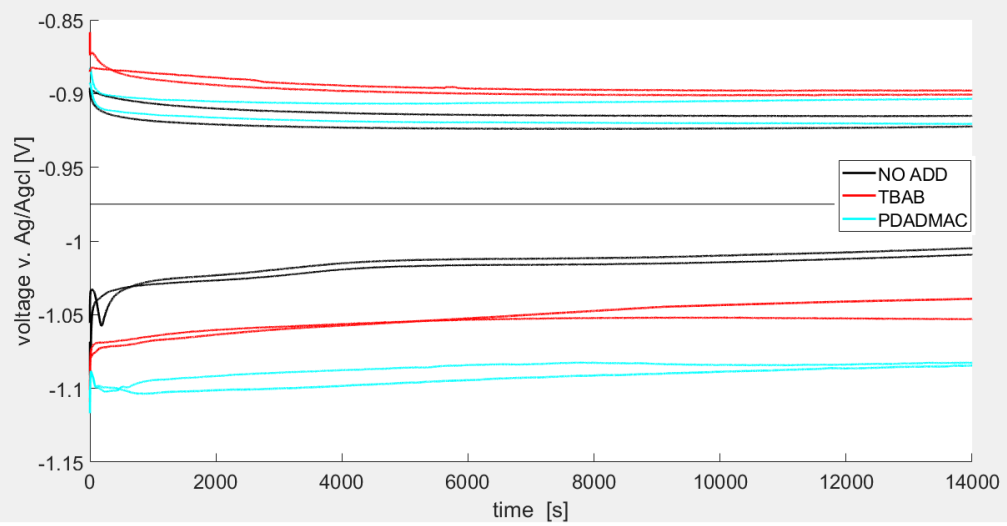


Figure 32 - Voltage profile of the galvanostatic depositions (down) and dissolution (up) on Zn substrate at 10 mA/cm$^2$.

Figure 32 reports the cathodic and anodic chronopotentiometric traces corresponding to galvanostatic measurements obteained with the experiment in section 2.4 carried out in solution without additive and with the two most prospective QASs: TBAB and PDADMAC, a picture of the galvanostaticlally obtained samples is given in figure 33.

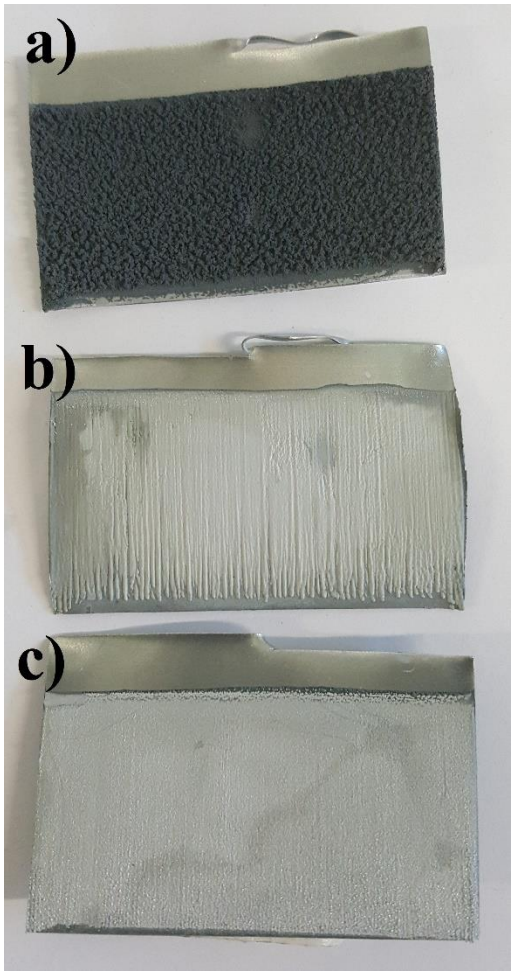


Figure 33 - Samples of Zn galvanostatically deposited at 10 mA/cm$^2$ for four hours, a) without additive (mossy structures), b) with TBAB (vertical patterns), c) PDADMAC (no vertical patterns).

The deposition without additives is characterized by an initial fast (range of ca. 100 s) decrease of the cathodic overvoltage, associated with Zn nucleation. Subsequently, After 1000s, the nucleation phase is complete, the cathodic overvoltage keeps decreasing due to increase in effective electrode area associated with the formation of mossy structures.

The presence of TBAB and PDADMAC results respectively in a rise of the overpotential of ca. 50 and 100 mV, respectively. This is consistent with the results from the CVs in section 3.1.2. In the presence of the additives, the nucleation interval is less evident and the overvoltage decrease rate corresponding to roughening is smaller than in the absence of the additive, indicating a lower increment in electrode area, corresponding to the suppression of mossy structures. The decrease of the overvoltage was visible, observed in the presence of additives can be associated with the active area increment due to the formation of compact vertically oriented structures, similarly to those described in section 3.2.3.
The galvanostatic dissolution of Zn also starts with a decrease of the anodic polarization on the timescale of a few hundred seconds, that can be ascribed to the buildup of a gradient of corrosion product in the electrolyte, resulting in ennobling. Longer-term decrease of anodic overvoltage can again be described in terms of electrode roughening, reaching an asymptotic value. The impact of the additives on the anodic overvoltage is smaller than that on the cathodic one, and – coherently with CV results, the presence of additives brings about an

increase in anodic polarization, with PDADMAC giving rise to lower overvoltages that TBAB.

## 3.3 Galvanostatic cycling at 1 mA/cm$^2$

In order to gain understanding of the behaviour of Zn electrodes in real operating conditions, we carried out a series of cycling test in split cells, that reproduce exactly the conditions of a coin cell, though with more flexibility in terms of mounting and access to the different components.

### 3.3.1 Galvanostatic cycling at 1 mA/cm$^2$ in the absence of additives

The measurement without additive showed a cell potential of ca. 100mV (figure 35), the voltage profile is symmetrical. This does not always happen in symmetrical cells cycling in the presence of additives, the asymmetry can be generated by gravitational phenomenon like those described in section 3.1.2. In this case, however, the influence of gravity seems to be minor, probably because at low currents (1 mA/cm$^2$) the creation of concentration gradients is slower and is compensated by diffusion.
After 90ks there is a potential build-up for 3 cycles (figure 36), this is associated to the passivation of the metal during anodic polarization, which is probably favoured by the slow alkalinization of the electrolyte happening with HER during the whole previous period.
When the potential reaches 2.6 V it suddenly drops to 200 mV, after which it keeps switching from + to -200 mV with an irregular signal disturbed by frequent potential spikes. The sudden drop is associated with the breakdown of the passive layer, this might be due to the overcoming of the passive breakdown potential, but also to a local re-equilibration of the electrolyte pH after the acidification of the solution caused by OER. After the breakdown of the passive layer the voltage applied to the full cell is almost doubled, meaning that probably the breakdown is imperfect and local, and most of the zinc surface is still insulated, hence the deposition is happening with increased current densities in a reduced portion of the area. After two cycles in this condition the cell short circuits, as indicated by the sudden drop to very low potentials, comparable to those yielded by the resistance of the series of ohmic contacts between metallic components of the cell and of the measurement circuitry. The short circuit happening soon after the passivation breakdown can also be explained by the local increment of CD described above: the increased deposition in one spot causes the formation of a tip and then of a tridimensional structure which short circuits the cell.
The images reported in figures (37,38,39 a) show SEM micrographs of the cell cycled without additives. This exhibits a low surface number density of crystallites, growing on the background of the corroded Zn foil, this morphology suggests a low nucleation rate, as expected in a process carried out at low current densities. The crystallites are covered with ZnO crystals, presumably formed by precipitation as described in section 1.1.3.

### 3.3.2 Galvanostatic cycling at 1 mA/cm$^2$ in the presence of additives

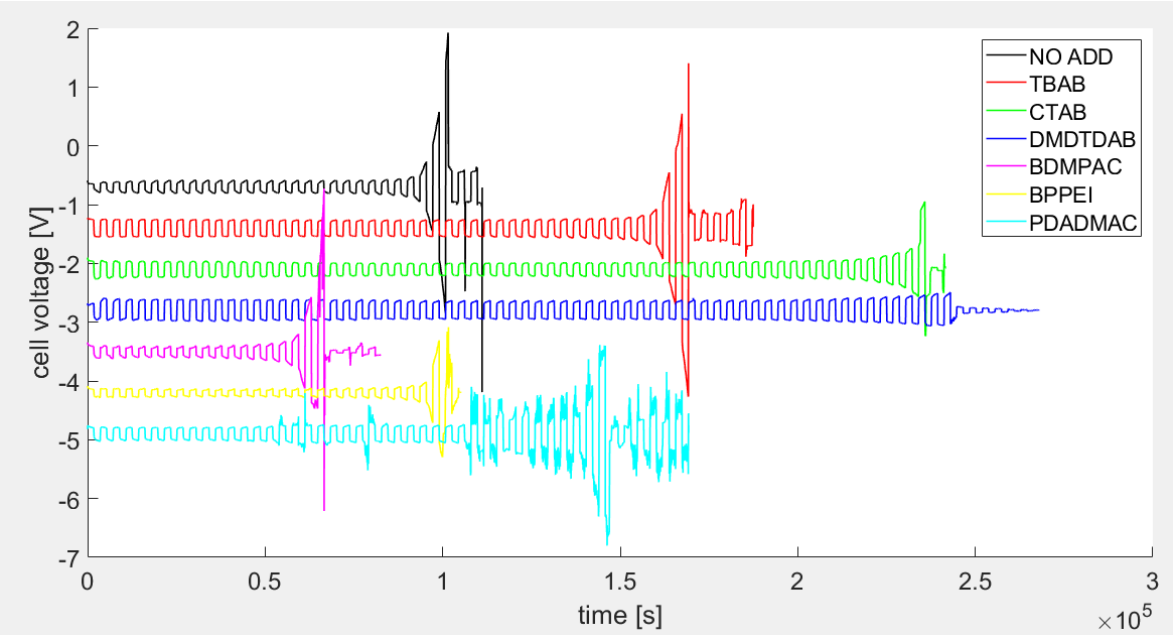


Figure 34 - Voltage profile of the symmetric cell cycling at 1mA/cm2 in 2M ZnSO4, with and without additives.

Even though the additives (with the exception of BDMPAC) demonstrated to increase the cell lifetime, this is not an improvement as radical as the one found in alkaline systems (as pinpointed in a work of our group that will be soon published), moreover, within the limits of the research carried out in this thesis, the time to failure time does not seem to be highly reproducible in the conditions investigated.
SEM images of the cycled samples confirmed the ability of TBAB and PDADMAC to suppress the formation of the tridimensional structures that are characteristic of operation at low current densities, also with the alternation of cathodic and anodic polarization. This is

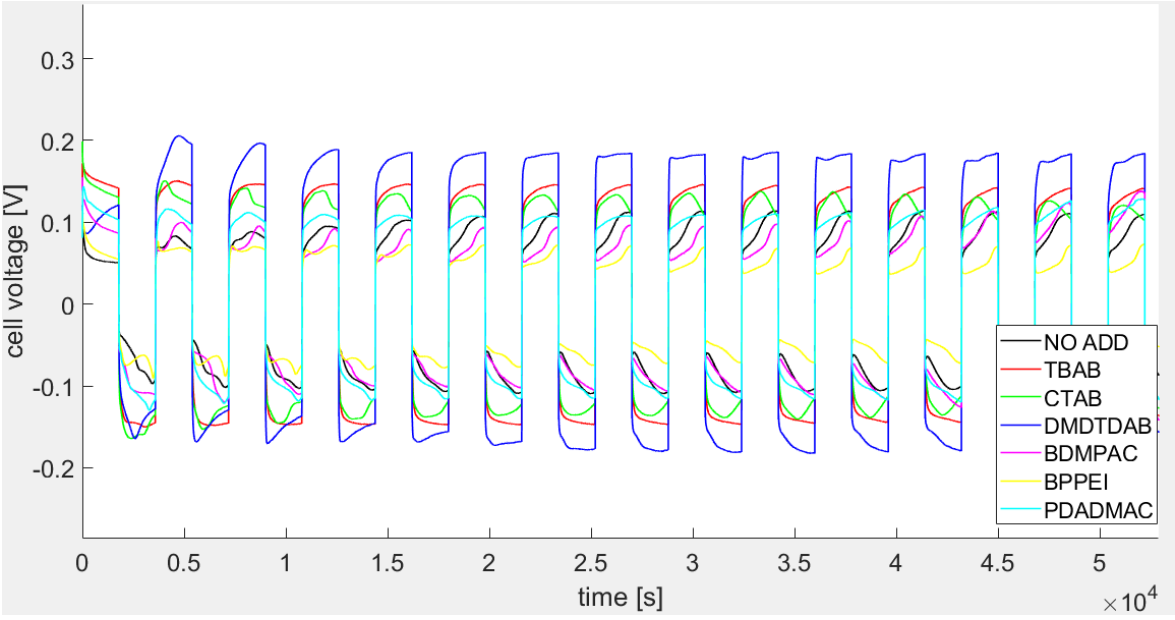


Figure 35 - Voltage profile of the symmetric cell cycling at 1mA/cm2 in 2M ZnSO4, with and without additives. First 13 cycles, before any sign of passivation.

not the case of CTAB, DMDTDAB, and BDMPAC, in which macroscopic structures grew bigger than in the absence of additives: no mossy structures were found, but rather vertically growing compact formations, which were not observed in cathodic depositions without the alternation of dissolution periods.

Below, we discuss the performance of each additive separately.

**TBAB**
TBAB shows a polarization that is 50 mV higher than in the additive-free system; the passivation, passivation breakdown and short circuit behaviour is similar to that observed without any additive. The SEM images however, reveal many differences: there are no sparse nuclei and the deposit is uniform: this is coherent with the increased nucleation rate, that is a typical effect of this additive (see section 1.2.1). Also in this case precipitated oxides crystals can be observed, which are in this case evenly distributed on the surface. In addition, fewer tridimensional structures can be noticed than in the case without additive. Micrographs at higher magnifications (figure 37b) show boulder like zinc electrodeposits and highlight that also the distribution of precipitated oxides is more even. This shows that at this CD TBAB allows a better distribution of the current and a more even deposit.

**CTAB**
CTAB shows high overpotentials, 150 mV, coherently with the CVs, and fails by short circuit soon after a slow potential build up. SEM micrographs show that the structures which lead to the short circuit are not mossy ones, but rather compact columns growing disorderly along multiple crystallographic directions. The background in which these features form, is deeply affected by corrosion, also exhibiting pits.

**DMDTDAB**
DMDTDAB, among the investigated additives, exhibits the highest overpotential and enables the longest cell lifetime, terminated by a short circuit preceded by limited passivation. SEM micrographs exhibit sparse nuclei forming on the background of the corroded Zn foil, similarly to the system without additive. At variance with the morphlogies developing in the additive-free case, oxide precipitates cannot be observed on the electrodes cycled in the DMDTDAB-containing electrolyte and the crystallites are similar to those forming in the presence of CTAB.

**BDMPAC**
As in the CVs, in the electrochemical cycling measurements BDMPAC shows small differences with respect to TBAB. SEM images, however, reveal different morphologies between BDMPAC and TBAB: the surface here completely covered with a precipitated oxides layer and some tridimensional outgrowth features can be noticed.

**BPPEI**
BPPEI exhibits a cycling behaviour an SEM morphologies that are very similar to those observed in the additive-free system, consistently with the cathodic CV behaviour that exhibits negligible effects of this additive at low CDs.

**PDADMAC**

PDADMAC has a polarization that is fully consistent with the CV behaviour and it presents random potential spikes, that were not observed with the other electrolyte chemistries investigated: this suggests the passivation behaviour prevailing in the presence of this additive exhibits some peculiarities that warrant further investigation. We stopped this measurement after a relatively long testing time, before it exhibited a tendency to short circuiting. SEM micrographs shows that the deposit of PDADMAC is highly uniform at low magnifications, coherently with the outcomes of GS growth tests: imaging at higher magnifications (figures 37,38 g) showed a deposit with morphologies that are similar to those found in the presence of TBAB.

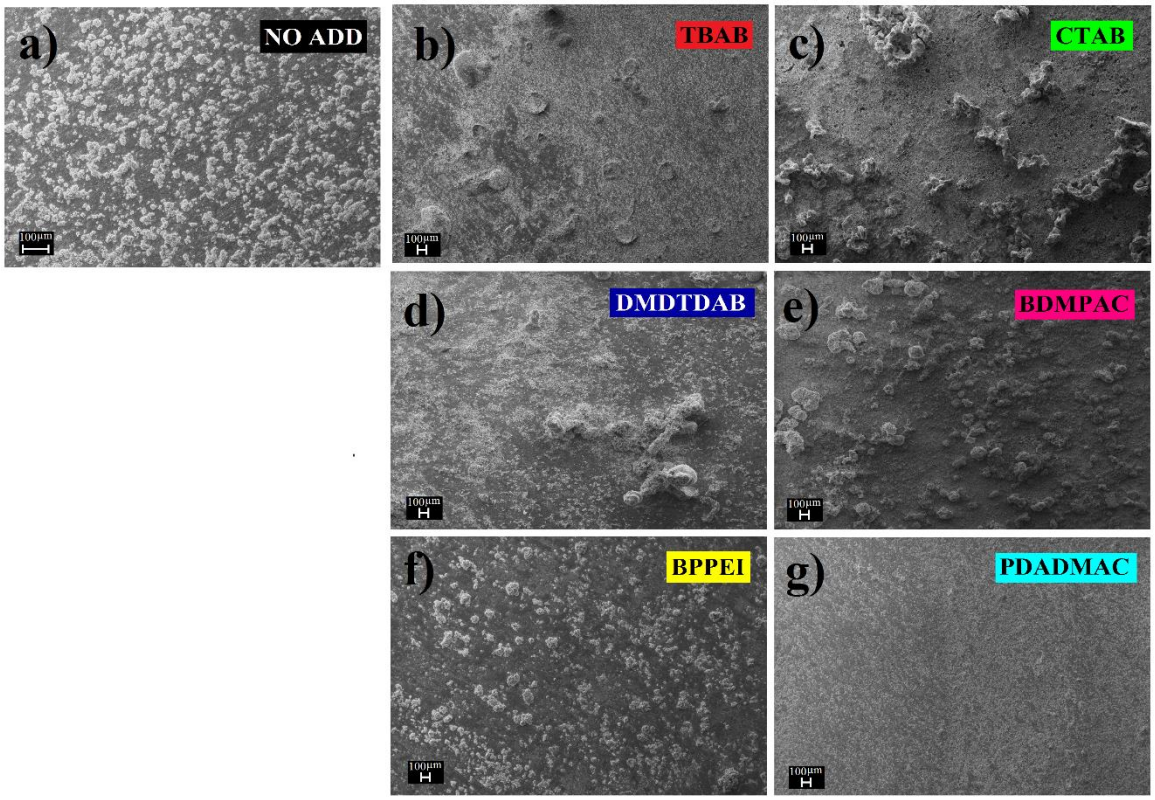


Figure 36 -100X SEM images of the cycled samples of figure 34.

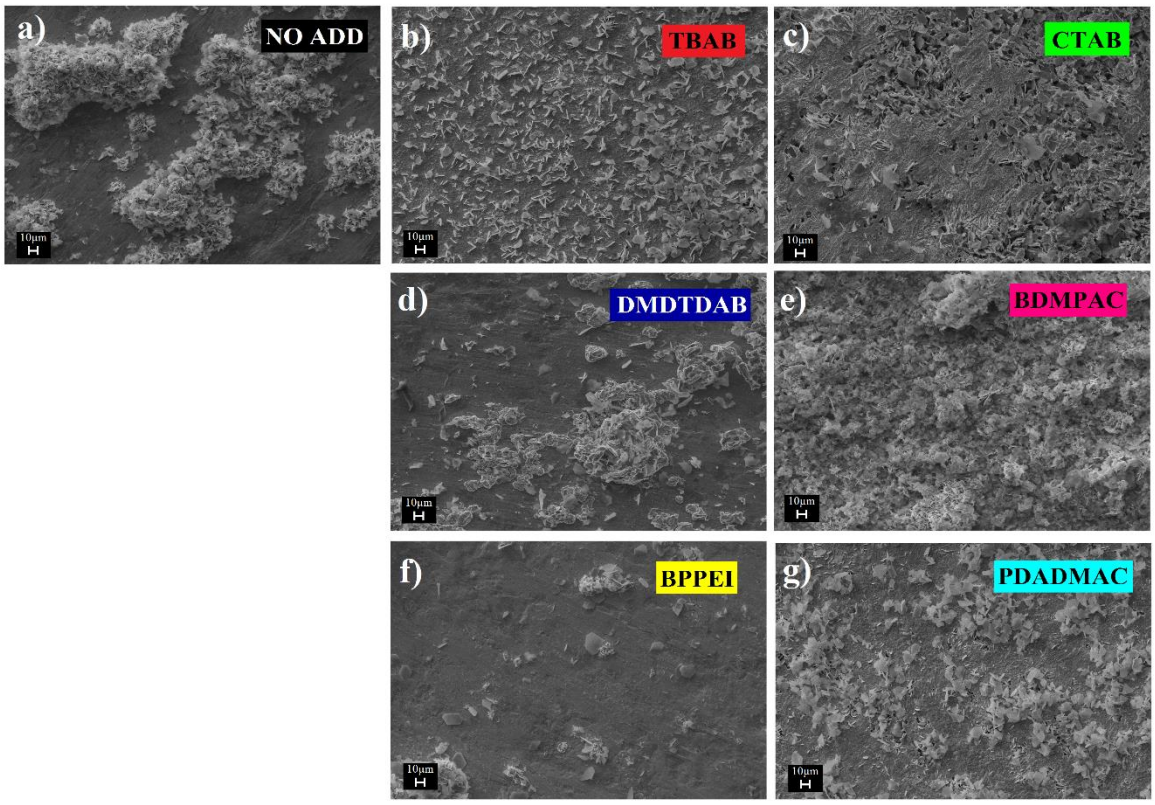


Figure 37 - 1000X SEM images of the cycled samples of figure 34.

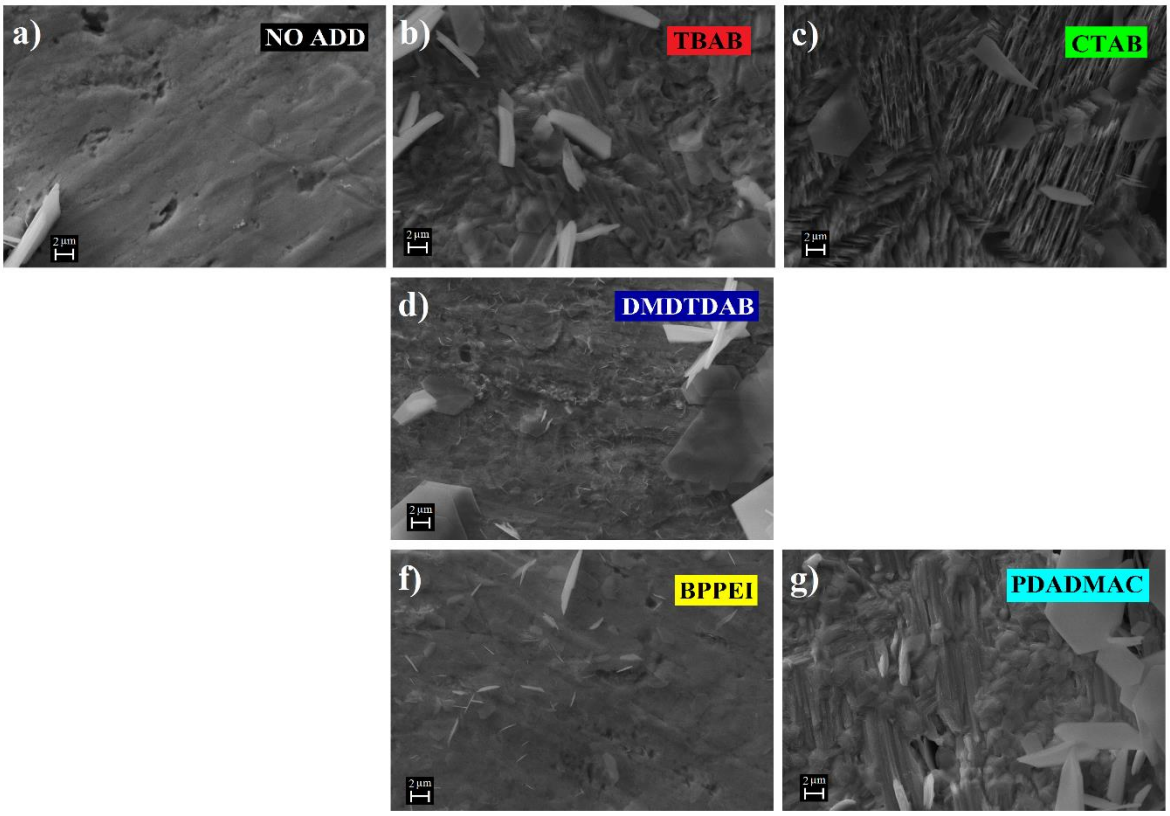


Figure 38 - 10000X SEM images of the cycled samples of figure 34

## 3.4 Cycled cell tomography

The method of election to follow morphology evolution of metal during an electrochemical process is *in situ* computed X-ray tomography. This technique allows to obtain a tridimensional reconstruction of the metal deposit with a good resolution in the intact reaction ambient and configuration. We resorted to this approach to gain in-depth understanding of the impact of the single most prospective additive on Zn cycling under representative battery conditions.

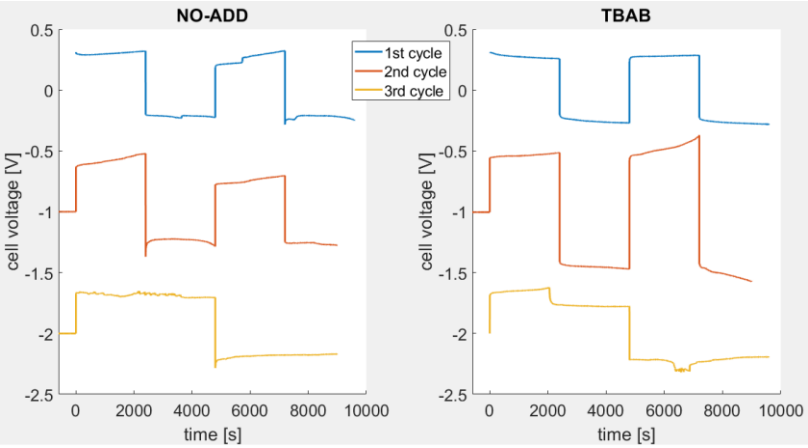


Figure 39 - Voltage profile of the electrochemical treatment on the tomography cells. Left: in 2M $ZnSO_4$. right: in 2M $ZnSO_4$ +0.1 g/l TBAB.

### 3.4.1 Case without additives

The voltage/time curves of the electrochemical treatments to which the tomography cell was subjected are represented in figure 39. The current densities employed for these cycling tests correspond to mild stress conditions for a practical reversible Zn cell, at variance with the experiments reported in section 3.3, were practically relevant low-stress conditions were instead selected. In addition, the cell geometry is different from that of the split cells used for the cycling experiments described in section 3.3 and, moreover, the current density on the two electrodes is not equal, as detailed in section 2.5.1 Nevertheless, the potential response to cycling with the different electrolytes is in line with the split-cell results. In particular, it is worth observing that no sign of passivation or short circuit could be spotted during these tests.

The 3D reconstructions refer to a representative section of each of the two cells. In the pristine cells, the internal and external electrodes were grown separately in four electrodeposition runs, carried out under nominally identical conditions: the observed differences in roughness correspond to the intrinsic variability of the process.

In the experiment carried out in the absence of additive, the morphology evolution of the inner rod during the first two cycles (figure 43,44) indicates progressive coarsening, with the formation on the whole surface of compact, tridimensional structures with a thin base, in addition a few isolated dendrites can be noticed. An interesting feature of the deposit after the second cycle, highlighted with the thin section in (figure 41), is that in some areas there is the formation of a crust which covers the original deposit leaving a cavity between the two. After the third cycle (figure 44d) the deposit results at least 30% thinner than the original one, with many particles of dead Zn close to the electrode surface, but detached from it. It is possible that the observed capacity loss happens because the thin bases of the structures visible after the second cycle dissolve faster than most of the rest of the structure, which disconnects from the electrode.
In figures 45 and 46 it is possible to observe that mossy structures form on the surface of the outer wall during the first two cycles. In the tomograms they appear as darker areas on the deposit surface. Thanks to their lower density, image analysis allows to segment off mossy structures from compact Zn, allowing to appreciate their complete space distribution (figure 41). Note that the formation of mossy Zn was expected at this CD (section 1.1.4). The holes already present on the pristine deposit (figure 45a) becomes larger after the first two cycles (figure 45c), and the thickness of the deposits clearly decreases, possibly owing to the detachment of mossy deposits. After the third cycle however (figure 45d) , the amount of mossy Zn on the external surface seems to be lower than after the second cycle and the deposit appears slightly thicker, correlating with the larger DOD.

### 3.4.2 Case with TBAB

In the experiment carried out with TBAB addition to the electrolyte, after the first cycle the roughness and the porosity of the deposit is increased (figure 43,44 f), with the formation of cavities, similarly to what happened after the second cycle in the deposit without additive. During the second cycle the potential trace shows (figure 39), after ca. 7000 s, a rise in potential: it is possible to relate this to an incipient passivation of the anode, which in that moment was the inner rod. After the second cycle the deposit appears profoundly modified (figure 43,44 g), some areas of the graphite substrate are exposed, and the surface is covered with large tridimensional structures with a thin base. After the third cycle the deposit on the internal rod underwent through major changes (figure 43,44 h). The chronopotentiogram (figure 39) shows a drop after ca. 2000s, which indicates the formation of an internal short circuit: the voltage measured in these conditions correspond to typical ohmic contributions of the contacts and graphite. From the 3D reconstruction, the short circuit can be visualized: most of the deposit on the inner rod has disconnected from the electrode and the resulting Zn particles accumulated in the electrolyte, causing a temporary and local short circuit, terminated by corrosion or decohesion of the contacting Zn objects, as witnessed by the behaviour of the potential trace after ca. 6000 s. Similar phenomena were observed in split cell test with CTAB and BDMPAC, see figure (34) in section (3.3.2). Differently from the inner rod, the pristine deposit on the outer wall of the TBAB cell was similar to that in the cell without additive. On the outer wall, after the first two cycles, no sign of mossy Zn formations is present: the deposit morphology is in fact smoother than that of the initial condition and thinning of the deposit was not clearly appreciable. After the third cycle the outer deposit exhibits only slight changed with respect to the condition observed after the second one, confirming that shorting derives from the morphology evolution of the inner rod.

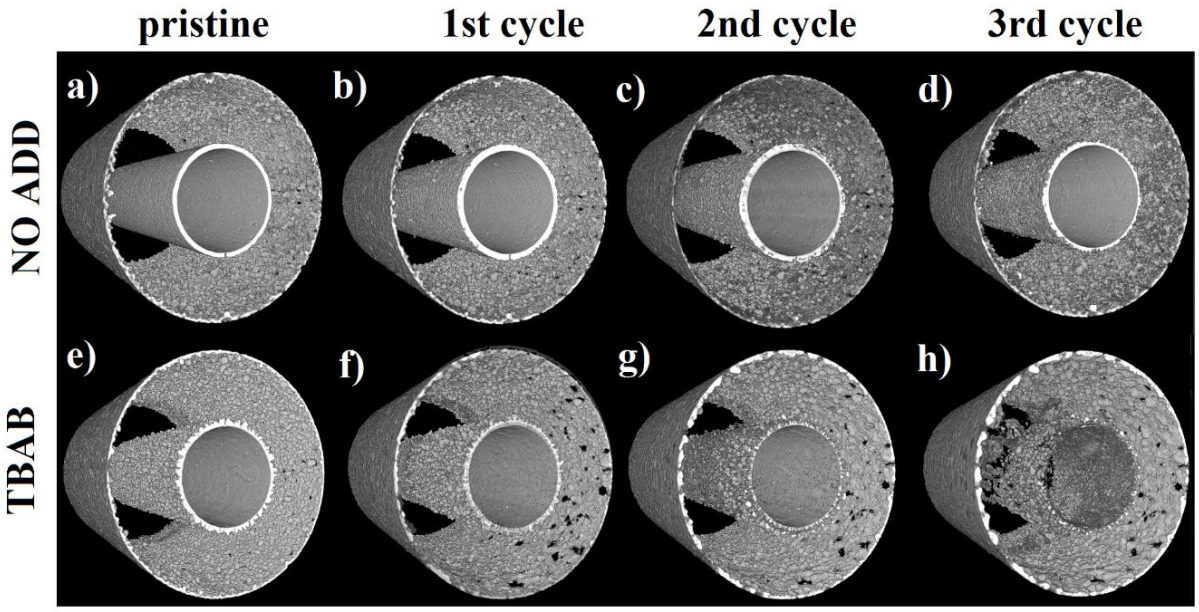


Figure 40 - 3D reconstruction of the inner rod deposit. Up: in 2M $ZnSO_4$. Down: in 2M $ZnSO_4$ +0.1 g/l TBAB. From left to right: pristine cell, after 1st cycle, after 2nd cycle, after 3rd cycle.

Figure 41- A thin section of the deposit on the inner rod of the cell without additive after the second cycle. It is visible that in this area the new deposit formed a crust above the previous layer, leaving a cavity in between.

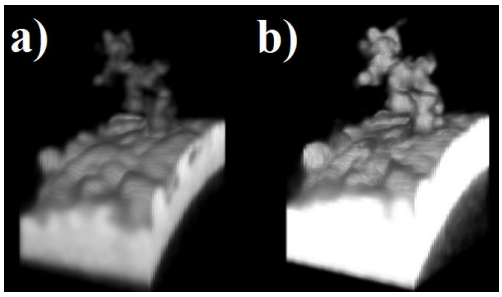


Figure 42 - A lonely mossy structure evolution on the inner rod after the last cycle on the cell without additive. In the image in the left the difference in density of this structure is appreciable thanks to its darker color. On the right the same structure with different parameters settings of brightness and luminosity allows to appreciate the full shape of the structure.

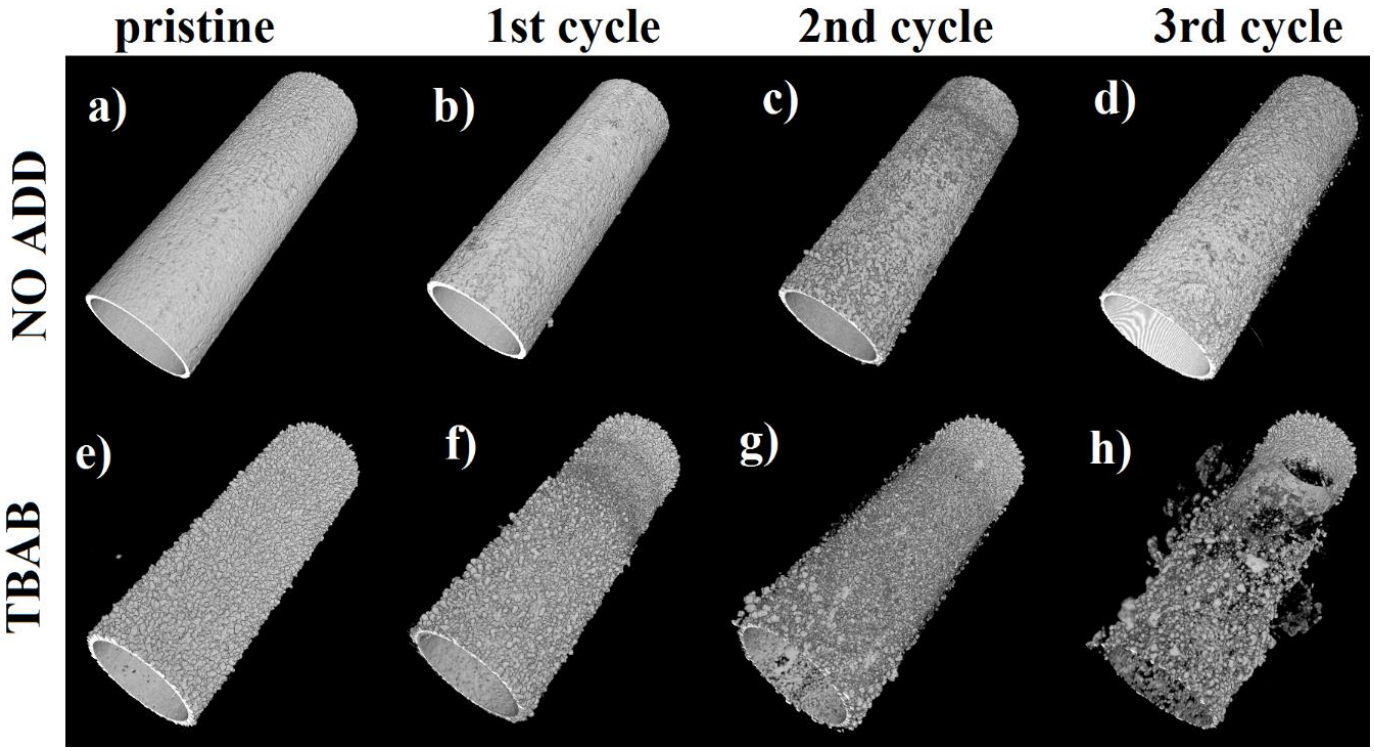


Figure 43 - 3D reconstruction of the inner rod deposit. Up: in 2M $ZnSO_4$. Down: in 2M $ZnSO_4$ +0.1 g/l TBAB. From left to right: pristine cell, after 1st cycle, after 2nd cycle, after 3rd cycle.

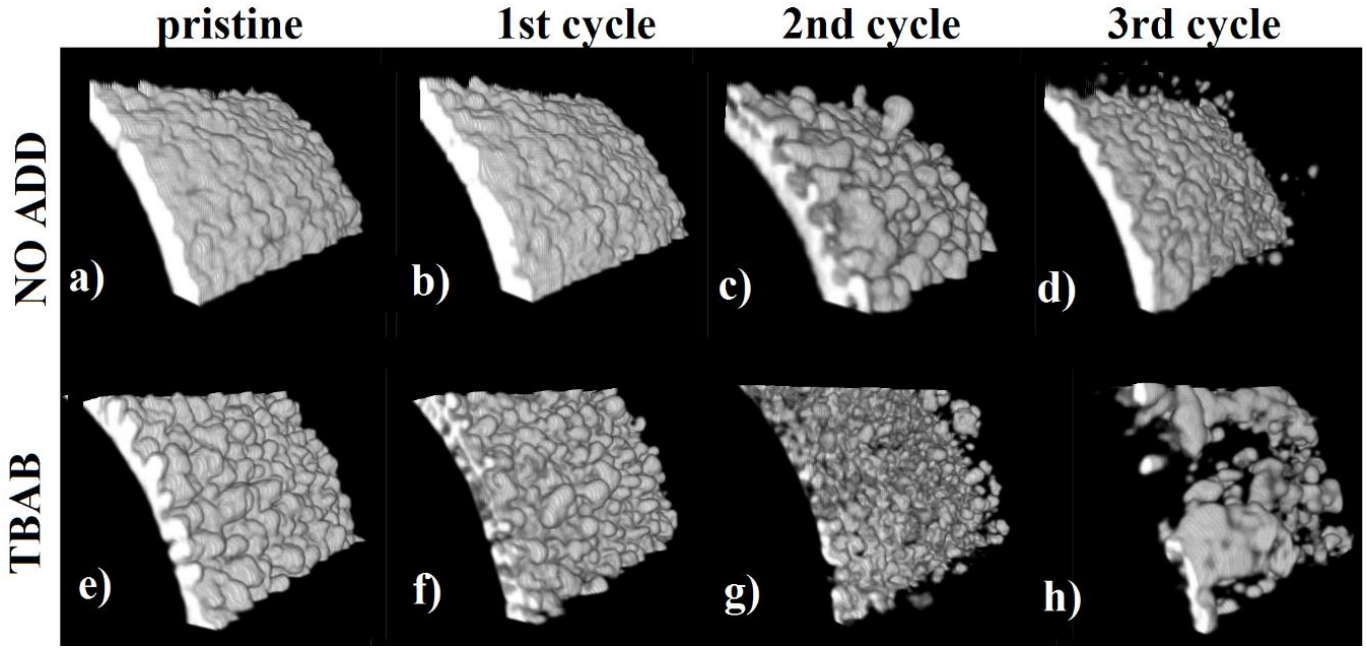


Figure 44 - A 1x1 mm section of the same area from the deposit in figure 43.

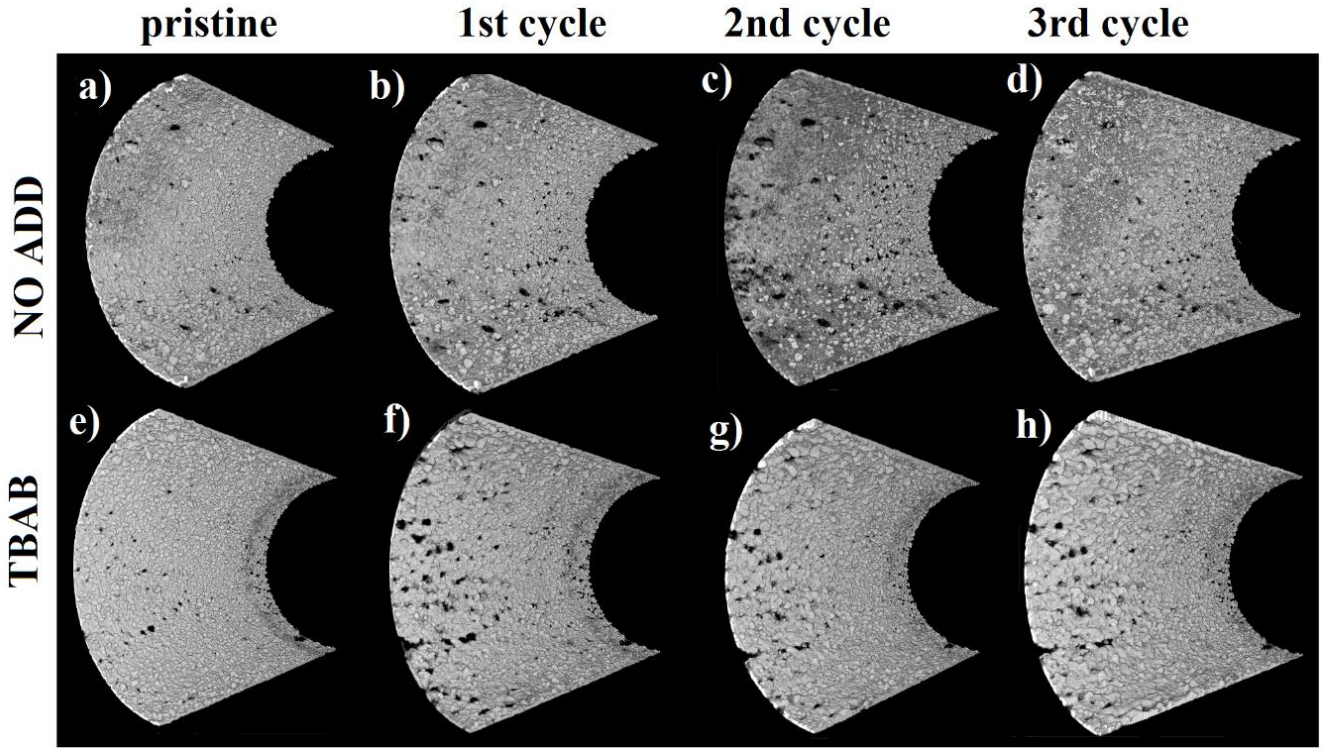


Figure 45 - 3D reconstruction of the outer wall rod deposit; Up: in 2M $ZnSO_4$. Down: in 2M $ZnSO_4$ +0.1 g/l TBAB. From left to right: pristine cell, after 1st cycle, after 2nd cycle, after 3rd cycle.

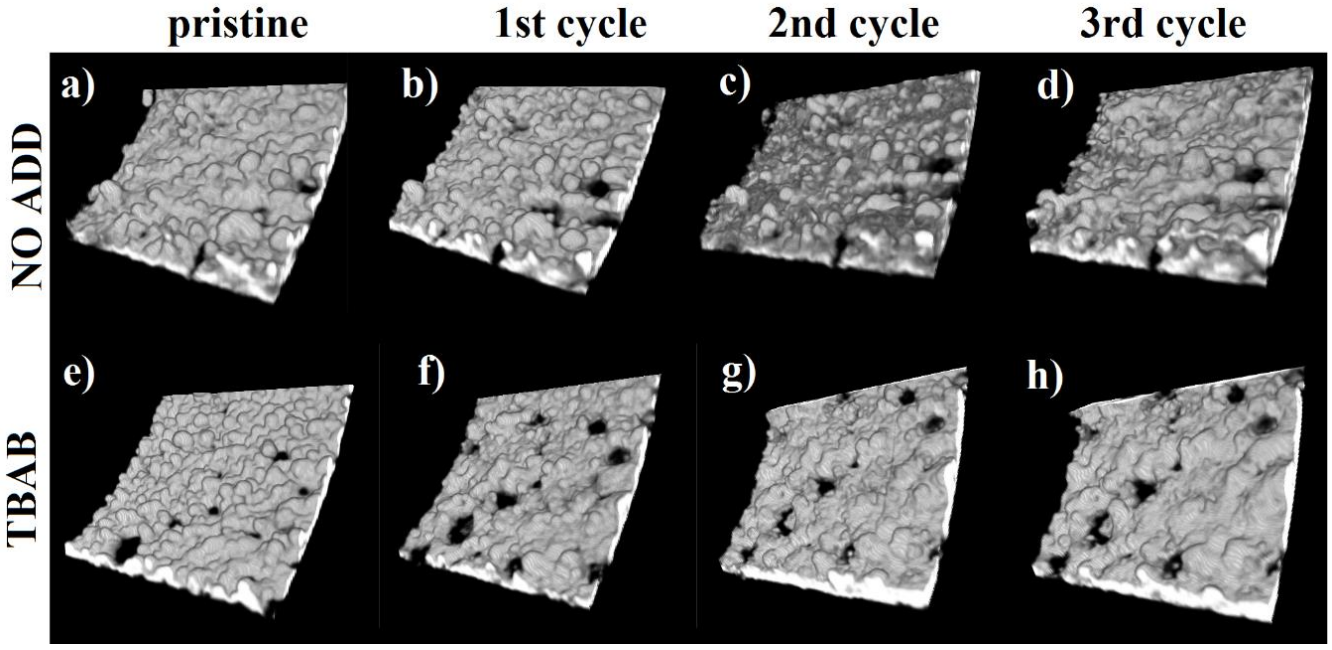


Figure 46 - A 1x1 mm section of the same area from the deposit in figure 45.

# Chapter 4
# Conclusions

In this work I concentrated on the electrochemical behaviour of Zn in secondary batteries with mildly acidic electrolytes, for which the literature information is scanty and fragmentary. Methodologically, this study has been developed against the background of cognate studies in alkaline environment, which is extensively documented, though perhaps not as systematically as one would wish.

I pinpointed that compact and uniform Zn electrodeposits can be obtained in a specific CD range. Above the upper CD limit dendrites tend to form under diffusion control. In neutral electrolytes, such upper CD limit was found to be above the range presently considered for battery recharge: this finding in principle points out the possibility of increasing the recharge rate of secondary batteries with Zn anodes. It is worth noting that since the concentrations of Zn ions currently proposed for neutral electrolytes are 4 to 20 times higher than those used in alkaline solutions, the former class of electrolytes intrinsically enables lower mass-transport limitations. The lower CD limit corresponds to the formation of non-compact, mossy structures: this lower limit is not appreciably different in neutral and alkaline electrolytes. Since mossy structures were found to grow even below 20 $mA/cm^2$, the suppression of these structures is currently more practically relevant that of high-CD dendrites.

As far as the anodic behaviour of Zn is concerned, I highlighted that it is of fundamental importance for the stabilization of anode morphology during extended cycling. In fact, at high anodic CDs, Zn tends to passivate. Moreover, I showed that, in neutral environment passivation is favoured by the local cathodic alkalinization linked to HER running concomitantly with Zn plating under strong cathodic polarization.

Since the anodic behaviour was suspected to be of fundamental importance for the evolution of the deposit morphology, visualization of the shape change of the electrode after the alternation of anodic and cathodic polarization periods was necessary. This was done in the split cell experiments in section 3.3, which showed that internal short circuits tend to occur after time intervals during which the cell exhibits drastic potential increases corresponding to the inception of passivation. At variance with alkaline systems, in which passivation typically leads to definitive cell failure, in neutral ambient passivation tends to be temporary, and probably leaves some active electrode areas on which the CD locally increases above the threshold leading to dendrite formation: in turn, dendrites tend to short the cell.

It is common practice to add $MnSO_4$ in the electrolyte to solve cathode-related issues: the effects of this compound on the ZIBs anodes behaviour are however not studied and have been considered in this work for the first time. The influence of $Mn^{2+}$ on the electrodeposit morphology was tested in section 3.2.1. Apparently, it has a minor influence on the deposit on the CD range of interest for ZIBs application, however, it might increase the CD limit below which mossy Zn can form.

The creation of an even Zn electrodeposited coating is traditionally achieved in industrial processes through the insertion of specific additives, such as QAS, in the plating bath. The applicability of these additives for ZIBs anodes in mildly acidic electrolytes and their behaviour during the anodic polarization has been attacked in this study. Seven different QASs were studied as candidate additives for the suppression of irregular structures on the battery anode. Systematic CV investigations, described in section 3.1.2, highlighted that these additives inhibit the cathodic reaction and have a lower effect on the anodic one: the increment of cathodic overpotential was associated to a kinetic inhibition of the deposition reaction as well as, to the formation of passivating layers after cycling. Galvanostatic electrodeposition experiments showed that three additives (TBAB, CTAB, PDADMAC) allowed a complete suppression of mossy structures. However, at CDs higher than that at which mossy structures are formed (> 30mA/cm$^2$), the deposit from the same additives was not as satisfying. The deposits resulted more irregular than these obtained without additives.

After having assessed the ability of these additives to suppress mossy deposits during low CD galvanostatic depositions, the additives were tested with low CD cycles. The aim here was to verify their performance with a treatment which included anodic polarization. The SEM inspection of the cycled samples at low CD unveiled that the morphology in presence of TBAB and especially of PDADMAC were smooth and uniform. The other additives exhibited deposit morphologies similar or more irregular than the ones obtained without additive. Systematic additive screening led to the selection of TBAB and PDADMAC as the most promising ones, and their behaviour was further investigated by galvanostatic deposition on Zn foil (section 3.2.3). In accordance with the CVs, TBAB exhibited a lower inhibition of the cathodic reaction than PDADMAC, leading to the selection of TBAB as the single most prospective additive. The differences in Zn cycling behaviour associated with TBAB in comparison with the additive-free case, were studied in depth by *in situ* tomography. Tomography confirmed a beneficial effect of TBAB at lower CDs (below 15 mA/cm$^2$), while at higher CDs (above 30 mA/cm$^2$ ) the additive induced a faster deterioration of the deposit, causing the formation of large amounts of dead metal and internal short circuits.

TBAB thus seem beneficial for ZIB operation at low CDs. It successfully inhibits mossy deposits and ensures uniform deposits even after cycling. At higher CDs, instead, the use of this additive was found to be detrimental for Zn cycling stability, owing to the anodic impact of these molecules, which favour Zn passivation and the subsequent evolution of the deposit in an irregular morphology. This might be caused by the irreversible adsorption of the molecule.

The performances of these additives must be further investigated to better asset their effects, with regard also on passivation and anodic polarization. The behaviour of these additives must be studied also in the presence of a separator since mass transport resulted to be an

important parameter for the effects of the additive. The further research for additives employable in a wider CD range is necessarily, specifically concentrating on the combined role of anodic and cathodic phase-formation processes.

# Acronyms

| | |
|---|---|
| ATV | anodic terminal voltage |
| BDMPAC | benzyl dimethyl phenyl ammonium chloride |
| BPPEI | benzyl-phenyl modified poly ethylene imine |
| CD | current density |
| CE | counter electrode |
| CMC | critical micellar concentration |
| CTAB | hexadecyl tri-methyl ammonium bromide |
| CTV | cathodic terminal voltage |
| CV | cyclic voltammetry |
| DMDTDAB | Di-methyl di-tetradecyl ammonium bromide |
| DOD | depth of discharge |
| HER | hydrogen evolution reaction |
| OER | oxygen evolution reaction |
| PDADMAC | poly di-allyl di-methyl ammonium chloride |
| PEI | poly ethylene imine |
| PVC | ploly vinil chloride |
| QAS | quaternary ammonium salt |
| REF | reference electrode |
| TBAB | Tetra-butyl ammonium bromide |
| WE | working electrode |
| ZAB | zinc air battery |
| ZIB | zinc ion battery |

# Bibliography


[1] Atlas of electrochemical equilibria in aqueous solutions marcel pourbaix

[2] Kinetics of Zinc Electrocrystallization Correlated with the Deposit Morphology ISRAEL EPELBOIN, MEKKI KSOURI AND ROBERT WIART

[3] the morphology study of Zinc Electrodeposits from Alkaline Zincate Solutions

[4] Morphology study of electrodeposited zinc from zinc sulfate solutions as anode for zinc-air and zinc-carbon batteries Nurhaswani Alias, Ahmad Azmin Mohamad

[5] the mechanism of the dendritic electro-crystallization of Zinc J. W. Diggle, A. R. Despic, J O'M. Bockris

[6] Dendritic and fractal patterns in electrolytic metal deposits Dendritic and fractal patterns in electrolytic metal deposits Yasuji Sawada

[7] Effects of Deposition Conditions on the Morphology of Zinc Deposits from Alkaline Zincate Solutions

R. Y. Wang, D. W. Kirk, and G. X. Zhang

[8] An experimental study of zinc morphology in alkaline electrolyte at low direct and pulsating overpotentials

[9] the acid-base behaviour of Zinc sulphate electrolytes: the temperature effects Weidon Wang

M.V. Simicˇic´ K.I. Popov N.V. Krstajic ´

[10] Passivation of Zinc Anodes in Alkaline Electrolyte: Part I. Determination of the Starting Point of Passive Film Formation Marina Bockelmann et al 2018 J. Electrochem.

[11] Electrochemical characterization and mathematical modeling of zincpassivation in alkaline solutions: A review Marina Bockelmann Laurens Reining Ulrich Kunz Thomas Turek

[12]Passivity and passivity breakdown of zinc anode in sulphate solutions E.E. Abd El Aa

[13] a kinetic model of the spontaneous passivation and corrosion of Znic in near neutral Na2SO4 solutions L.sziraki

[14] EIS investigation of zinc dissolution in aerated sulfate medium. Part I: bulk zinc C. Cachet

[15] EIS investigation of zinc dissolution in aerated sulphate medium. Part II: zinc coatings C. Cachet

[16] Designing Dendrite-Free Zinc Anodes for Advanced Aqueous Zinc Batteries Junnan Hao

[17] 3D Porous Copper Skeleton Supported Zinc Anode toward High Capacity and Long Cycle Life Zinc Ion Batteries Zhuang Kang

[18] The Three-Dimensional Dendrite-Free Zinc Anode on aCopper Mesh with aZinc-Oriented Polyacrylamide Electrolyte Additive. Qi Zhang

[19] 3D zinc carbonfiber composite framework anode for aqueous Zn–MnO2batteries Wei Dong

[20] Dendrite-Free Zinc Deposition Induced by Multifunctional CNT Frameworks for Stable Flexible Zn-Ion Batteries Yinxiang Zeng

[21] Nanoporous CaCO3Coatings Enabled Uniform Zn Stripping/Plating for Long-Life Zinc Rechargeable Aqueous Batteries Litao Kang

[22] Long-life and deeply rechargeable aqueous Zn anodes enabled by a multifunctional brightener-inspired interphase. Zhiming Zhao

[23] Manipulating the ion-transfer kinetics and interface stability for high-performance zinc metal anodes Xuesong Xie

[24] Ultrathin Surface Coating Enables Stabilized Zinc Metal Anode Kangning Zhao

[25] A Corrosion-Resistant and Dendrite-Free Zinc Metal Anode in Aqueous Systems Daliang Han

[26] Highly reversible zinc metal anode for aqueous batteries Fei Wang

[27] Cation-Deficient Spinel ZnMn2O4Cathode in Zn(CF3SO3) Electrolyte for Rechargeable Aqueous Zn-Ion Battery Ning Zhang

[28] Fundamentals and perspectives in developing zinc-ion battery electrolytes: a comprehensive

Review Tengsheng Zhang

[29] Some fundamental aspects of levelling and brightening in metal electrodeposition L. ONICIU, L. MURESAN

[30] SOME MECHANISMS OF ACTION OF ADDITIVES IN ELECTRODEPOSITION PROCESSES T. C. FRANKLIN

[31] Fundamentals and perspectives in developing zinc-ion battery electrolytes: a comprehensive review Tengsheng Zhang, Yan Tang, Shan Guo, Xinxin Cao

[32] Effect of lead and tin additives on surface morphology evolution of electrodeposited zinc. Tomohiro Otani, Yasuhiro Fukunaka, Takayuki Homma

[33] inhibition Role of Trace Metal ion Additives on Zinc Dendrites during Plating and Stripping Processes, Ge Chang, Shijun Liu, Yanan Fu.

[34] Suppressing Dendrite Growth during Zinc Electrodeposition by PEG-200 Additive. Stephen J. Banik and Rohan Akolkar

[35] Surface Adsorption of Polyethylene Glycol to Suppress Dendrite Formation on Zinc Anodes in Rechargeable Aqueous Batteries. Aly Mitha, Alireza Z. Yazdi, Moin Ahmed, and Pu Chen

[36] The effect of polyethyleneimine as an electrolyte additive on zinc electrodeposition mechanism in aqueous zinc-ion batteries Amir Bani Hashemi, Ghoncheh Kasiri, Fabio La Mantia

[37] Tetra-alkyl ammonium hydroxides as inhibitors of Zn dendrite in Zn-based secondary batteries. C.J. Lan, C.Y. Lee, T.S. Chin

[38] Cationic Surfactant-Type Electrolyte Additive Enables Three-Dimensional Dendrite-Free Zinc Anode for Stable Zinc-Ion Batteries Aruuhan Bayaguud, Xiao Luo, Yanpeng Fu, and Changbao Zhu

[39] Electrodeposition of Zinc from Alkaline Electrolytes Containing Quaternary Ammonium Salts and Ionomers: Impact of Cathodic-Anodic Cycling Conditions Francesca Rossi, Claudio Mele, Marco Boniardi, Benedetto Bozzini

[40] Lead ion and tetrabutylammonium bromide as inhibitors of the growth of spongy zinc in single flow zinc/nickel batteries Yuehua Wena, Tian Wangb, Jie Cheng, Junqing Pan, Gaoping Cao, Yusheng Yang

[41] MECHANISM OF ZINC ELECTRODEPOSITION IN ACIDIC SULFATE ELECTROLYTES CONTAINING Pb2 + IONS R. ICHINO, C. CACHET and R. WIART

[42] Scientific Challenges for the Implementation of Zn-Ion Batteries Lauren E. Blanc, Dipan Kundu, and Linda F. Nazar

[43] Bright zinc electrodeposition and study of influence of synergistic interaction of additives on coating properties K.O. Nayana, T.V. Venkatesha

[44] Suppression of Dendrite Formation and Corrosion on Zinc Anode of Secondary Aqueous Batteries Kyung E. K. Sun, Tuan K. A. Hoang

[45] Evaluation of organic additives as levelling agents for zinc electrowinning from chloride electrolytes D. J. MacKINNON, J. M. BRANNEN

[46] Studies of corrosion inhibitors for zinc manganese batteries: quinoline quaternary ammonium phenolates. Dongshe Zang, Lidong Li, Lixin Cao.

[47] MECHANISM OF ZINC ELECTRODEPOSITION IN ACIDIC SULFATE ELECTROLYTES CONTAINING Pb2 + IONS R. ICHINO, C. CACHET and R. WIART

[48] Effect of Mn2+ ions on the electrodeposition of zinc from acidic sulphate solutions Qi Bo Zhang, Yixin Hua

[49] Lee, T. S.: Hydrogen overpotential on zinc alloys in alkaline solution, 1. Electrochem. Soc.

[50] the morphology study of Zinc electrodeposits from alkaline zincate solutions by Rainey Yu Wang

[51] OperandoVisualization and Multi-scale Tomography Studies of Dendrite Formation and Dissolution in Zinc Batteries Vladimir Yufit, Farid Tariq, David S. Eastwood, Moshiel Biton, Billy Wu, Peter D. Lee, Nigel P. Brandon

[52] Dendrite growth in the recharging process of zinc–air batteries.di Keliang Wang, Pucheng Pei,* Ze Ma, Huicui Chen, Huachi Xu, Dongfang Chen
and Xizhong Wang

[53] Crystallographic and morphological studies of electrolytic zinc dendrites grown from alkaline zincate solutions JOHN W. DIGGLE, ROBERT J. FREDERICKSt

[54] Corrosion and Electrochemistry of Zinc. Xiaoge Gregory Zhang

[55]Corrosion of Zinc as a Function of pH. S. Thomas, N. Birbilis, M.S. Venkatraman, and I.S. Cole

[56] Diethyl ether as self-healing electrolyte additive enabled long-life rechargeable aqueous zinc ion batteries Weina Xua,b, Kangning Zhao, Wangchen Huob

[57] Dendrite-Free Lithium Deposition via Self-Healing Electrostatic Shield Mechanism Fei Ding, Wu Xu, Gordon L. Graff,

[58] Inhibited zinc electrodeposition: electrode kinetics and deposit morphology J. BRESSAN, R. WIART

[59] The Electrochemical Degradation of Quaternary Ammonium Salts. II. The Mechanism of the Coupling Reaction By Sidney D. Ross, Manuel Finkelstein and Raymond C. Petersen

[60] Quaternary ammonium compounds (QACs): A review on occurrence, fate and toxicity in the environment Chang Zhang *, Fang Cui, Guang-ming Zeng

[61] The adsorption, CMC determination and corrosion inhibition of some
N-alkyl quaternary ammonium salts on carbon steel surface in 2M H2SO4
R. Fuchs-Godec

[62] Studies for corrosion inhibitors for zinc-manganese batteries: quinoline Quaternary ammonium phenolates. Dongshe Zang, Lidong Li

[63] Influence of surfactants on electrochemical behaviour of zinc electrodes in alkaline solution. JiLing Zhu, YunHong Zhou ), CuiQin Gao

[64] Surfactant widens the electrochemical window of an aqueous electrolyte for better rechargeable aqueous sodium/zinc battery. Zhiguo Hou, Xueqian Zhang

[65] Performance improvements of alkaline batteries by studying the effects of different kinds of surfactant and different derivatives of benzene on the electrochemical properties of electrolytic zinc
Robab Khayat Ghavami, Zahra Rafiei

[66] Effects of BTA and TBAB electrolyte additives on the properties of zinc electrodes in zinc–air batteries Pengpeng Wang, Fangxia Zhao

[67] Tetra-alkyl ammonium hydroxides as inhibitors of Zn dendrite in Zn-based secondary batteries C.J. Lan, C.Y. Lee, T.S. Chin

[68] Semipermanent capillary coatings in mixed organic–water solvents for CE. Abebaw G. Diress, Mahmoud M. Yassine, Charles A. Lucy

[69] Aqueous rechargeable zinc/sodium vanadate batteries with enhanced performance from simultaneous insertion of dual carriers. Fang Wan, Linlin Zhang,

[70] Translating Materials-Level Performance into Device-Relevant Metrics for Zinc-Based Batteries Joseph F. Parker, Jesse S. Ko, Debra R. Rolison, and Jeffrey W. Long

[71] C. *Monticelli*, in *Encyclopedia* of Interfacial *Chemistry*

[72] Characterization of the particulate anode of a laboratory flow Zn–air fuel cell Claudio Mele, Angelo Bilotta, Patrizia Bocchetta, Benedetto Bozzini

[73] An Electrochemical and in situ SERS Study of Cu Electrodeposition from Acidic Sulphate Solutions in the Presence of 3-Diethylamino-7-(4-dimethylaminophenylazo)-5-phenylphenazinium chloride (Janus Green B)" Benedetto Bozzini, Claudio Mele, Lucia D'Urzo, Vincenzo Romanello. Journal of Applied Electrochemistry.

[74] 2001 - bozzini b., e. Griskonis, a. Sulcius and p.l. cavallotti. (2001). Influence of selenium-containing additives on the electrodeposition of zinc-manganese alloys. Plating and surface finishing. Vol. 88, pp. 64-70

[75] 1999 - bozzini b., f. Pavan, v. Accardi and p.l. cavallotti. (1999). Electrodeposition and plastic behaviour of low-mn zn-mn alloys for automotive applications. Metal finishing; preparation electroplating coating. Vol. 97, pp. 33-42 issn: 0026-0576.

[76] 1998 - bozzini b., f. Pavan, p.l. cavallotti. (1998). Experience with a pilot plant for the electrodeposition of zn-mn on wire. Transactions of the institute of metal finishing. Vol. 76, pp. 171-178 b. Bozzini*, p.l. cavallotti, f. Pavan
“metastable intermetallics in the zn-mn system obtained by electrodeposition”

[77] Journal de Chimie Physique et de Physico-Chimie Biologique, 94 (1997) 1009-1013.

[78] Coupling Phenomena between Zinc Surface Morphological Variations and Ionic Mass Transfer Rate in Alkaline Solution I. Arise,a S. Kawai,a Y. Fukunaka,b, and F. R. McLarnonc,